UC San Diego

UC San Diego Electronic Theses and Dissertations

Title

Lineage mapping of brain tumors

Permalink

https://escholarship.org/uc/item/9w01168g

Author

Jandial, Rahul

Publication Date

2008

Peer reviewed|Thesis/dissertation

eScholarship.org Powered by the California Digital Library
University of California

UNIVERSITY OF CALIFORNIA, SAN DIEGO

Lineage Mapping of Brain Tumors

A Dissertation submitted in partial satisfaction of the
Requirements for the degree Doctor of Philosophy

in

Molecular Pathology

by

Rahul Jandial

Committee in charge:

Professor Evan Y. Snyder, Chair
Professor Tony L. Yaksh, Co-Chair
Professor Henry C. Powell
Professor Hoi Sang U
Professor Alexey Terskikh

The Dissertation of Rahul Jandial is approved, and it is acceptable in quality and form for publication on microfilm:

Co-Chair

Chair

University of California, San Diego

2008

DEDICATION

To my wife Danielle for her unwavering love, support, and understanding.

EPIGRAPH

Time grows for all those who know how to use it.

Leonardo da Vinci

TABLE OF CONTENTS

Signature page……iii

Dedication……..iv

Epigraph……..v

Table of Contents……....vi

Acknowledgements……vii

Vita……..viii

Abstract……...xi

Introduction……1

Methods……...22

Results……..44

Discussion……73

Conclusion……...88

Figures……..93

References……125

ACKNOWLEDGEMENTS

With an enterprise as immense as the preparation of a dissertation, undoubtedly many people have contributed and deserve to be acknowledged. Foremost, my thesis committee members, Drs. Snyder, Yaksh, Powell, U, and Terskikh have helped and encouraged me as I navigate the unconventional and difficult path of being both surgeon and scientist. Without their invaluable support, this endeavor would be futile.

In the proverbial trenches where the science and writing took place, Joseph Krueger was my peer and in some ways my mentor from the initial graduate classes all the way to the proof reading of this dissertation. To him I am very grateful. Likewise, Allen Ho provided consistent and valuable effort and energy to all aspects of this work. Again, I am grateful. Lastly Anders Persson was instrumental in much of this work and our collaboration yielded results and brought ideas to fruition, which alone we would not have been able to achieve.

VITA

1995 Bachelor of Arts, University of California, Berkeley

2000 Doctor of Medicine, University of Southern California, Los Angeles

2008 Neurosurgeon, University of California, San Diego

2008 Doctor of Philosophy, University of California, San Diego

Ames CP, Boriani J, Jandial R. *Spine and Spinal Cord Tumors: Advanced Operative Techniques*. QMP Inc. Saint Louis, Missouri; Winter 2009.

Jandial R & Teng Y. *Spine and Spinal Cord Repair and Regeneration.* Springer/Landes Bioscience, Georgetown, Texas; Spring 2008.

Jandial R & Snyder EY. *Frontiers in Brain Repair*. Springer/Landes Bioscience, Georgetown, Texas; Spring 2008.

Toy E, Jandial R, Snyder EY. *Case Files: Neuroscience*. Lange Medical Books/ McGraw Hill, New York, New York: April 2008.

Jandial R, *100 Questions and Answers About Spinal Disorders*. Jones and Bartlett Publishing, Boston, Massachusetts: Winter 2007.

Jandial R, Hughes SA. *100 Questions and Answers About Head Injury*. Jones and Bartlett Publishing, Boston Massachusetts: Spring 2008

Jandial, R. *Code Blue: Emergent Clinical Scenarios*. Quality Medical Publishing, Inc., St. Louis, Missouri, In Press.

Jandial, R. (Associate Editor) *TRAUMA: Resuscitation, Anesthesia, & Critical Care*. Marcel Dekker, Inc., New York, New York. 2007.

Jandial R, Aryan HE, Nakaji P. *Neurosurgical Essentials*. Quality Medical Publishing, Inc., St. Louis, Missouri, 2004.

Jandial R, Snyder ES. Stem cell regeneration of the intervertebral disc-molecular and cellular challenges. Submitted Neurosurgical Focus.

Jandial R. Biologics and intervertebral disc repair. Biomaterials. Accepted.

Jandial R. Spinal fusion and bone morphogenic proteins-integrating scaffolds. *Biomaterials*. Accepted.

Jandial R, Snyder ES. Genetic Modification of Neural Stem Cells. *Molecular Therapy*. Accepted.

Jandial R, Snyder ES. Exploiting Genetically Modified Neural Stem Cells for Neurological Disease. *Molecular Therapy*. Accepted.

Jandial R, Snyder ES. Central Nervous System Repair. *International Congress Series*. Accepted.

Singec I, Jandial R, Snyder ES. The Leading Edge of Stem Cell Therapeutics. *Annual Review of Medicine*. 2006 Nov 13.

Jandial R, Levy ML, Sturdivan L, Apuzzo ML. Ballistics for the Neurosurgeon. *Neurosurgery*. Accepted.

Levy ML, Nguyen A, Aryan H, Jandial R, Meltzer HS, Apuzzo ML. Robotic virtual endoscopy: development of a multidirectional rigid endoscope. *Neurosurgery*. 2006 Jul;59(1 Suppl 1):ONS134-41

Jandial R, Greenberg MS, Aryan HE, Taylor WR. Sutherland-Smith, M; Kearns, K; Morris, K. Lumbar Diskectomy In A Human-Habituated Western Lowland Gorilla. *The Internet Journal of Neurosurgery*. 2005. Volume 2 Number 1.

Ozgur BM, Jandial R, Levy ML. Complications of Interhemispheric Transcallosal Approach in Children. *Clin Neurol Neurosurg*. 2005.

Aryan HE, Jandial R, Farin A, Chen JC, Granville R, Levy ML. Intradural cranial congenital dermal sinuses: diagnosis and management. *Childs Nerv Syst.* 2006 Mar;22(3):243-7. Epub 2005 Sep 29.

Aryan HE, Ghosheh FR, Jandial R, et al. Retinal Hemorrhage and Pediatric Brain Injury: History, Etiology, and Review of the Literature. *Journal of Clinical Neuroscience* 12(6): 624-631, August 2005.

Aryan HE, Ozgur BM, Jandial R, Levy ML. Subfrontal Transbasal Approach for Resection of Craniopharyngioma. *Neurosurgical Focus* 18(6a): E10, June 2005.

Aryan HE, Jandial R, Ozgur BM, et al. Surgical Correction of Metopic Synostosis. *Child's Nervous System* 21(5): 392-398, May 2005.

Aryan HE, Meltzer HS, Park MS, Jandial R, Levy ML. Antibiotic-Impregnated Silicone Catheters for Shunting of Cerebrospinal Fluid (CSF) in Children. C*hild's Nervous System* 21(1): 56-61, January 2005.

Jandial R, Hughes SA, Aryan HE, Marshall LF, Levy ML. The Science of Shrinking Human Heads: Tribal Warfare and Revenge Among the South American Jivaro-Shuar. *Neurosurgery* 55(5): 1215-1221, November 2004.

Jandial R, Aryan HE, Hughes SA, Levy ML. Effect of Vagus Nerve Stimulator (VNS) Magnet on Programmable Shunt Settings. *Neurosurgery* 55(3): 627-630, September 2004.

Aryan HE, Meltzer HS, Gerras GG, Jandial R, Levy ML. Leptomeningeal Cyst Development After Endoscopic Craniosynostosis Repair. *Neurosurgery* 55(1): 235-238, July 2004.

Jandial R, Aryan HE, Bennett RL, Masri LS, Lavine SD, Levy ML. Gunshot Wounds to the Head: Gang and Non-Gang Related Injuries and Outcomes. *Brain Injury*. 2004

Aryan HE, Yanni DS, Nakaji P, Jandial R, Marshall LF, Taylor WR. Syringocephaly. *Journal of Clinical Neuroscience* 11(4): 421-423, May 2004.

Park MS, Aryan HE, Ozgur BM, Jandial R, Taylor WT. Stabilization of Anterior Cervical Spine with Bioabsorbable Polymer in One- and Two-Level Fusions. *Neurosurgery* 54(3): 631-635, March 2004.

Jandial R, Snyder ES. Neural repair and stem cells. *New Encyclopedia of Neuroscience*. Elsevier. Oxford, UK. In Press.

Lee JP, Clark D, Jeyakumar M, Gonzalez R, McKercher S, Park KI, Jandial R, Seyfried TN, Platt FM, Snyder EY. Neural Stem Cell Therapy in Lysosomal Storage Disease. *Lysosomal Storage Diseases*. Springer Publishing. New York, New York. In Press.

Jandial R, Aryan HE, Hughes SA, U HS. Management of Intracerebral Vascular Catastrophes. *TRAUMA: Resuscitation, Anesthesia, & Critical Care*. Marcel Dekker, Inc., New York, New York. 2007.

Hamid RK, Newfield P, Levy ML, Jandial R, Davis PJ. Pediatric Neurologic Trauma and Other Emergencies. *TRAUMA: Resuscitation, Anesthesia, & Critical Care*. Marcel Dekker, Inc., New York, New York. 2007.

ABSTRACT OF THE DISSERTATION

Lineage Mapping of Brain Tumors

by

Rahul Jandial

Doctor of Philosophy in Molecular Pathology

University of California, San Diego, 2008

Professor Evan Y. Snyder, Chair
Professor Tony L. Yaksh, Co-Chair

Identifying the cellular origins of gliomas has been elusive, partly due to the lack of models in which the neurodevelopmental biology of brain tumors can be investigated. Using molecular and genetic tools a transgenic mouse model that develops high grade gliomas was studied. We hypothesized that the neurogenic subventricular zone to be the brain region from which the glioma cell of origin would arise. This area was characterized and labeled with a oligonucleotide library that allow for lineage tracing of

gliomas once formed. Gliomas were comprised of heterogeneous clones, with the consistent presence of a dominant overrepresented clone. In animals with gliomas, neurogenesis is altered with loss of neuronal committed progenitor markers. This process is partly mediated by map kinases, and their inhibition leads to increased neuronal differentiation in vitro of transgenic mouse neurospheres and human glioma cells.

INTRODUCTION

Parallels between cancer and normal development have begun to emerge with recent molecular and cellular advances. Molecules originally discovered based on their role in cancer—oncogenes and tumor suppressors—have now been shown to function as fundamental regulators of cell growth and differentiation during development. Genes identified as regulators of pattern formation in invertebrates and vertebrates have been implicated in a variety of human cancers. The fields of developmental biology and tumor biology have clear convergence, and for the central nervous system (CNS) the interface between development and cancer is the investigation of gliomas. (Wechsler-Reya and Scott, 2001)

Adult neurogenesis

Neurogenesis, the process of generating functionally integrated neurons from progenitor cells, was believed to occur only during embryonic stages in the mammalian central nervous system (CNS). (Ramon y Cajal, 1913) Current evidence indicates new neurons are added in discrete regions of the adult mammalian CNS. (Gross, 2000, Kempermann and Gage, 1999, Lie et al., 2004) Santiago Ramon y Cajal (1913) also concluded that neurons are generated exclusively during the prenatal phase of development. Existence of dividing cells in the postnatal CNS was suggested at that time, (Allen, 1912, Hamilton, 1901) but with methods of the time, fate determination was not

possible. (Ramon y Cajal, 1913) Subsequently “no new neurons after birth” became a central dogma in neurobiology for almost a century. (Gross, 2000)

In the 1950s, a new method was developed to label dividing cells with [H3]-thymidine, which incorporates into the replicating DNA during the S-phase of the cell cycle and is detected with autoradiography. (SIDMAN et al., 1959) The generation of new neurons was first reported using this technique in three-day old mouse brains. (Smart, 1961) Altman and colleagues published a series of papers reporting [H3]-thymidine evidence for new neurons in various regions of adult rats, including the dentate gyrus of the hippocampus, (Altman and Das, 1965) neocortex, (Altman and Das, 1966) and olfactory bulb (Altman, 1969) The functional relevance of these findings remained undetermined.

The potential for adult neurogenesis was investigated in the 1970s when Kaplan & Hinds (1977) demonstrated that newborn neurons in the hippocampus survived past the postnatal period. These new neurons also appeared to receive synaptic inputs and extend axon projections to their target area. (Kaplan and Bell, 1983, Stanfield and Trice, 1988) A series of studies of adult neurogenesis in songbirds started to provide evidence for functional roles of postnatal neurogenesis in seasonal song learning. (Nottebohm, 2004)

With advancing molecular techniques, adult neurogenesis was demonstrated with BrdU incorporation in all mammals examined, including samples from human patients. (Eriksson et al., 1998) BrdU can be detected by immunocytochemistry for phenotypic analysis and stereological quantification. This was corroborated with combined retroviral-based lineage tracing. (Price et al., 1987, Sanes et al., 1986) Electrophysiological studies provided further evidence that newborn neurons in the adult

mammalian CNS are indeed functional and synaptically integrated. (Belluzzi et al., 2003, Carleton et al., 2003, van Praag et al., 2002)

Adult neurogenesis has been proven by technical advances to facilitate identification of newborn neurons and three approaches have been explored so far. During DNA replication in the S-phase of the cell cycle, exogenous nucleotides such as [H3]-thymidine or BrdU are incorporated into newly synthesized DNA and then passed on to cell progeny. By varying the pulsing paradigm and the examination time points after pulsing, this technique allows quantitative analysis of proliferation, differentiation, and survival of newborn cells. (Kempermann et al., 1997, Miller and Nowakowski, 1988) The expression of transgenes from retroviruses requires viral integration into the host genome, (Lewis and Emerman, 1994) and can be used for lineage analysis based on genetic marking with retroviruses. Developing neurons express distinct markers during their maturation process. (Kempermann et al., 2004) Common markers used for immature neurons include PSANCAM (poly-sialylated-neural cell-adhesion molecule), Tuj1 (β-tubulin isoform III), CRMP (collaspin response-mediated protein 4, also known as TOAD4), and DCX (doublecortin). Markers used for mature neurons include MAP-2ab (microtubule associated protein-2 a and b isoforms) and NeuN (neuronal nuclei). Newborn neurons can be identified by the presence of immature markers and absence of mature markers of neurons.

Neurogenic zones in the adult mammalian CNS

In the intact adult CNS, active neurogenesis occurs in discrete regions. (Alvarez-Buylla and Lim, 2004, Lie et al., 2004) From rodents to primates, neurons are generated continuously in the subventricular zone (SVZ) [See Figure 1] and migrate anteriorly through the rostral migratory stream (RMS) into the olfactory bulb to become interneurons. [See Figure 2] The olfactory bulb has two types of output neurons, i.e., tufted and mitral cells, and two types of local neurons or interneurons, i.e., periglomerular and granule cells. (Cajal, 1955, Brunjes and Frazier, 1986) Until recently it was thought that a RMS-like structure does not exist in the human brain since humans are less dependent on olfaction compared with rodents. Curtis et al. describe a RMS that originates from the proliferative cells of the SVZ and leads to olfactory neurogenesis in humans. (Curtis et al., 2007) The subgranular zone (SGZ) of the dentate gyrus in the hippocampus, is another discrete region from which new granule neurons are continuously born locally in all mammals examined, including humans. Recently another substantial area of neurogenesis has been described. The subcallosal zone (SCZ) localizes beneath the corpus callosum and many cells in the SCZ appear to have similar characteristics to those observed in the SVZ. Using epidermal growth factor (EGF) and fibroblast growth factor (FGF), the SCZ is a rich source of neurosphere-forming cells; these neurospheres can generate oligodendrocytes, neurons, and astrocytes. (Seri et al., 2006) The SVZ, SCZ, and the corpus callosum are associated with transcription factors involved with cell migration and differentiation. [See Figure 3]

Neural stem cells (NSCs)

Multipotent neural progenitors have been isolated from various regions of the adult mammalian CNS, including human CNS regions. (Gottlieb, 2002) These cells can be expanded and genetically modified with preservation of their multipotentiality over many passages. Because of easy access and defined culture conditions, manipulation of adult neural progenitors in monolayer (Deisseroth et al., 2004, Song et al., 2002a) or slice cultures (Bolteus and Bordey, 2004, Raineteau et al., 2004) allows precise analysis of the intrinsic and extrinsic mechanisms that control the various steps of neurogenesis, including proliferation, survival, fate specification, neuronal migration, maturation, and synapse formation.

Cultures of neural progenitors from the adult CNS are largely established on the basis of self renewal; a process of cell division to generate more cells of the same type. Preferential growth over other cell types, when grown in defined media with specific growth factors, is a hallmark property of stem cells. (Gottlieb, 2002) Stem cells can accomplish self-renewal by undergoing asymmetric divisions, in which a faithful copy of the mother cell and a more mature progenitor are generated. The same result is achieved when, within a given stem-cell pool, equivalent numbers of symmetrical cell cycles take place, yielding either two stem cells or two more mature progenitors. Cells dissociated from specific tissues are plated either directly (Reynolds and Weiss, 1992) or after partial purification steps to remove major contaminants. (Palmer et al., 1999) Prospective isolation methods using fluorescence-activated cell sorting (FACS) have recently been developed on the basis of cell properties and/or cell-surface antigens, (Rietze et al., 2001,

Temple, 2001, Uchida et al., 2000) or the expression of reporters under specific promoters. (Roy et al., 2000)

Two types of progenitor cultures are commonly used. (Gottlieb, 2002) In the neurosphere culture, individual neural progenitors proliferate on a non-adhesive substrate and generate suspended clusters of cells. (Reynolds and Weiss, 1992) In the adhesive culture, neural progenitors grow as a monolayer on coated substrates, such as laminin. (Ray et al., 1993) The most commonly used growth factors to maintain self-renewal of cultured adult neural progenitors are epidermal growth factor (EGF) and basic fibroblast growth factor (FGF-2).

The identity of neural stem cells is of significant investigation and several cell types have been proposed as the resident adult NSC, (Doetsch et al., 1999a) multiciliated ependymal cells (Johansson et al., 1999) and subependymal cells. (Morshead et al., 1994) The astrocyte hypothesis is the prevailing view. (Alvarez-Buylla and Lim, 2004) In the SVZ of rodents, a subset of astrocytes (GFAP+) gives rise to rapidly proliferating transient amplifying cells (GFAP−Dlx2+), which in turn generate migrating neuroblasts (GFAP−Dlx2+PSA-NCAM+). The ability of SVZ astrocytes to act as primary progenitors in the generation of new neurons is attributable to both the effects of the germinal niche microenvironment and the intrinsic properties of parenchymal astrocytes. While the niche clearly has significant effects on stem cell proliferation and differentiation, niche-derived signals do not appear to be sufficient to confer progenitor-like capabilities on ectopically transplanted astrocytes. The transplantation of parenchymal tissue to the SVZ of adult parenchymal astrocytes is intrinsically different from astrocytes that lie within germinal regions and that function as adult neural stem

cells. One study indicates that whereas adult parenchymal astrocytes cannot give rise to neural stem cells in culture, adult astrocytes isolated from germinal niches. Also, SVZ astrocytes express LeX and can form multipotent neurospheres or demonstrate neurogenic potential under the appropriate culture conditions, astrocytes derived from the cerebral cortex are LeX-negative and non-neurogenic. A similar observation has been made with astrocytes derived from adult human brain (Sanai et al., 2004) In the SGZ, a subset of astrocytes has also been proposed as the stem cells that give rise to new granule neurons. (Seri et al., 2001)

The SVZ and SGZ are regions in the CNS with proliferation and neuronal differentiation of multipotent neural progenitors (Doetsch, 2003, Lie et al., 2004) and the astrocytes provide a unique neurogenic niche. (Doetsch, 2003, Lie et al., 2004, Palmer et al., 2000, Lim and Alvarez-Buylla, 1999, Song et al., 2002a) The astrocytes in the adult CNS are not merely supporting cells as traditionally believed. Similar to neurons, astrocytes have a broad diversity of subtypes and functions; some behave like stem cells, (Doetsch et al., 1999a, Seri et al., 2001) some provide neurogenic signals, (Lim and Alvarez-Buylla, 1999, Song et al., 2002a) and some provide synaptogenic factors. (Song et al., 2002b, Ullian et al., 2004)

Astrocytomas

Astrocytomas are graded according to guidelines by the World Health Organization (WHO) using histological criteria. [See Figure 4] Grade I astrocytomas are benign, slow growing, well-circumscribed tumors that rarely progress to malignancy (e.g.

pilocytic astrocytomas). The remaining three grades (WHO II–IV) form a progression series of increasing malignancy, although high-grade tumors are often found *de novo* without evidence for a lower-grade precursor lesion. Low-grade diffuse astrocytomas (WHO II) are diagnosed based on atypical nuclear morphology. Anaplastic astrocytomas (WHO III) show mitotic figures in addition to nuclear atypia, and can be diffuse or focal. The most malignant grade astrocytoma is termed glioblastoma multiforme (GBM) (WHO IV) due to its extreme pleomorphism, and is diagnosed based on the presence of necrosis and/or microvascular proliferation, showing multi-layering of nuclei in the walls of blood vessels. Glioblastomas have been further subdivided into those that are identified *de novo* without any precursor lesion, termed primary glioblastomas, and those that arise through progression from anaplastic astrocytomas, termed secondary glioblastomas. Primary glioblastomas tend to arise later in life and are faster growing, whereas secondary glioblastomas arise earlier and are slower growing.

In addition to these diagnostic criteria, there are many histological and immunohistochemical features characteristic of astrocytomas. (Kleihues and Cavenee, 1997) Histologically, malignant astrocytomas have very diffusely infiltrative margins, and tumor cells tend to accumulate around brain architecture to form secondary structures, first identified by Scherer. (Scherer, 1940) These structure form along blood vessels, surrounding neurons, and along the subpial zone of the cortex. Glioblastomas are by characterized by distinctive cell types, such as multinucleated giant cells or gemistocytic astrocytes. (Kleihues and Cavenee, 1997) Regions of necrosis in glioblastoma are often surrounded by pseudopalisading tumor cells. In addition, astrocytomas are immunoreactive for the glial marker, glial fibrillary acidic protein

(GFAP), although higher-grade, more poorly differentiated tumors show variable expression. (Marsden et al., 1983) Because brain tumors stimulate normal astrocytes to react to damage to the brain (Janeczko, 1989) GFAP-positive reactive astrocytes can also be found within the tumors, but should not be confused with GFAP-positive tumor cells. In contrast, astrocytomas do not stain with antibodies to the neural markers synaptophysin (Gould et al., 1986) and NeuN (Wolf et al., 1996) and this can be used to distinguish them from brain tumors of other cellular origins.

Molecular alterations in gliomas

In addition to the cellular and histological basis for classifying gliomas, new information regarding molecular alterations in gliomas helps further define their formation and progression. One major molecular alteration encountered in gliomas is loss of p53. The p53 protein acts as part of a checkpoint mechanism for uncontrolled proliferation and DNA damage in the cell. (Sherr and Weber, 2000) A tetramer of p53 acts as a transcription factor to turn on genes responsible for growth arrest and apoptosis. Within the tetramer, a single mutant copy of p53 in the cell can act as a dominant negative oncomplexes containing wild-type p53. The *p53* gene is located on chromosome 17p in humans and loss of heterozygosity at 17p is one of the earliest and most common deletions in astrocytoma. Loss of heterozygosity at 17p and/or mutation of *p53* is found in up to 50% of WHO II and WHO III astrocytomas.63–65,67 Mutation of *p53* is correlated to secondary glioblastomas, and is found in 67% of secondary glioblastomas, as opposed to 11% of primary glioblastomas. In addition, patients with Li- Fraumeni

disease carrying germline mutations of *p53* are at an increased risk for developing astrocytoma. (Kleihues et al., 1997) Recent findings have shown that SVZ stem cell astrocytes express a receptor for platelet-derived growth factor (PDGF), suggesting that the ability to respond to specific growth factor stimuli, such as PDGF, epidermal growth factor and others, may be unique to these stem cell astrocytes.

EGFR gene amplification occurs in 40% of allcGBMs, and the amplified genes are frequently rearranged (Libermann et al. 1984, 1985; Ekstrand et al. 1991; Wong et al. 1992; Louis et al. 2007). An *EGFR* mutant allele with deletion of exons 2–7 (known variously as EGFRvIII occurs in 20–30% of all human GBM (and in 50%–60% of those that have amplified wild-type EGFR), making it the most common *EGFR* mutant (Sugawa et al. 1990; Frederick et al. 2000). EGFRvIII is a highly validated glioma target as evidenced by the capacity of activated EGFR mutants to enhance tumorigenic behavior of human GBM cells by reducing apoptosis and increasing proliferation (Nishikawa et al. 1994; Nagane et al. 1996; Huang et al. 1997; Narita et al. 2002) and to malignantly transform murine *Ink4a/Arf*null neural stem cells (NSCs) or astrocytes in the mouse brain (Holland et al. 1998a; Bachoo et al. 2002). Activation of these same signaling pathways is widely implicated in brain tumor formation. (Jackson and Alvarez-Buylla, 2008)

Another common molecular alteration in gliomas is with the *p14ARF* gene. p14ARF is an alternate reading frame of the *INK4a* locus on chromosome 9, which commonly shows loss of heterozygosity in astrocytomas. Mutation of *p14ARF* occurs in 40–70% of glioblastomas (Ichimura et al., 2000, Fulci et al., 2000) and appears to be mutually exclusive with *p53* mutations. Together these three gene alterations suggest that the p53 pathway is altered in 75–90% of glioblastomas.

Among the signaling pathways activated by receptor tyrosine kinases, p21-ras is of importance as reflected by the presence of oncogenic activating p21-ras mutations in 30% of all human cancers. (Bos, 1989) The lack of either primary p21-ras mutations or the loss of p21-ras-GAPs in GBMs therefore suggests that the elevated p21-ras-GTP levels are secondary to activation of this signaling pathway from over-expressed and activated receptor tyrosine kinases such as EGFR. Activation of the p21-ras pathway is functionally important in stimulating astrocytoma proliferation and angiogenesis. (Guha et al., 1997, Feldkamp et al., 1999)

Origin of brain tumors – historical insights

In trying to understand the origin of cancer, the German pathologist Julius Cohnheim noted the similarities between tumors and embryonic cells. (Rather, 1978) He suggested, more cells might be produced than are necessary for the construction of a particular tissue. These excess cells (which he called “embryonic rests”) would persist in that tissue until later in life and, because they were embryonic in origin, would retain the capacity for growth. Tumorgenesis, then, would result from abnormal activation of a growth program in these cells. The primitive cytoarchitecture and embryonic features of many malignant brain tumors have also suggested that these tumors may arise from transformed neural stem or progenitor cells. (Bailey and Cushing, 1926)

In 1942 and 1944, Joseph Globus and Hartwig Kuhlenbeck called attention to the subependymal cell plate in the adult brain and recognized its identity, as a cellular structure, with the mantle or matrix layer of the embryonic or newborn mammalian brain.

They proposed, on the basis of study of a number of human brain tumors, that there may be a relationship between the primitive cells of the subependymal plate and those of telencephalic tumors. Specifically, they stated that "one of the most important sources for such immature embryonal residue from which neuroectodermal tumors are likely to develop under certain still unknown conditions is the subependymal plate". (Globus, 1944)

This “subependymal plate,” originally described by Globus and Kuhlenbeck, was better characterized as a “mitotically active and well defined subependymal layer is present in mammalian brains throughout life.

> a distinct subependymal layers is present in the monkey as a discontinuous band of cells beneath the surfact of the ventricles, separated from the ependyma by a fibre layer of variable thickness. It is most marked anteriorly in the lateral ventricles and is tenuous and sometimes difficult to recognize posteriorly and in the wall of the third and fourth ventricle and the aqueduct. In addition to astrocytes and microglia the layer contains cells of an unusual type. These cells are most numerous in two prolongations of the subependymal layer in the anterior part of the brain, on dorso-lateral and spreading from the angle of the lateral ventricle between the undersurface of the corpus callosum and the caudate nucleus, an the other ventral and passing below the head of the caudate to the olfactory area. Here the cells are often in nests, which are sometime related to small blood vessels. The subependymal cells suggests that they could be a possible source of different histological varieties of glioma, in particular those tumors in paraventricular situation and butterfly gliomas of the corpus callosum…

A scrutiny of these neoplasms in the light of the present findings led to a reappraisal of Globus and Kuhlenbeck’s theory, and with our current understanding of adult neurogenesis, their description provides early histological demonstration of the RMS. (Lewis, 1968) [See Figure 5]

Experimental evidence for the propensity of subventricular cells to become transformed was provided by Hopewell in 1969. (Hopewell and Wright, 1969) They placed carcinogenic pellets (either 20-methylcholanthene or 3,4-benzpyrene) in the meninges of rats and reported no glial tumors. Whereas, with placement of the pellets "deeply within the brain so as to involve the lateral ventricles", a high proportion of tumors, the majority of which were of glial origin, were produced. [See Figure 6] These results showed that site of implantation is important for induction of experimental glial tumors in the rat. A possible explanation of this result is that, in the deeply implanted position, the carcinogen is in contact with the cells of the subependymal layer. This is a primitive layer of cells which are mitotically active throughout the life of the animal. (Allen, 1912, Bryans, 1959) As a result, these dividing cells that exist for long periods of time are candidates for accumulating multiple genetic hits and consequently more prone to tumor induction. In support of this they suggested that the "subependymal plate as the site of origin of several glioma types in man". (Globus and Kuhlenbeck, 1942, Globus, 1944, Kuhlenbeck, 1947, Lewis, 1968)

In 1976 transplacental injection of N-ethyl-N-nitrosourea (ENU) of pregnant rats let to foci of proliferation and gliomas near the "subependymal plate." (Lantos and Cox, 1976) In 1977, Vick et al suggested the following:

> …while it is possible that any quiescent, mature, non-mitotic glial cell may become transformed, divide excessively and form a tumor, it seems more attractive, a priori, to think that there may be a role in glial tumorigenesis for the primitive mitotic cells of the subependymal plate…it seems likely that the postnatal brain contains a continually dividing pool of cells (in the subependymal zone) which have as their normal destiny an outward migration pattern providing, perhaps, a continual source of new

> glial cells for telencephalic structures. It is these cells which may, when neoplastically transformed (by whatever cause), provide the clone (or clones) for the development of glial brain tumors…

Vick et al's foresight into the potential origin of gliomas gained further support by other investigators in the 1970s. (Vick et al., 1977) Periventricular tumors were then demonstrated to occur in the subventricular region after intraventricular inoculation with avian sarcoma viruses, with a much higher rate of tumors occurring in neonatal rats versus adult rats. [See Figure 7] (Copeland et al., 1975, Copeland and Bigner, 1977, Vick et al., 1977) A single dose of ethylnitrosurea administration to pregnant rats also induced periventricular tumors in the offspring. (Koestner et al., 1971)

Evidence for neural stem cells as the glioma cell of origin

The neurogenenic zones within the human CNS with their resident NSCs are considered the leading candidates for neoplastic transformation. Specifically mitotically active cells (NSCs and their direct progeny, transit amplifying cells (TACs)) are the cells that have the greatest probability to be the brain tumor cell of origin.

NSCs and gliomas share histological and biological similarities: Gliomas have long been described by pathologists as having remarkable cellular heterogeneity. The most aggressive and malignant glioma (glioblastoma multiforme) was named based partly on the histological diversity comprising this tumor-hence "multiforme." A transformed NSC could provide this cellular landscape due to their mulitipotential capacity (ability to differentiate into the cell types that constitute their respective germ

line). Mixed cell gliomas, such as oligoastrocytomas, have both oligodendrocytes and astrocytes (Valtz et al., 1991) and could be independent transformation of two differentiated cells. More plausible would be the transformation of a single, bipotential progenitor cell such as a NSC or a transit amplifying cell. (Chekenya and Pilkington, 2002) These mixed cell gliomas also exhibit loss of heterozygosity on chromosomes 1p and 19q in both the astrocytic and oligodendrocytic components, (Kraus et al., 1995) suggesting that in oligoastrocytomas, the astrocytes and oligodendtocytes comprising the tumor have a shared cell of origin.

Further, many glioma cells are undifferentiated and lack expression of differentiated cell makers, as well as demonstrate staining with markers for nestin. Nestin is a Class VI intermediate filament expressed in the developing CNS in early embryonic neuroepithelial stem cells. This protein has been widely used as a predominant marker for stem / progenitor cells, glioma cells, and tumor endothelial cells in the mammalian CNS. Nestin expression is one hallmark features of NSCs. (Dahlstrand et al., 1992, Tohyama et al., 1992, Lendahl et al., 1990) Gliomas and NSCs also exhibit characteristic overlapping behavior, such as high motility, association with vasculature and white matter tracts. (Shoshan et al., 1999, Doetsch et al., 2002, Palmer et al., 2000)

NSCs more likely to accumulate oncogenic mutations: Accumulation of oncogenic genetic hits by cells is an infrequent stochastic event that most likely requires the cell to exist for a considerable period or time. NSCs, defined by their ability to self renew are both mitotically active and exist during the lifetime of the animal, allowing them to potentially accumulate the necessary multiple mutations for tumor formation. Accordingly, the cellular origin of gliomas would most likely occur from the proliferative

zones in the mammalian CNS such as the SVZ contain at least two types of mitotically active cells – NSCs and transit amplifying cells. (Merkle et al., 2007) TACs exist only briefly and then differentiate, and although their total cellular compartment is significantly larger than NSCs, their transient existence makes them less likely then NSCs to accumulate the necessary genetic hits for transformation (See Figure 8). (Vescovi et al., 2006)

Cancer stem cells: Approximately 150 years ago pathologists Rudolph Virchow and Julius Cohnheim suggested there were histological similarities between the developing fetus and certain cancers (such as teratocarcinomas) and that both tissues have the capacity to differentiate and proliferate. This "embryonal-rest hypothesis" is the historical version of today's cancer stem cell hypothesis. (Huntly and Gilliland, 2005) As defined at the American Association for Cancer Research workshop on cancer stem cells: cancer stem cells are cells that (1) self renew and (2) re-supply the tumor with the various lineages of cells of which it is comprised. Self renewal can only be defined experimentally by the ability to recapitulate the generation of a continuously growing tumor-or tumor initiation cell. (Clarke et al., 2006, Lee and Herlyn, 2007) [See Figure 9]

The first report of cells with stem-like properties in brain tumors was by Ignatova et al. in 2002 where surgical specimens of glioblastoma multiforme were shown to have clonogenic neurosphere forming cells that expressed both neuronal and glial markers upon differentiation. [See Figure 10] (Ignatova et al., 2002, Vescovi et al., 2006) Subsequently, the Dirks group demonstrated CSC in brain tumors by intracerebral transplantation of CD133+ or CD133- populations into immunodeficient mice. With as few as 100 CD133+ cells from the primary tumor, a new phenocopy of the tumor could

be created in the transplanted mice; and un-sorted or CD133- primary tumor cells were unable to cause de novo tumor generation. As part of what has come to define CSCs-self-renewal capacity was also shown by confirming the ability of serially transplanted CD133+ cells to recapitulate the original tumor. The identity of the cancer initiating cell within the CD133+ population remains unknown. (Buzzeo et al., 2007, Singh et al., 2004) These findings established the presence of BTSCs, cells which can differentiate into the neural lineages, and exhibit self renewal – as demonstrated by recapitulation of primary tumors with serial transplantation. This has been shown for other types of brain tumors as well. (Taylor et al., 2005, Merkle et al., 2004) The existence of these BTSCs adds further evidence toward the NSCs origin of gliomas by confirming that different brain tumors contain transformed, undifferentiated neural precursors that respond to the same mitogens that activate adult neural stem cells. (Vescovi et al., 2006) Second, they indicate that tumor stem-like cells possess some of the molecular features of neural stem cells. Third, BTSCs, through asymmetric division, could generate a BTSCs and a progenitor cell, the latter of which may migrate away to either form or contribute to the tumor mass. (Vescovi et al., 2006, Berger et al., 2004)

Gliomas and NSCs have common regulatory pathways: Neural stem cells and progenitor cells have activated cellular pathways, such as promitotic genes, telomerase activity, and antiapoptotic genes. This innate capacity overlaps with the mechanisms underlying tumor initiation, progression, or both. EGFR expression is up-regulated in primary glioblastoma multiforme and transiently dividing progenitors (type C cells). (Mellinghoff et al., 2005) Fibroblast growth factors (FGFs) are involved in tumor proliferation and angiogenesis (Joy et al., 1997, Auguste et al., 2001) and also shown to

regulate NSC proliferation and cell fate. (Palmer et al., 1999, Gritti et al., 1996, Vescovi et al., 1993)

Notch receptors and signaling is involved in NSC renewal (Hitoshi et al., 2002, Shen et al., 2004) and related to proliferative capacity of gliomas. (Purow et al., 2005) PTEN is a tumor suppressor with an important function in the control of proliferation of neural stem cells and progenitor cells *in vivo* and *in vitro*. (Baker and McKinnon, 2004, Reya and Clevers, 2005, Groszer et al., 2001) *PTEN* is inactivated in glioblastomas (Wechsler-Reya and Scott, 2001, Rasheed et al., 1999) and its preservation in glioblastoma multiforme is clinically favorable. (Mellinghoff et al., 2005) The Wnt-catenin pathway regulates adult neurogenesis (Chenn and Walsh, 2003, Lie et al., 2005) modulating its activity may increase glioma cell growth. (Roth et al., 2000)

Recent experiments have also highlighted the increased ability of progenitor cells to be transformed versus differentiated cell types. If epidermal growth factor receptor (EGFR) is transfected into transgenic *Ink4a-Arf-/-* mouse (lacking genes for cell-cycle arrest) neural stem cells, the cells lead to glioma formation. (Bachoo et al., 2002) This contrasted with similar manipulation of differentiated mouse astrocytes. Further, if the undifferentiated mouse astrocytes were transfected with platelet-derived growth factor (*pdgf*) transgene and converted to a less differentiated state, they showed increased oncogenicity. (Bachoo et al., 2002, Dai et al., 2001, Uhrbom et al., 2002)

Mouse models for investigation of glioma origin

Mouse models gliomas are available and offer a unique opportunity to investigate tumor origin. These models, unlike glioma models in *Drosophila* and *C. elegans*, recapitulate the human pathology with characteristic structures including pleomorphic nuclei, diffusely infiltrative margins, secondary structures of Scherer, necrosis with pseudopalisading tumor cells, and microvascular proliferation. Xenograft models fail to phenocopy the classic histopathological features and are not an option for elucidating developmental mechanisms. Ultimately, these models of spontaneous tumor development and progression allows for the potential identification of novel mechanisms for tumorgenesis. (Ding et al., 2001) Genetically engineered mouse (GEM) models predictably develop gliomas with many of the features of the human disease Weissenberger et al. 1997; Uhrbom et al. 1998; Kamijo et al. 1999; Holland et al. 2000; Reilly et al. 2000; Dai et al. 2001; Ding et al. 2001, 2003; Rich et al. 2001; Sonoda et al. 2001; Bachoo et al. 2002; Uhrbom et al. 2002; Xiao et al. 2002; Weiss et al. 2003; Holmen and Williams 2005; Zhu et al. 2005; Charest et al. 2006; Tchougounova et al. 2007). Given the experimentally tractable nature of the mouse, these glioma-prone GEM models are beginning to shed light on a number of key issues such as, for example, the glioma cell of origin (Zhu et al. 2005), the ordering of mutations and whether such events underlie various glioma subtypes (Hu et al. 2005), the cooperative and epistatic relationship of such mutations, and the complex heterotypic interactions between the evolving tumor cell and the host microenvironment, among other issues central to the problem of gliomagenesis.

Toward this goal, Ding et al. 2001 used an ES cells-based transgenic approach with *in vitro* selection to overexpress oncogenic V12Ha-*ras* specifically in astrocytes

using the *GFAP* promoter. Ninety-five percent of the mice with moderate V12Ha-*ras* expression and activity, which did go on to germ-line transmission, also developed and died from astrocytomas of varying grades, with 50% of these mice developing their astrocytomas by 3 months. To address whether the astrocytes in astrocytoma-like lesions of GFAP-V12Ha-*ras* transgenic mice represent transformed cells, derivative astrocyte cultures demonstrated formation of astrocytomas when transplanted into immuno-deficient mice. These transgenic astrocytomas are pathologically similar to human astrocytomas. [See Figure 11] The transgenic astrocytomas exhibit additional molecular alterations associated with human astrocytomas, and this transgenic mouse astrocytoma model recapitulates many of the molecular histopathological and growth characteristics of human malignant astrocytomas in a reproducible, germ-line transmitted, and high-penetrance manner. (Ding et al., 2001)

Relevance of identifying the glioma cell of origin

Brain tumor classification with current histological criteria fails to accurately categorize patients as many patients with similar grade brain tumors have highly variable clinical outcomes. Clearly, this classification is one that at a minimum needs molecular modifiers. Defining the cell of origin, and confirming whether NSCs are indeed the cell of origin would improve not only glioma classifications, but also detection and treatment. The differential antigenic and molecular attributes of NSCs responsible for tumorgenesis could be exploited to target malignant cells prior tumor progression to clinical

presentation. Indeed, defining cell of origin could help expand the concept of chemoprevention – targeting cells in the pre-morbid state.

METHODS

Our experiments begin with labeling of transgenic mice neurogenic zones with a library containing unique genetic tags. This library was constructed and concentrated with the methods described below. Animals that were injected with this virus were sacrificed and sectioned at various time points and stained for the marker (alkaline phosphatase) carried by the library transgene. The cells carrying this transgene were selected and sequence to identify the clonality of cellular composition. Also, the experimental protocols included staining for proliferation markers and immuo-fluorescense of candidate transcription factors during assessment of neurogenesis in transgenic animals.

Creation of BOLAP plasmid

DPLl was prepared by PCR amplification of the following reaction mix: 1 ,ul of 1: 100 diluted DPL (0.6 mg/ml), 1 ~1 of DPLP (0.44 mg/ml), 1 ~1 of DPLPS (0.2 mg/ml), 5 ~1 of 2.5 mM dNTP mix, 10 ~1 of 10X PCR buffer (Boehringer Mannheim), 79 ~1 of water, and 2 pl of Taq DNA polymerase (Boehringer Mannheim). The amplification program was 93” for 2.5 min; (94” for 45 set, 70” for2 min) for 30 cycles; and 72” for 5 min. The product was phenol-chloroform extracted, ethanol precipitated, digested with AscI and XhoI, gel purified, and ethanol precipitated. Approximately 3 pg of AscIIXhoI-digested BABE-AP-X was ligated to 25 ng ofAscI-XhoI-digested DPLl in a loo-p1 ligation reaction at 16 degrees overnight. The product was phenol-chloroform

extracted, ethanol precipitated, and resuspended in 50 ~1 of Tris-EDTA (TE). Twenty microliters of ligation product was used to transform ElectroMax DHlOB (GIBCO/BRL, Gaithersburg, MD) competent cells according to the manufacturer instructions. The transformed cells are pooled. One microliter of the pooled cells was serially diluted and plated on Luria-Bertani/ampicillin (LB/amp) plates. The remainder of the pool was split into five l-liter cultures of TB containing ampicillin and kanamycin sulfate (each at 50 pg/ml) and shaken overnight at 37 degrees. BOLAP plasmid (3.7 mg) was extracted from the overnight cultures by Triton lysis, followed by purification via CsCl gradient.

Virus production

A population of double-stranded DNA molecules that includes a short degenerate region, [(G or C)(A or T)] 12, was generated by PCR amplification of a chemically constructed single-stranded oligonucleotide population of the same sequence. The oligo preparation was ligated into a retrovirus vector and a preparation of highly competent Escherichia coli was transformed. The library was then grown as a pool and a preparation of plasmids from the pool was made. The DNA of the pool was transfected into a mammalian packaging cell line to produce a library of virus particles. Eleven confluent l0-cm dishes of Bosc23 cells9 are split into fifty l0-cm dishes. The next morning, 350 pg of BOLAP DNA was combined with 1.5 ml of LipofectAMINE (GIBCO-BRL) in 25 ml of Opti-MEM (GIBCO-BRL).

The mixture was incubated for 20 min at room temperature and then added to 200 ml of Dulbecco's modified Eagle's medium (DMEM). The 50 plates are washed with

DMEM and 5 ml of the DNA-LipofectAMINE-DMEM mixture was added to each plate. The plates are incubated for 5 hr at 37 degrees. Five milliliters of 20% fetal bovine serum in DME was then added to each plate and the plates returned to the incubator overnight. The next morning the supernatant was harvested and replaced with 5 ml of 10% (v/v) fetal calf serum (FCS) in DMEM. The next morning, this supernatant was harvested. The supernatants are pooled, filtered through a 0.45~pm pore size filter unit.

Virus concentration

For lineage applications it was necessary to concentrate virus in order to achieve sufficient titer. This was due to a limitation in the volume that can be injected at any one site. Virus was concentrated by a short high centrifugation step, at 20,000 rpm for 2 hr at 4 degrees. The VSV G protein was used as the viral envelope protein to make the virions more stable, allowing high speed centrifugation. To prepare the highest titered stock for multiple experiments, we usually concentrate several hundred milliliters of producer cell supernatant. The final concentration of the viral supernatant was 1 X 10-8 CFU/ml. The concentrated stocks are tittered and tested for helper virus contamination, and stored indefinitely at -80 degrees in small (lo- to 50-~1.1) aliquots, with a drop of mineral oil to prevent dehydration.

BOLAP complexity

A test of the complexity of the library was performed by infecting NIH 3T3 cells *in vitro*, as described previously for BOLAP. (Golden and Cepko, 1996, Cepko et al., 1998) Bulk-infected NIH 3T3 cells were cloned by limiting dilution in 96 well tissue-culture plates, and the resultant colonies were fixed with 4% paraformaldehyde and stained for detection of human placental alkaline phosphatase (PLAP) activity, as described below. These cell cultures were washed with PBS and then lysed by mechanical agitation in PCR buffer (Roche, Hertforshire, UK) containing 400 g/ml proteinase K and 0.02% Tween 20. The lysate was transferred to 96 well PCR plates and covered with mineral oil. The plate was heated to 65°C for 2 hr, 85°C for 20 min, and 95°C for 10 min. Two rounds of nested PCR were performed as described below, and the 10 l of the PCR product was run on a 2% NuSieve (Rockland, ME) 1% SeaKem GTG agarose gel (Bioproducts, Rockland, ME). Wells that yielded an amplified 123 bp DNA product were later sequenced using an Exo-Pfu Cyclist kit (Stratagene, La Jolla, CA) as described below. One hundred PCR products were sequenced; none contained the same sequence.

Transplantation

Pups postnatal age 2d were removed one at a time and transplanted with inoculum of BOLAP retrovirus. BOLAP retrovirus mixed with 2 ul of trypan blue dye to facilitate visualization of intraventricular injection. Each pup was anesthetized with ice and placed above a high intensity focused light for trans-illumination. Using cranial surface landmarks, a single insertion with a micropipette was inserted into the right lateral

ventricle. Upon entry into the lateral ventricle, 4ul of inoculum was injected. Successful injection leads to visualization of blue dye within all the entire ventricular system. Subsequently, animals were warmed by heated pads and allowed to become vigorous prior to return with adult female mouse for nursing. Any pups that failed to demonstrate complete ventricular encasement with blue dye with a single micropipette insertion, were sacrificed and not used for investigation. Animals were observed up to 60 days after injection and were sacrificed at established time points to evaluate SVZ labeling (day 7 and day 14), as well as when animals became symptomatic and ill.

Sectioning

Mice were deeply anesthetized with 4% chloral hydrate (15 lL/g body weight) and perfused transcardially with 20 mL of 0.9% saline followed by 100 mL of 4% paraformaldehyde (PFA). The brains were removed from the skull and post fixed in the 20% sucrose overnight. For paraffin embedded sections, brains were then embedded in paraffin and serially cut into 4μm sections and mounted on slides. For frozen sections, brains were embedded in optimum cutting temperature (OCT) embedding medium for frozen tissue specimens. Brains were then serially sectioned using a cryostat (-20^{o}C) at 20 μm into free floating sections that were suspended in tissue collecting solution (TCS, 250 mL glycerin, 300 mL ethylene glycol, 500 mL 0.1M PB) or mounted directly onto slides. Frozen sections are stored at -20^{o}C until ready for use.

BOLAP staining

Brain sections were transferred to 12-well plates into floating nets immersed in PBS. They were then washed with fresh PBS three times for 10 minutes each. Sections were then transferred into a PBS solution with 2mM $MgCl_2$ and heated to 65^{o}C for 1 hour. Sections were then suspended in a freshly made alkaline phosphatase detection buffer (0.1 M tris-HCl, pH 9.5, 0.1 M NaCl and 0.05 M $MgCl_2$) for 5 minutes. Sections were then incubated in NBT/BCIP buffer solution (200µl of NBT/BCIP stock solution (Invitrogen) to every 10 mL of the alkaline phosphatase detection buffer) for 2 hours in the dark. Staining was performed before mounting on slides with Aquamount (VWR Scientific) with cover slips, or mounting on membrane mounted metal frame slides (MMI) for laser microdissection. Membrane slides were dried and stored in 4^{o}C.

Laser microdissection

Brain sections on membrane slides were observed using a MMI CellCut Laser Dissection Microscope. Placement of sections on membrane slides allows for laser capture of cells directly onto isolation caps without any contamination from specimen transfers. Images prior to and after laser capturing were banked for reference. Tissue samples were viewed and laser captured at varying magnifications (4x, 20x, etc.) into MMI isolation caps with adhesive lids for sequencing.

Polymerase chain reaction

Single cells or small clusters of cells containing purple NBT were laser capture microdissected. The cells are transferred to a 96-well PCR (Hybaid, Teddington, UK) plate with 10 ~1 of a proteinase K solution [50 mM KCl, 10 mM Tris-HCl (pH 7.5) 2.5 m&f MgCl, 0.02% (v/v) Tween 20, proteinase K (200 wg/ml)]. Each well was overlaid with 1 drop of light mineral oil (Sigma) and the plates are heated to 60" for 2 hr, to 85" for 20 min, and to 95" for 10 min in a Hybaid OmniGene thermocycler. The first PCR was accomplished by adding 0.15 ~1 of Taq polymerase (Boehringer Mannheim, Indianapolis, IN), 0.15 ~1 of dNTP mix (Boehringer Mannheim), 0.75 ~1 each of 10 pM oligonucleotide 0 (5'-TGTGGCTGCCTGCACCCCAGGAAAG-3') and 10 pM oligonucleotide 5 (5'-GTGTGCTGTCGAGCCGCCTTCAATG-3'), 2 ~1 of PCR buffer with MgC12 (Boehringer Mannheim), and 16.2 ~1 of H20 to each well of the lo-p1 proteinase K solution (final volume, 30 ~1). This was cycled at 93" for 2.5 min; [(94" for 45 set) (72" for 2 min)] for 40 cycles; 72" for 5 min.

The second PCR was performed with 1 ~1 of reaction product from the first PCR added to 0.25 (~1 of Taq polymerase (Boehringer Mannheim), 0.25 ~1 of dNTP mix (Boehringer Mannheim), 1~1 each of 10 pM oligonucleotide 2 (5'-GCCACCACCTACAGCCCAGTGG-3') and 10 pM oligonucleotide 3 (5'-GAGAGAGTGCCGCGGTAATGGG-3'), 2 ~1 of PCR buffer with MgC& (Boehringer Mannheim), and 14.5 ~1 of Hz0 (final volume, 30 ~1). The reaction was thermocycled at 93" for 2.5 min; [(94" for 45 set) (70" for 2 min)] for 30 cycles; 72" for 5 min. An aliquot of DNA was run on a 1.5% (w/v) agarose gel [0.75% (w/v) Seakem, 0.75% (w/v) NuSeive; FMC Bioproducts, Rockland, ME] to ensure that the appropriate insert was present.

Sequencing

DNA was extracted from tissue samples with PicoPure DNA Extraction kit (Arcturus, Mountain View, CA) as follows: 10 ul of Proteinase K extraction solution was added to the LCM sample, covered with 10 ul of sterile mineral oil, and incubated at 65^{o}C for 3 hours. The sample was centrifuged at 1000 X g for 1 min. and then incubated at 95^{o}C for 10 min. The sample was cooled to room temperature prior to use in the PCR. Two rounds of PCR amplification were performed essentially as described by Cepko et al. (1998). Primer sequences were Bolapo5: 5'CCAGGGACTGCAGGTTGTGCCCTG T3'; Bolapo6: 5'AGACACACATTCCACAGGGTCGAAG3'; Bolapo7: 5'GGCTGC CTGCACCCCAGGAAAGGAG3'; Bolapo8: 5'GGTCTCGGAAGCCCTCAGCCCAGT C3'. Ten ul of the extracted DNA samples were added to 2 ul 10X PCR Buffer with 20 mM $MgCl_2$ (Roche, Indianapolis, IN), 0.15 ul of 1.25 mM dNTP mix (Roche), 0.15 ul of 5U/ul FastStart Taq (Roche), 0.75 ul of 10 uM of each primer (Bolapo5 and Bolapo6) and 16.2 ul of nuclease-free water (Hyclone, Logan, UT). PCR amplification was performed in a GeneAmp PCR System (Applied Biosystem, St. Louis, MO) with the following conditions: 1 cycle of 93^{o}C, 2.5 min.; 33 cycles of 94^{o}C, 45 sec.; 67^{o}C, 2 min.; 72^{o}C, 2 min. and 1 cycle of 72^{o}C, 5 min. For the second round of amplification, 1 ul of the first round reaction was added to 2 ul 10X PCR Buffer with 20 mM $MgCl_2$ (Roche), 0.25 ul of 1.25 mM dNTP mix (Roche), 0.25 ul of 5U/ul FastStart Taq (Roche), 1 ul of 10 uM of each primer (Bolapo7 and Bolapo8) and 14.5 ul of nuclease-free water. Cycling conditions were: 1 cycle of 93^{o}C, 2.5 min.; 30 cycles of 94^{o}C, 45 sec.; 72^{o}C, 2

min. and 1 cycle of 72^{o}C, 5 min. Ten ul of the second round amplification products were separated on 3% agarose by gel electrophoresis and products were visualized using ethidium bromide staining to detect amplification of a 185 bp product. Four ul of the second round amplification reaction mix was used to clone the products into the pCR2.1-TOPO vector using a TA cloning kit (Invitrogen, Carlsbad, CA) following the manufacturer's protocol. Twenty-five ul of the transformation mix was plated on LB media containing 100 ug/ml ampicillin. Single, well-isolated colonies were chosen and re-streaked for isolated colonies on LB + 100 ug/ml ampicillin plates. DNA was recovered from these clones using a plasmid mini-prep DNA extraction kit (Qiagen, Valencia, CA) following the manufacturer's protocol. Bolap primer 7 was used for nucleotide sequence analysis which was performed by the University of Missouri DNA Core (Columbia, MO). The unique tag contained in each clone was determined.

BrdU staining

Mice at varying ages received intraperitoneal (i.p.) injections of 5-bromo-29-deoxyuridine (BrdU). Two hours after the last injection, mice were deeply anesthetized with 4% chloral hydrate (15 lL/g body weight) and perfused transcardially with 20 mL of 0.9% saline followed by 100 mL of 4% paraformaldehyde (PFA). The brains were removed from the skull and postfixed in the 20% sucrose overnight. They were then embedded in optimum cutting temperature (OCT) embedding medium for frozen tissue specimens. Brains were then serially sectioned using a cryostat (-20^{o}C) at 20 μm into free floating sections that were suspended in tissue collecting solution (TCS, 250 mL glycerin,

300 mL ethylene glycol, 500 mL 0.1M PB). Sections were immersed in tris buffered saline (10X TBS, 0.5M Tris Base, 9% NaCl, pH 7.6) and washed with fresh TBS 3x for 10 minutes each. Then sections were submerged and shaken in 0.6% H_2O_2 in TBS for 30 minutes before another series of washes with fresh TBS 3x for 10 minutes each. Sections were then prehybridized in formamide SSC solution (50% formamide in 2x SSC solution) at 65^{o}C for 2 hours. After incubation, sections were washed with cold 2xSSC, and then with 2M HCl at 37^{o}C for half an hour. Next sections were shaken with cold 0.1M borat buffer pH 8.5 for 20 minutes on ice. Sections were then washed thoroughly with TBS 6x for 10 minutes each, then blocked with TBS-Plus for 30 minutes at room temperature with agitation. Finally, sections were incubated with 2^{o} biotinylated anti-rat antibody (Jackson, 1:200 in TBS-Plus) at room temperature for 2 hours. While incubating sections in 2^{o} antibody, ABC Elite solution was prepared at least 30 minutes prior to use (preferably 1-2 hours) by first pouring solution A into TBS (9µl/1ml TBS) and mix, then adding solution B. Store ABC Elite solution away from the light. Sections were again washed with TBS after removing them from 2^{o} antibody incubation, then incubated with ABC Elite solution for one hour at room temperature. Sections were again washed 3x in TBS at room temperature with agitation then developed with DAB. To do this, a DAB tablet was diluted in 1ml of pyrogen free water immediately before use. Then a solution of 40 ml TBS, 12 µl 30% H_2O_2, 200 µl NiCl (8%) and 500 µl of DAB solution was made. Sections were incubated in this solution for 5 minutes then staining was observed under a microscope. After development, sections were washed 3x in tap water for 2 minutes, then in TBS 2x for 5 minutes. Sections were then mounted onto positively charged slides, then dehydrated using 100% EtOH 2x for 1 minute, then in 100% xylene

2x for 3 minutes. Finally, cover slips were applied with Aquamount (VWR Scientific) and store in 4^{o}C.

Ki-67 staining

Frozen, free floating were removed from TCS and washed with TBS 2x for 10 minutes with agitation. Sections were then submerged and shaken in 0.6% H_2O_2 for half an hour, then washed again with TBS 3x for 15 minutes with agitation. Next, a citrate buffer pH 6.0 was used for antigen-retrieval for 5 minutes on ice, and sections were then washed again with TBS 3x for 15 minutes with agitation. Sections were blocked with TBS-Plus for 1 hour with agitation at room temperature. Finally, incubated in 1^{o} rabbit anti-Ki-67 (1:100 in TBS-Plus) antibody at 4^{o} for two days. Sections were washed after 1^{o} antibody incubation with TBS 3x for 15 minutes at room temperature with agitation. Then blocked sections again with TBS-Plus for 15 minutes at room temperature before incubating with biotinylated anti-rabbit 2^{o} antibody 1:200 (Vector 1:200 in TBS-Plus) in 4^{o}C for 24 hours. While incubating sections in 2^{o} antibody, ABC Elite solution was prepared at least 30 minutes prior to use (preferably 1-2 hours) by first pouring solution A into TBS (9µl/1ml TBS) and mix, then adding solution B. Store ABC Elite solution away from the light. Sections were again washed with TBS after removing them from 2^{o} antibody incubation, then incubated with ABC Elite solution for one hour at room temperature. Sections were again washed 3x in TBS at room temperature with agitation then developed with DAB. To do this, a DAB tablet was diluted in 1ml of pyrogen free water immediately before use. Then a solution of 40 ml TBS, 12 µl 30% H_2O_2, 200 µl

NiCl (8%) and 500 µl of DAB solution was made. Sections were incubated in this solution for 5 minutes then staining was observed under a microscope. After development, sections were washed 3x in tap water for 2 minutes, then in TBS 2x for 5 minutes. Sections were then mounted onto positively charged slides, and dried overnight at room temperature. Sections were then dehydrated using 70% EtOH 2x for a few minutes, then in 96% EtOH 2x for a few minutes, then 100% EtOH 2x for a few minutes, then 100% EtOH/100% xylene 2x for a few minutes, and finally in 100% xylene 2x for 3 minutes. Finally, cover slips were applied with Aquamount (VWR Scientific) and store in 4^{o}C.

H&E Staining

First, frozen, free floating sections were removed from TCS and mounted onto positively charged cover slips. Sections were then dried on slides overnight at room temperature. We rehydrated the slides by dipping into tap water 2 to 3 times until clear. Next, slides were dipped in hematoxylin with agitation for 2 minutes, then rinsed in running tap water until the water ran clear. Next, the slides were dipped 3 times into differentiating solution with agitation, then rinsed again in running tap water for 20 seconds. Next, slides were dipped in blueing solution with agitation for 1 minute, then rinsed again with running tap water for 20 seconds. Finally, slides were dipped in eosin for 4 minutes with agitation. Slides were washed by dipping in 70% EtOH 3-5 times. We then dehydrated the slides by dipping in 70% EtOH for 5-10 minutes with agitation, then 80% EtOH for 5-10 minutes with agitation, then 95% EtOH for 5-10 minutes with

agitation, 100% EtOH 2x for 5-10 minutes with agitation, then 100% EtOH for 10-20 minutes with agitation. Slides were cleared through 100% xylene 3x with agitation for 5-10 minutes and left in xylene before affixing cover slips. Finally, cover slips were applied with Aquamount (VWR Scientific) and stored.

Immunohistochemistry

In vivo (Free floating sections): Frozen free floating sections were removed from TCS and wash in TBS 3x for ten minutes with agitation. Sections were then prehybridized in formamide SSC solution (50% formamide in 2x SSC solution) at 65^{o}C for 2 hours. After incubation, sections were washed with cold 2xSSC, and then with 2M HCl at 37^{o}C for half an hour both with agitation. Next sections were shaken with cold 0.1M borat buffer pH 8.5 for 20 minutes on ice. Sections were then washed thoroughly with TBS 6x for 10 minutes each, then blocked with TBS-Plus for 30 minutes at room temperature with agitation. Sections were then incubated in primary antibody solution (primary antibody diluted with TBS-Plus) at 4^{o}C for 48 hours. After primary antibody staining sections were washed with TBS for 10 minutes 3x for ten minutes with agitation, and incubated in secondary antibody solution (secondary antibody diluted with TBS-Plus) for two hours protected from light at room temperature. Sections were then washed with TBS for 10 minutes protected from light with agitation. Next, sections were shaken with DAPI for nuclear staining while being washed in TBS again for 10 minutes. Sections were then washed one last time after DAPI staining in TBS for 10 minutes with

agitation. Sections were then mounted onto slides and cover slipped with Aquamount (VWR Scientific), and stored in 4^{o}C protected from light.

In vitro (cells)

Sterile cover slips were transferred using tweezers under the hood into 24 well plates. 250 µg of polyporin (rat tail protein) per 50 mls of pyrogen free water was added to the cover slips in wells. Cover slips were incubated for one hour at 37^{o}C. Cover slips were then washed in wells with pyrogen free water. Polyporin and pyrogen free water were aspirated from wells, and 40-45µgs of laminin for every 50mls of phosphate buffered solution (PBS) were added to wells. Cover slips were incubated for two hours at 37^{o}C. The laminin solution was aspirated out, and cover slips were stored in a 37^{o}C incubator until ready for use. Cells were pipetted out of flasks into 15ml falcon tubes and spun down at 1000rpm for 10 minutes. Supernatant was poured off, and approximately 4 ml of sterile D-PBS (w/o Ca and Mg) was added to cell pellet. Cell mix was lightly vortexed to create cell suspension before being spun down once again at 800rpm for 5 minutes. Supernatant was poured off and cell pellet was incubated in 2ml of Accutase to dissociate neurospheres. Cell pellet was shaken vigorously to create cell suspension before being incubated at 37^{o}C for 15-20 minutes depending on average neurosphere diameter. Cell mix was then spun down at 800rpm for 5 minutes. After pouring off supernatant Accutase, 1-5ml of neural basal media (w/EGF and FGF) was added, and a single cell suspension was created with a light vortex. 15µl of trypan blue was added to 15µl of cell mix and injected onto a hemocytometer cell counting chamber to obtain a

cell mix dilution. Cell mix was then diluted to obtain an appropriate dilution of cells/1ml of media/well, and 1ml of diluted cell mix was added per well of 24 plate with polyporin and laminin coated cover slips. Cells were allowed to adhere to cover slips for 48 hours in the 37^{o}C incubator. Media was then flushed out of wells, and 4% paraformaldehyde was added and cover slips were stored in 4^{o}C for 15 minutes for fixation. PFA was aspirated out and cover slips were washed with PBS 3 times for 10 minutes with agitation. Cover slips were then blocked with PBS blocking solution for half an hour with agitation. Primary antibody solutions were prepared with appropriate concentrations diluted in PBS blocking solution, and an incubation chamber was prepared to insure that adequate moisture levels were maintained. For every cover slip around 100µl of antibody solution was dropped onto parafilm, and cover slips were removed from wells and carefully inverted onto the solution to stain the cells with primary antibody. Cover slips were incubated for two nights at 4^{o}C. Cover slips were then placed back into wells with cells facing upward and shaken with PBS 3x for 10 minutes to wash off primary antibody solution. 300-400µls of secondary antibody solution (secondary antibody diluted in PBS blocking solution) was added per well, and cover slips were incubated in secondary for two hours at room temperature with agitation protected from the light. Secondary solution was then aspirated out and cover slips were washed with PBS for 10 minutes with agitation protected from the light. Cover slips were then washed once more with PBS with agitation for 10 minutes this time with DAPI (1:500) for nuclear staining. Finally, cover slips were washed once more with PBS for 10 minutes with agitation before cover slips were removed from wells to be mounted. Cover slips were inverted onto a drop of Aquamount (VWR Scientific) on a slide and stored at 4^{o}C.

Neurosphere isolation

Papain solution was prepared by diluting a spatula tip's worth of papain (Sigma) in 5mls of papain activation buffer (10 ml of 0.01M EDTA, 0.1 ml of 0.06 M mercaptoethanol, 10ml of 0.05M cysteine*HCl, diluted with 70ml of reagent grade water), and solventing for 30 minutes at 37^{o}C. 1ml of solvented papain solution was then diluted with 4mls of Hanks Balanced Salt Solution (w/out Ca 7 Mg and phenol red) into a 50ml falcon tube before being mixed and sterile filtered with a 22µm Millipore filter and 10ml syringe into a 15 ml falcon tube. 3-4mls of sterile Hanks Balanced Salt Solution was added to a petri dish for dissection and each falcon 15ml collection tube, and kept on ice until ready for use. All dissection equipment was cleaned with 20% butadiene diluted in PBS and washed with ethanol before use. Mice were deeply anesthetized with 4% chloral hydrate (15 lL/g body weight) before cervical dislocation. The brains were then removed wholly intact in a sterile fashion and placed on a 1mm coronal mouse brain cutting matrix (WPI). 1mm slices of the brain cut and deposited into the dissection dish. The subventricular zones were then dissecting out under a dissecting microscope and placed in collection tubes. Hanks Balanced Salt Solution was then pipetted out under the hood and tissue was incubated in 2-3mls of diluted papain solution for 30 minutes at 37^{o}C. Tissue samples were then loosened physically with a 1ml pipet tip to mix the tissue in papain under the hood. Samples were spun down at 1000rpm for 10 minutes. The diluted papain solution supernatant was removed and replaced with 1ml of neural basal media (w/epidermal growth factor EGF, and fibroblast growth factor FGF). Tissue was

lightly vortexed to create a single cell suspension before 1 more ml of neural basal media (w/EGF and FGF) was added. 1ml of cell mix plus an addition ml of neural basal media (w/EGF an FGF) was added per well on a 24 well plate. Cells were incubated for 2-7 days until neurospheres formed, then passaged and expanded to more wells with the addition of more neural basal (w/EGF and FGF) media. Cells were then similarly grown and expanded and eventually combined into flasks or frozen for storage.

Single cell neurosphere formation assay

Cells were pipetted out of flasks into 15ml falcon tubes and spun down at 1000rpm for 10 minutes. Supernatant was poured off, and approximately 4 ml of sterile D-PBS (w/o Ca and Mg) was added to cell pellet. Cell mix was lightly vortexed to create cell suspension before being spun down once again at 800rpm for 5 minutes. Supernatant was poured off and cell pellet was incubated in 2ml of Accutase to dissociate neurospheres. Cell pellet was shaken vigorously to create cell suspension before being incubated at 37^{o}C for 15-20 minutes depending on average neurosphere diameter. Cell mix was then spun down at 800rpm for 5 minutes. After pouring off supernatant Accutase, 1-5ml of neural basal media (w/EGF and FGF) was added, and a single cell suspension was created with a light vortex. 15µl of trypan blue was added to 15µl of cell mix and injected onto a hemocytometer cell counting chamber to obtain a cell mix dilution. Cell mix was diluted until a 1 cell/200µl of neural basal media (w/EGF and FGF) dilution was obtained. 20mls of this mix was prepared for each 96 well plate. Using a multipipet and mulipipet well, 200µl of this mix was added per well of a 96 well plate

to deposit a single cell per well. Cells were then grown for 2-7 days with or without treatment of map kinase blockers before neurosphere forming wells were counted, and a % of neurosphere formation and/or average diameter of neurospheres figure was obtained.

Proliferation assay

A sterile 96 well plate was prepared by first washing once with PBS under the hood. The plate was then coated with polyporin (150µl to 25ml of PBS), distributing enough to completely cover the bottom of each well. Polyporin was then removed, and the plate was again washed with PBS. The plate was then coated with laminin (40µl to 25ml of PBS), distributing enough to completely cover the bottom of each well, and incubated at 37^{o}C for one hour. Cells were pipetted out of flasks into 15ml falcon tubes and spun down at 1000rpm for 10 minutes. Supernatant was poured off, and approximately 4 ml of sterile D-PBS (w/o Ca and Mg) was added to cell pellet. Cell mix was lightly vortexed to create cell suspension before being spun down once again at 800rpm for 5 minutes. Supernatant was poured off and cell pellet was incubated in 2ml of Accutase to dissociate neurospheres. Cell pellet was shaken vigorously to create cell suspension before being incubated at 37^{o}C for 15-20 minutes depending on average neurosphere diameter. Cell mix was then spun down at 800rpm for 5 minutes. After pouring off supernatant Accutase, 1-5ml of neural basal media (w/EGF and FGF) was added, and a single cell suspension was created with a light vortex. 15µl of trypan blue was added to 15µl of cell mix and injected onto a hemocytometer cell counting chamber

to obtain a cell mix dilution. A target density of 3000 cells/200µl of cell mix/well was reached after dilution. A multipipet and multipipetting well was utilized to add 200µl of cell mix/well. Cells were allowed to adhere to plate for 48 hours in the 37^{o}C incubator. Map kinase blockers were then added at a dilution of 3µl/well along with an added 100µl of neural basal media (w/EGF and FGF) per well. Cells were incubated for 3 more days and then the CyQuant Cell Proliferation Assay (Molecular Probes) was conducted. 11ml of 1x Hanks Balanced Salt Solution buffer was prepared per 96 well plate by diluting 2.2ml of 5x Hanks Balanced Salt Solution with 8.8ml of deionized water. 22µl of dye reagent was then added per every 11ml of 1x Hanks Balanced Salt Solution buffer. Media was drawn from plates using a multipipet. 100µl of 1x Hanks Balanced Salt Solution with dye reagent was added to each well using a multipipet. Plates were incubated for 1 hour at 37^{o}C protected from the light. Then using the Turner BioSystems TD-700 Laboratory Fluorometer with the Molecular Probes CyQuant Cell Proliferation Assay the plates were analyzed for density of cells in cell culture.

Differentiation

Sterile cover slips were transferred using tweezers under the hood into 24 well plates. 250 µg of polyporin (rat tail protein) per 50 mls of pyrogen free water was added to the coverslips in wells. Coverslips were incubated for one hour at 37^{o}C. Cover slips were then washed in wells with pyrogen free water. Polyporin and pyrogen free water were aspirated from wells, and 40-45µgs of laminin for every 50mls of phosphate buffered solution (PBS) were added to wells. Cover slips were incubated for two hours at

37°C. The laminin solution was aspirated out, and cover slips were stored in a 37°C incubator until ready for use. Cells were pipetted out of flasks into 15ml falcon tubes and spun down at 1000rpm for 10 minutes. Supernatant was poured off, and approximately 4 ml of sterile D-PBS (w/o Ca and Mg) was added to cell pellet. Cell mix was lightly vortexed to create cell suspension before being spun down once again at 800rpm for 5 minutes. Supernatant was poured off and cell pellet was incubated in 2ml of Accutase to dissociate neurospheres. Cell pellet was shaken vigorously to create cell suspension before being incubated at 37°C for 15-20 minutes depending on average neurosphere diameter. Cell mix was then spun down at 800rpm for 5 minutes. After pouring off supernatant Accutase, 1-5ml of neural basal media (w/ EGF and FGF) was added, and a single cell suspension was created with a light vortex. 15µl of trypan blue was added to 15µl of cell mix and injected onto a hemocytometer cell counting chamber to obtain a cell mix dilution. Cell mix was then diluted to obtain an appropriate dilution of cells/1ml of media/well, and 1ml of diluted cell mix was added per well of 24 plate with polyporin and laminin coated cover slips. Map kinase blockers were then added in desired quantities to wells to investigate the effects of inhibition on cell growth and differentiation. Cells were allowed to adhere to coverslips and grown and/or differentiated for a predetermined treatment period. Media was then flushed out of wells, and 4% paraformaldehyde was added and cover slips were stored in 4°C for 15 minutes for fixation. PFA was aspirated out and cover slips were stored in PBS at 4°C.

autoMACS cell separation

Target cell mix was emptied into 50ml falcon tubes and spun down at 800 rpm for 5 minutes. Supernatant media was poured off and replaced with 10 ml of D-PBS (w/o Ca and Mg) and spun down again at 800rpm for 5 minutes. Supernatant PBS was poured off and replaced with Accutase to dissociate neurospheres. Cells were shaken vigorously to create a cell suspension before being incubated for 15-30 minutes (depending on average neurosphere diameter) at 37^{o}C. Cells were spun down again at 800rpm for 5 minutes after incubation, and the supernatant Accutase was poured off and replaced with 4mls of separation buffer (autoMACS wash solution with .5% BSA). Cells were shaken vigorously to create a single cell suspension before being spun down again at 800rpm for 5 minutes. Supernatant separation buffer was poured off and replaced with primary antibody solution (180µl separation buffer, 20µl FC block, 6-10µl CD133-PE). Cells were shaken vigorously to create a single cells suspension and incubated in primary antibody for one hour at 4^{o}C. From this step on, everything was done at 4^{o}C. Cells were then spun down at 800rpm for 5 minutes and resuspended in separation buffer twice. After aspirating off all the buffer supernatant, cells were then dissolved with PE beads (1:5 beads to separation buffer dilution). 100µl bead mix was added to sample, mixed with a 1ml pipet, and incubated at 4^{o}C for 30 minutes. 4ml of separation buffer was then added per sample, and each sample was then spun down at 800rpm for 5 minutes. autoMACS Separator and autoMACS Columns and Filters were then set up, and washed with separation buffer. Columns were never allowed to run dry. Media was aspirated out of sample tubes, and 1ml of separation of buffer was added to each sample. Samples were deposited and mixed in the autoMACS filter to ensure cells trained through autoMACS columns. Separation buffer was added to wash out all negative cells into collection tubes.

Columns were removed from antoMACS Separator and flushed with 1ml of separation buffer and plunger to obtain positive fraction of cells. Cell fractions were then spun down, and used as needed.

Media preparation

Neural Basal Media

1 bottle of 500 ml of neural basal media (-L-Glut)

Add 10 ml B27 supplement w/o vit A

Add 5 ml 100x penicillin streptomycin

Add 500 μm of FGF and EGF

Add 5 ml of L-Glut

EGF and FGF

We made 200 microgram/ml preparations of both (FGF comes as 50 micrograms/ml and EGF comes as 0.2 milligrams/ml). FGF was combined with 5mM Tris-HCl, pH 7.4. EGF was combined with 10mM HAc + 0.1% BSA. Diluent solutions were sterile filtered and a portion of the sterile filtered solution was added directly to EGF or FGF. EGF and FGF were mixed with diluents with a 1ml pipet, then fully diluted. Solutions were then aliquotted to 1ml solutions in sterile eppendorf tubes and stored at -20^{o}C.

RESULTS

SVZ cells in GRASp53+/+ and GRASp53+/- mice are multipotent and capable of differentiation into three major neural lineages (neurons, astrocytes, oligodendrocytes)

We selected the GRASp53 genetically engineered mouse model because the transgenic astrocytomas exhibit additional molecular alterations associated with human astrocytomas, and this transgenic mouse astrocytoma model recapitulates many of the molecular histopathological and growth characteristics of human malignant astrocytomas in a reproducible, germ-line transmitted, and high-penetrance manner. By having high frequency of glioma formation this allowed us to lineage map the brain tumors and those transgenic mice that failed to develop gliomas were used as controls. The effects of the transgene on the fundamental properties of neurogenic regions needed to first be elucidated.

First, we demonstrated that the NPCs from the P30 SVZ of the GRASp53+/+ and GRASp53+/- mice are multipotent. Similar to normal non-transgenic animals, the cells isolated from the SVZ of these mice form neurospheres and differentiate into multiple cell types constituting the neural lineage, but do not remain undifferentiated and immortalized, as would be expected of transformed cells (See Figure 12).

A total of 3 adult (d30) GRASp53+/+ and 3 adult (d30) GRASp53+/- mice were sacrificed when they displayed the classical features or neurological deterioration (circling, hemiplegia). These signs were used as a method of detecting animals with gross glioma formation, due to the presence of mass effect leading to alterations in motor

function. The lateral walls of the lateral ventricle of the mice were enzymatically dissociated in 0.8 mg/ml hyaluronidase and 0.5 mg/ml trypsin. The dissociated cells were strained through a 70-μm strainer,and cultured in media containing 20 ng/ml EGF and 20ng/ml bFGF. Through a series of 2-5 passages, the non-proliferating cells were eliminated and the proliferative neurospheres were isolated. These neurospheres were identified on the basis of their ability to form anchorage independent spheres of cells that maintained their proliferative and undifferentiated state. (Singec et al., 2006) Additional immunological criteria validated their undifferentiated state by examining the expression of primitive neuroepithelial markers such as Nestin, Sox2, Mushashi. (Maurer and Kuschinsky, 2006) Nestin is a Class VI intermediate filament expressed in the developing CNS in early embryonic neuroepithelial stem cells. This protein has been widely used as a predominant marker for stem / progenitor cells, glioma cells, and tumor endothelial cells in the mammalian CNS. In mammals, the Musashi family is important for cell fate determination, playing roles in maintenance of the stem-cell state, differentiation and tumorigenesis. Musashi1 (also known as Msi1), is selectively expressed in neural progenitor cells, including neural stem cells. SRY-related HMG-box 2 (SOX2) is a transcription factor involved in the regulation of embryonic development and only found in primitive cells Together, these three markers identify NSCs **.**

Typical of undifferentiated NPCs, the cells stopped proliferating and differentiated into the glia and neurons upon removal of the mitogens. The presence of the oligodenroglial-specific marker GalC, astrocytic maker GFAP, and neuronal specific marker B-tubulin verified their differentiation state. (Zhu and Dahlström, 2007) This demonstrates the multipotency of the neurosphere forming cells, which establishes them

as NPCs. In addition, 3 non-transgenic animals were treated in an identical fashion to serve as controls. In these animals, cells isolated from the SVZ formed neurospheres in the presence of mitogens, and differentiated upon the removal of mitogens. In all cases of the experimental and control animals, there was no immortalization or continued proliferation of the differentiated cells. Together, this data indicates that the NPCs isolated from the SVZ of the GRASp53+/+ and GRASp53+/- mice are not transformed or lineage committed, as one would expect if the tumors observed in the GRASp53+/+ and GRASp53+/- mice were contiguous with the SVZ or if the SVZ was populated with tumor cells.

Enhanced neurosphere forming ability of SVZ NPCs in GRASp53+/+ and GRASp53+/- mice

Since NSCs are characterized by their ability to differentiate into the cells that comprise the neural lineage (neurons, astrocytes, and oligodendrocytes), the ability of undifferentiated neurosphere forming cells isolated form the SVZ to differentiate into these lineages is an accepted measure of multipotentiality. While in vitro, NSCs are maintained in their undifferentiated state as floating aggregates (neurospheres) in media with mitogens (bFGF and EGF); upon removal of these mitogens the neurospheres differentiate and become adhesive to the substrate. This neurosphere assay was applied to the SVZ cells of GRASp53+/+ and GRASp53+/- mice. Mice that did not have tumors (n=3 each) were sacrificed at ages 30 - 45 days and evaluated for the ability to generate neurospheres. Cells from the SVZ were microdissected and plated as single cells in 96

well plates, as well as 10 cells per well. At 14 days, neurospheres (any aggregate three dimensional floating cell cluster >10um and >20um) were counted. For each initial cell plating density (1,10) and for each defined minimum size, the cells in an aggregate cluster were categorized as a neurosphere (>10um and >20um). GRAS animals contained greater neurospheres in culture than the WT animals, most likely due to the proliferative effects of the oncogene in the transgenic animal (See Figure 13). Interestingly, the GRASp53+/- mice formed significantly more neurospheres (at all sizes and plating densities) than the GRASp53+/+ mice. The differences in proliferation seen are similar to prior work in which cells that demonstrated anchorage independent growth were more likely to form tumors when transplanted. Later experiments will detail the tumor initiating potential of GRASp53+/+ and GRASp53+/- cells.

Tumor cells from adult (p30-p45) GRASp53+/+ and GRASp53+/- mice exhibit normal differentiation pattern upon mitogen withdrawal

Similar to NSCs, tumor cells often have the characteristics of undifferentiated cells due to their oncogenic plasticity and show significant heterogeneity in their state of differentiation. Specific markers of differentiation for various cell types are used to identify their lineage, as described previously. We quantitatively measured the differentiation state and response to withdrawal of mitogens by gliomas from 6 GRASp53+/+ and 6 GRASp53+/- mice, which although not consistently, predictably form gliomas by day 60. (Ding et al., 2001) This in vitro percentage of differentiated cells

under proliferative conditions (mitogens present) and differentiation conditions (mitogens absent) can be compared to assay the differentiation potential of cells within the tumor.

To do this, mice were sacrificed randomly at day 45 to identify tumor bearing mice. The gliomas from tumor bearing mice were microdissected and cultured with mitogens until tumor sphere formation, as done for cells from the SVZ. Upon withdrawal of EGF and bFGF as before, most of the cells from the tumorspheres differentiated and became adherent. Subsequent staining for neurons (B-Tubulin for immature, Map 2ab for mature), astrocytes (GFAP) and oligodendrocytes (NG2 for immature, GalC for mature) revealed their state of differentiation. Cells that remained undifferentiated were determined by staining for nesting and Musashi-1 as before. As expected, and similar to NSCs, GRAS tumorspheres are multipotent. In contrast to the neurosphere assay, there was no difference between the GRASp53+/+ and GRASp53+/- mice, indicating that p53 status likely has little bearing on the ultimate differentiation state of the tumor cells upon removal of mitogens (See Figure 14). Under proliferative conditions, GRAS NPCs are more proliferative and form more neurospheres in a p53 dependent fashion. However, this most likely does not affect the final differentiation of the tumor cells, as shown in this neurosphere assay using cells derived from tumors.

Increased BrdU labeling in SVZ and decreased BrdU labeling in RMS in P10 and P30 GRASp53+/+ and GRASp53+/- mice compared to wild type controls

Being in vitro assays, the neurosphere and differentiation assays may be subject to artifacts due to the contrasts between the in vitro environment and in vivo environment.

To better evaluate the effect of p53 status in proliferation in vivo, in situ evaluation of proliferative state of cells in the SVZ was determined using BrdU incorporation in vivo. Likewise, proliferation was assayed in comparable cells in the RMS, which consists of cells migrating from the SVZ. (Murase and Horwitz, 2004) To accomplish this, 1mg per mouse bromodeoxyuridine (BrdU) was administered IP to the mice 24 hours before sacrifice, and sections of the brain containing the SVZ and RMS were assayed for the number of cells that actively incorporated BrdU. Since the BrdU nucleotide analogue is only taken up by cells which are undergoing active DNA replication, it is widely considered to be correlative to the active proliferative state of the cells. This assay was used to determine the amount and distribution of BrdU labeling on mitotically active cells in the SVZ of 8 GRAS animals (4 $p53^{+/+}$ and 4 $p53^{+/-}$) at ages 10 and 30 days. Non-transgenic animals were treated in an identical manner at age 10 and 30 to serve as a control. In coronal sections of all the animals, the characteristic labeling of the SVZ on the lateral ventricular boundaries was seen and the RMS was identified as it extends from the SVZ toward the olfactory bulbs (See Figure 15).

These findings were quantified. The SVZ of non-transgenic mice contained 63,000 BrdU+ cells/ mm2 and 59,000 BrdU+ cells/mm2 for animals age 10 days and 30 days, respectively. In comparison, GRASp53+/+ animals contained 83,000 BrdU+ cells/mm2 and 70,000 BrdU+ cells/mm2, GRASp53+/- contained 84,000 BrdU+ cells/mm2 and 73,000 BrdU+ cells for animals age 10 days and 30 days, respectively. The RMS of non-transgenic mice contained 81,000 BrdU+ cells/mm2 and 98,000 BrdU+ cells/mm2 for animals age 10 days and 30 days, respectively. The RMS of GRASp53+/+ animals contained 59,000 BrdU+ cells/mm2 and 41,000 BrdU+ cells/mm2, GRASp53+/-

contained 56,000 BrdU+ cells/mm2 and 36,000 BrdU+ cells for animals age 10 days and 30 days, respectively. This quantification of BrdU labeling in non-transgenic and GRASp53+/+ and GRASp53+/- animals clearly shows an increased proliferation of GRASp53+/+ and GRASp53+/- SVZ cells compared to WT SVZ at age 10 days and 30 days.

This data is consistent with the observed effect of the $HRas^{V12}$ transgene and p53 alelle deletion on proliferation in the SVZ neurosphere eassay. However, when the RMS was quantified there is significantly less BrdU labeling with GRASp53+/+ and GRASp53+/- animals both at age 10 days and 30 days, with the difference greatest at 30 days. This reciprocal relationship between SVZ BrdU incorporation and RMS BrdU incorporation in GRASp53+/+ and GRASp53+/- animals compared to the non-transgenic animals indicates that there is a potential effect of the transgene/KO in the GRASp53+/+ and GRASp53+/- in either RMS cells proliferation or alternatively, RMS migration, which would reduce the number of migrating and thus BrdU positive cells.

To examine this closer, the degree of BrdU staining in the SVZ of the non-transgenic animals was evaluated and compared to the transgenic animals. It was found to be contiguous with cells comprising the RMS at day 10 or day 30; but not in the GRAS mice (in both GRASp53+/+ and GRAS53+/- animals), which showed a dramatic decrease in proliferative cells in the RMS at both time points compared to the SVZ. These results indicate that the difference is due to the presence of the HRas oncogene rather than the p53 status. Thus, the changes in proliferation observed in vitro using the neuropshere assay are correlative in vivo in the developing brain but not the adult brain. The inverse difference in proliferation between the RMS and SVZ in the GRAS mice

may be a biological response to the increased proliferative potential of the GRAS cells; but this is not fully understood.

Increase in apoptosis is likely to maintain the homeostasis (cell numbers) in SVZ of GRASp53+/+ and GRASp53+/- mice

Because net proliferation in vivo and in vitro is always a balance between cell division and cell death due to apoptosis, the in vivo apoptotic and proliferative component was examined in the GRASp53+/+ and GRASp53+/- mice. To accomplish this, the SVZs were microdissected from 6 day 30 GRAS (both $p53^{+/+}$ and $p53^{+/-}$) and from 6 day 30 control (non-transgenic) mice as described previously. To analyze proliferation and apoptosis in the same tissue section, the animals were treated with BrdU as before, and BrdU incorporation was examined and the section subjected to Terminal deoxynucleotidal-transferase-dUTP Nick End Labeling (TUNEL) as a maker of apoptosis. These methods were used to quantify both proliferation and cell death in vivo (See Figure 16). Since the in vitro experiments demonstrated increased proliferation of isolated SVZ and tumor cells from GRASp53+/+ and GRASp53+/- versus control animals, this method sought to explain the balance between proliferation and apoptosis.

As the data demonstrates in Figure 15, there is an increase in proliferation (BrdU) in the SVZ at day 30, in the GRAS mice compared to the control (non-transgenic) mice. When evaluating rates of apoptosis, the GRASp53+/+ and GRASp53+/- mice also have an increase in the cell death in comparison to the SVZ cells of non-transgenic mice. We believe this may explain the histological findings of the GRASp53+/+ and GRASp53+/-

SVZ maintaining normal cytoarchitectural characteristics. However, the net difference between increased proliferation and increases apoptosis is increased in GRASp53+/+ and GRASp53+/- SVZ cells. Why this doesn't lead to histological changes in the transgenic animals remains to be understood.

SVZ-resident cells, but not cortex or olfactory bulb-resident cells from tumor bearing GRASp53+/+ and GRASp53+/- mice initiate tumors in syngeneic mice.

To determine the tumor initiating capability of the SVZ cells forming neurospheres isolated from the SVZ of GRASp53+/+ and GRASp53+/- mice , these cells were re-implanted into the right cereberal hemisphere of syngeneic (non-transgenic), immunocompetent mice and allowed to form tumors. The mice were then sacrificed at day 14 after implant or when the mouse begins to exhibit signs of tumor growth. To accomplish this, isolated GRASp53+/+ and GRASp53+/- SVZ cells were grown as neurospheres (in 3-D aggregate clusters) as before from 4 different animals that were tumor bearing. Subsequently, the cells comprising the neurospheres were inoculated into the right cerebral hemisphere of immune-competent mice. With transplantation of as little as 4000 GRASp53+/+ and GRASp53+/- tumor bearing SVZ cells, 25% of the transplanted mice developed gross tumors within 2 weeks. With greater than 40,000 cells implanted, tumors formed 100% of the time by 2 weeks (See Figure 17).

As a negative control for this assay, the olfactory bulb, cortical cells were microdissected from the same GRASp53+/+ and GRASp53+/- tumor bearing animals and transplanted into the right cerebral hemisphere of syngeneic immunecompetent mice.

In this transplantation assay, no tumors developed in the transplanted animals, indicating that the SVZ cells from the tumor bearing mice but not other NSC derived cells in the same mouse have tumorgenic potential. Most importantly, isolated SVZ neurospheres from non-transgenic mice from 3 different animals were implanted into syngeneic, immunocompetent mice, in an identical manner, did not from tumors. This transplantation assay demonstrates the ability of SVZ cells from the GRASp53+/+ and GRASp53+/- mice, cultured as neurospheres, to initiate and recapitulate gliomas; but not from the control mice (both WT and non-tumor bearing GRASp53+/-). Upon histological evaluation, transplanted SVZ cells demonstrated the same archetypal histopathological features as the original tumor. This data indicates that the tumor initiating component of the GRASp53+/+ and GRASp53+/- mice is indeed the neurosphere forming population of the SVZ; which is the canonical NSC. Furthermore, this tumor forming component is only present in the GRAS mice, indicating that oncogenic transformation may begin in the NSCs of the SVZ, in these genetically manipulated animals. This suggests that the greatest role is the intrinsic capacity of the SVZ cells in these GRASp53 animals, and a smaller role for the microenvironment.

Intraventricular injection of BOLAP retrovirus infects NPCs in SVZ

The BOLAP retrovirus is a retroviral tagging library which uniquely and independently labels mitotically active cells. The library contains approximately $1*10^8$ unique genetic tags, with only one tag per virus, located within the terminal repeats (LTRs) of the viral construct. Additionally, the viral construct encodes for alkaline

phosphatase (AP), effectively labeling each transduced cell with a unique tag that is traceable through PCR and renders the cells trackable through alkaline phosphatase staining in tumor sections. Furthermore, since retroviral genome is unable to enter the nuclear pore, it only transduces actively proliferating cells which no longer have a nuclear envelope due to mitosis. Finally, due to the nature of retrovirus, it cannot transduce cells with a high multiplicity of infection (MOI). For these reasons, the BOLAP retrovirus is a unique tool created to only label proliferating cells with a single copy of a unique and traceable genetic tag and marker amenable for use in immunohistochemical techniques. Thus, injection of a modest titer of BOLAP virus into the ventricles of the developing mouse pups results in efficient but selective tagging of NSCs in the subventricular zone.

To label the NSCs of GRAS animals (p53 +/+ and p53 +/-) using the BOLAP library, pups age 2d were injected in the right lateral ventricle with 2ul of BOLAP retrovirus. Upon successful entry into the right lateral ventricle, encasement of the entire ventricular system was visualized (See Figure 18, Part A). This was accomplished by sacrificing injected animals at day 7 and day 14, and evaluating sections of the SVZs with alkaline phosphatase staining. This methodology demonstrated transfection of the SVZ as well as the subcallosal zone. To further evaluate that the NPCs were specifically tagged using BOLAP sections of olfactory bulbs (OB) from injected animals demonstrate alkaline phosphatase cells, further verifying that the SVZ is successfully transfected (See Figure 18, Part B). Since the SVZ cells migrate via the RMS to the olfactory bulb, positive AP staining occurred in cells in the SVZ, through the RMS and in the OB.

These data demonstrate the ability of the BOLAP virus to efficiently and selectively tag the NSC component through intraventricular injection.

Oncogenic H-Ras in GFAP-positive glial cells induces astrocytoma in mice

Although the GRAS animals are well established to reliably form gliomas, the effect of p53 on the grade of glioma is entirely unknown. To determine the aggressiveness of the tumors formed, the entire population of GRAS animals was followed to establish survivability curves. The GRASp53 +/+ had a survival probability of or 55% by 12 weeks, whereas the GRAS p53+/-, mice had a survival probability of 35% by 12 weeks. The GRAS p53-/- did not survive long enough to assay, and the limited subset of data is included in the graph (See Figure 19). The interplay of both genetic changes (GRAS and p53) in contributing to tumor formation can not be separated and must be considered collectively.

Robust alkaline phosphatase expression in SVZ and glioma

In addition to uniquely labeling the transduced cells with one of $1*10^8$ unique genetic tags, the BOLAP virus also encodes for the alkaline phosphatase (AP) gene. This allows sections containing BOLAP labeled cells to be tracked. Using this methodology, GRAS mice injected with BOLAP retrovirus were reared until ages 30 days to 60 days. For this study, 6 GRAS p53+/- animals which displayed neurological deterioration and were sacrificed for analysis. As a control, the same age matched non-transgenic animals

were labeled with BOLAP and sacrificed for analysis**.** Staining for AP revealed what appears to be selective labeling of the SVZ in 100% of the animals examined. Identical results were seen in age matched control animals.

The 6 GRASp53+/- mice also had robust labeling in the glioma (See Figure 20). Serial sections though the entire brain demonstrated persistent AP positive cells in the neurogenic zones, specifically the SVZ, subcallosal zone, hippocampus, and the OB. The cortex did not label significantly, with few cortical cells being AP positive. These cortical findings are consistent with those seen in non-transgenic animals.

This data supports the observation that the BOLAP virus is selectively labeling the mitotically active cells in the SVZ, as intense staining is seen in the anatomical structures that support NSC populations. As may be expected, the cerebral hemispheres, cerebellum, and brain stem demonstrated very few AP positive cells, and at the same frequency as in control mice. This is most likely due to the typically low NSC content in these anatomical structures.

In contrast to the control animals, that lack gliomas, 100% of the cortical gliomas in the mice examined are robustly positive for AP. The ability of gliomas to exist some distance from the SVZ could be explained by the innate property of NSC to undergo asymmetric cell division and is described further in the discussion. These mice all had one dominant glioma in the cortex, which was discernible by gross examination and confirmed histologically. This observation shows the presence of BOLAP labeled NSC derived cells in the gliomas that originated from the SVZ. Furthermore, the high percentage of AP positive cells within the tumor indicates that a population of BOLAP positive cells contributed to the formation of the tumor. Although the location and

intensity of staining is highly suggestive that the tumors arose, at least in significant portion, from the SVZ, it is not definitive proof that the tumor cells are progenitors of the originally labeled SVZ cells. However, since the BOLAP library allows direct tracking of the SVZ labeled in these GRAS mice and the gliomas that developed as these mice matured both contain AP positive cells that were also identified through the unique oligonucleotide sequences that are part of the transfected plasmid. The strength of this determination undoubtedly demonstrates that a significant portion of the gliomas in the GRAS mice are constituted of cells from the SVZ. However, distinguishing which of the mitotically active cells residing in the SVZ is responsible for tumor formation will require further investigation.

Alkaline phosphatase labeled regions are gliomas in GRASp53+/- mice

Although both the GRAS p53+/- mice reliably form tumors, and the tumors from the examined animals that were injected with BOLAP virus all contained a large population of AP positive cells, we sought to verify that the lesions containing the AP positive cells were indeed tumors. To evaluate this, 6 GRASp53+/- with tumors were sectioned and stained using the alkaline phosphatase reaction. Multiple sections were taken through the brain and sections incorporating the gross tumor were separated for analysis. Regions with robust focal staining were proven to be gliomas based on staining and histopathology of adjacent, non treated H&E sections and BrdU labeling (See Figure 21). As expected, the tumor sections had had markedly increased BrdU labeling compared to the same brain region in non-transgenic mice. Thus, several independent

methods demonstrated that the vast majority of cells in the areas positive for AP were actively proliferating, consistent with the transformed, aggressive phenotype of AP-positive tumor cells.

Importantly, 100% of the GRASp53+/- mice with tumors had robust AP positive labeling. All GRASp53+/- animals that were injected with the BOLAP retrovirus as pups were followed into maturity, and those that developed tumors were consistently AP positive. In contrast, in BOLAP injected non-transgenic mice, which were devoid of tumors, did not show any AP positivity outside of the expected anatomical structures such as the SVZ, subcallosal zone, RMS, and OB.

Laser capture microdissection and sequencing of AP+ cells

To definitively identify if the tumors are 1) directly formed from BOLAP labeled SVZ cells and 2) polyclonal or monoclonal in origin, we utilized the unique genetic tags that were conferred to BOLAP labeled cells that are also AP positive. To accomplish this, we sought to isolate individual cells that were AP positive from the tumors and analyze the makeup of their BOLAP tags. For this clonal analysis of AP positive cells, AP labeled sections of the tumors were microdissected using laser capture technology to isolate the cells. In these gliomas, some cells were laser captured as a cluster of cells (See Figure 22) and some areas of the glioma were also captured as single cells. As a control, normal structures (olfactory bulb, subcallosal zone, hippocampus, and SVZ) that also contained AP positive cells were targeted for capture. The BOLAP specific sequence

within these laser captured cells could then be analyzed through PCR amplification, followed by sequencing.

As a proof of concept for this methodology, the isolated cells positive for AP also were able to be sequenced using RT-PCR specific to the flanking regions of the unique nucleotide region in the BOLAP construct. To identify the unique oligonucleotide library sequence, the individual cells were captured for analysis and the sequence determined. Here, the entire PCR product was submitted for sequencing. For the groups of cells, they were also subjected to RT-PCR, but the PCR products separated through TOPO-TA cloning (Invitrogen). TOPO-TA cloning is a method of capturing individual PCR products from a mixture of PCR products. Here, the overhanging adenines at the end of a PCR product, added on by DNA polymerase, are captured by an "open" plasmid with overhanging thymidines. When the two products meet, they form a complete "closed" vector. The "closed" vector, which is used to transform bacteria, confers antibiotic resistance and thus individual colonies of bacteria can be isolated. The "captured" PCR product from each of these colonies can be determined.

In the case of the multi-cell captures, the overall PCR product could not be directly sequenced, due to varying sequences of multiple clones if present in the group of cells. To isolate the individual tags within the group of cells, individual bacteria clones from the TOPO-TA cloning procedure were propagated to sufficient quantity to isolate the genetic tag, and then sequenced. This proof-of-concept study showed that 1) the unique BOLAP tags could be isolated and identified from individual cells that were laser captured, and that 2) unique BOLAP tags could be separated, isolated and identified from the multi-cell samples using the TOPO-TA technique.

Clonal analysis of tumors reveals dominant clone

Using the BOLAP oligonucleotide library to lineage map brain tumors, we sequenced the labeled cells (AP+) to identify the distribution of tags. In each of the 6 GRASp53+/- animals that were both injected with the oligonucleotide library in the early neonatal period which subsequently developed gliomas as adults, the gliomas robustly expressed AP. These tumors were identified by various methods, including gross observation, histopathology, and proliferative marker uptake. Using laser capture microdissection, both single and cluster of cells from the tumors were captured and sequenced. From the entire pool of sections incorporating the tumor, the sections were chosen randomly with the aid of a number generator. In addition, the single cells that were generated were also chosen randomly for increasing statistical significance. The composition of the clones (See Figure 23) in each animal was similar. A great majority of the clones consisted mostly of singletons or doublets. Further, each glioma also is comprised of a clone that is represented significantly greater than the other clones. Each glioma has one clone that occurs 8-12 times, depending on the experimental animal from which it was investigated. Based on the extremely high complexity of the BOLAP oligonucleotide retroviral library, the cells that carry the same tags are clonally related and siblings. Clearly the bulk of the contribution to the tumor from the SVZ is polyclonal and heterogeneous. This may represent the migration of SVZ cells to the tumor which are responsible for tumor growth and bulk. Each tumor bearing animal, possesses a clone that is present at a significantly higher rate than other clones within the

tumor. Although, this quantitatively does not comprise a significant portion of the glioma, it could represent a dominant of master clone that was the original cell in the SVZ that received the transformation event or events. From increasing data with cancer stem cells, a precedent exists for a very small subpopulation of tumor cells being responsible for a tumor's aggressiveness, ability to metastasize, and initiate other tumors.

BOLAP-RV staining revealed less positive cells in the olfactory bulb of GRASp53+/- mice

Although the effect on tumor formation of the GRAS transgene in the p53 +/- mice is obvious, the effect of this transgene on normal anatomic structure for which there is a significant SVZ contribution is unknown. The mouse olfactory bulb (OB) continues to develop after birth, and there have been a large number of studies describing the role of SVZ derived NSCs in this development. Cells from the SVZ are known to migrate (as migratory neuroblasts) to the OB via the RMS. Utilizing this phenomenon, we sought to examine the role of the GRAS transgene in the context of the p53+/- mouse. We performed histological analysis of GRAS and control animals infected with BOLAP retrovirus in day 30 pups. First, we qualitatively verified that the SVZ cells in each animal type were successfully infected with BOLAP RV expressing AP to a similar degree. To make this determination, we sectioned the brains of random BOLAP injected mice 6 weeks after injection, and looked for the constitution of AP positive cells in the SVZ. Repeatedly, there was strong AP positivity in the cells of the RMS and corpus callosum to a similar degree within the animals examined.

Next, we examined the SVZ and OB for the presence of AP positive cells (See Figure 24). Qualitatively, this study revealed less AP positive cells in the OB of GRAS p53+/- animals compared to control animals. These histological findings led to further investigation into alterations in differentiation, specifically why fewer SVZ cells are migrating through the RMS.

Decreased alkaline phosphatase labeling of RMS in GRASp53+/- mice

In the 6 GRAS p53 +/- mice examined, we observed a significant decrease in AP positive cells in the olfactory bulb (OB). Although we observed a defect in proliferation in the OB in these mice compared to control animals, it remained unclear if this was entirely responsible for the significant decrease in cells that migrated from the SVZ. To explore the possibility that the reduction of AP positive cells is at least in part due to alterations in the RMS, we examined coronal sections containing the RMS and quantified the number of AP positive cells in the RMS of the GRAS p53+/- mice compared to the control animals. This histological analysis of adult WT and GRAS mice utilized AP as a marker for SVZ derived cells.

This analysis demonstrated marked differences in coronal section labeling of AP in the RMS. As previously stated, in the GRAS animals the SVZ labeling was similar to WT animals, but a dramatic decrease in AP labeled cells was observed in the OB. Normally, the RMS is contiguous to the SVZ of the lateral boundaries of the each lateral ventricle and provides a path of migrating neuroblasts toward the olfactory bulb where these cells differentiate into the neurons of the OB. However, at the apex of the ventricle

where the RMS originates, the RMS is altered in all the GRAS p53+/- mice that are tumor bearing (See Figure 25). As would be expected, this was not observed in the control mice. These findings were consistent with the decrease in AP positive cells in the OB as shown in Figure 24 and the decrease in BrdU positive cells in Figure 25. Thus, the reduction of proliferating cells in the OB as seen in the GRAS p53+/- mice was not due to a defect in proliferation, but rather a defect in migration across the RMS into the OB. Importantly, the sum of these observations indicate that there is not a defect in NSC proliferation in the GRAS p53-/- mice (although there is an increase in apoptosis) leading to a decrease in cells in the RMS and OB.

Decreased BrdU labeling of the RMS is observed only in the presence of oncogenic RAS

The previous studies determined that decreased proliferative cells in the RMS is most likely the cause of decreased AP positive and proliferating cells in the OB. Since the animals used are $HRas^{V12}$ transgenic, we suspected that this transgene is responsible for the observed effect. The minor difference in proliferation between the GRAS p53 +/- and GRAS p53+/+ mice observed suggests that there is very little contribution to proliferation by this knockout. However, these studies did not make it clear if this alteration of RMS is due to the oncogenic Ras transgene or the p53 partial knockout. To determine this, we utilized syngeneic p53 +/- mice with and without oncogenic Ras in this system. We performed BrdU labeling on the GRASp53+/- and p53+/- mice at age P10 and P30. At P30, the cortical labeling remains minimal in both models and in the p53+/- background the RMS is present and contiguous with the labeling in the SVZ (See

Figure 26). However, at P30 in the GRASp53+/- mice, the BrdU positive cells fail to appear in the RMS near its origin at the apex of the ventricle, where it should be contiguous with the SVZ. Thus, oncogenic GRAS is required for the observed disruption in the RMS and the contribution of the p53+/- background is not relevant to this phenomenon.

Dramatic decrease of DCX+ cells in the RMS of GRASp53+/- tumor bearing mice

Since we identified oncogenic Ras as the key factor disrupting the RMS stream, we sought to identify potential roles for oncogenic Ras in this aspect of biology. Also, with migratory neurblasts being a major component of the RMS, we quantified these cells that were positive for doublecortin (DCX). DCX is a 40 kDa microtubule-associated protein (MAP) that is expressed in a precise temporal manner in migrating neuroblasts during early embryonic development. It is also retained in neurogenic areas in the adult (the subventricular zone/rostral migratory stream/olfactory bulb axis and the dentate gyrus of the hippocampus), a pattern that suggests it is an ideal marker of both embryonic corticogenesis and adult neurogenesis. Using mice pre-treated with BrdU, we were able to co-stain the same sections for BrdU as a marker of proliferation. Therefore, using this system, we examined the SVZ and RMS labeling with GFAP (astrocytes) and DCX (migratory neuroblasts) in day 30 mice**.**

As expected, the control (non-transgenic) mice demonstrate an increase in DCX labeled cells from the SVZ to the RMS, with a concomitant decrease in GFAP (astrocytes or NSCs). In GRASp53+/- tumor bearing mice, the GFAP labeled cells decreased from

the SVZ to the RMS as with non-transgenic animals. However, there was a dramatic decrease in the DCX labeled cells in the GRASp53+/- tumor bearing animals (See Figure 27). This finding is consistent with what would be expected with a disrupted RMS, which typically labels strongly for DCX.

In addition, control mice demonstrate obvious DCX and BrdU labeling at day 10 and at day 30. In the GRASp53+/- mice, substantially less BrdU and DCX labeling is observed in the early postnatal period (day 10) in both the SVZ and RMS. By day 30 the expression in the GRASp53+/- mice expression is still markedly decreased in both the SVZ and RMS. This data suggests that the defect is due to a complete disruption of the RMS. Since the cells labeled with DCX are migratory neuroblasts which become the neurons of the olfactory bulb, the decreased neurogenesis is concordant with the decrease in DCX expression in the cells comprising the SVZ and RMS.

Decreased Pax6 expression in GRASp53+/- SVZ & RMS

The SVZ and corpus callosum express various transcription factors that mediate cell fate for the neural progenitor cells and cells fated to become glia or neurons. This expression occurs with some regional specificity. The corpus callosum has robust labeling Olig2, a marker for oligodendrocytes. The *Olig* family of bHLH transcription factors are essential regulators of ventral neuroectodermal progenitor cell fate and oligodendrocyte development in the murine CNS (Ligon 2004). The SVZ adjacent to the lateral ventricle primarily expresses Sox2, a marker for glial committed progenitor. The transition of the SVZ to the RMS and the RMS proper primarily expresses Pax6, a

marker for neuronal committed progenitors. In this way, Pax6 acts as a specification cue for migrating progenitor cells to become periglomerular and granular interneurons upon reaching the olfactory bulb (Hack et al., 2005). Pax6 is one of the key factors for central nervous system patterning and plays an essential role in the differentiation of cortical radial glia during development.

Since we observed a defect in the RMS, which is constituted with committed progenitor cells, we examined if the defect in migration through the RMS is associated with the failure of these cells to become committed progenitors and perhaps infers a different "programming" in the GRASp53+/- tumor bearing mice. We accomplished this by qualitatively examining the amount of Pax6 positive cells in the SVZ and RMS of the control and GRAS p53+/- mice. The amount of Olig2 positive cells (for oligodendrocytes) was also examined. By day 30 in the control mice, we observed the expected absence of BrdU positive but a strong presence of Pax6 expressing cells, due to this later stage in development where cells in the RMS should be lineage committed. As well, significant numbers of Olig2 positive, lineage committed cells are present. However, in the GRASp53+/- mice, cells a proliferating (BrdU+) population of cells in the RMS is still present, with a dramatic decrease in Pax6 expressing cells (See Figure 28). These results indicate that the reduction of migratory neuroblasts in the RMS is less likely from a general defect in proliferation, but more likely a consequence of the failure of SVZ cells to lineage commit in the RMS. More specifically, there seems to be a "switch" in the commitment of the cells towards oligodendroglial cells, rather than the Pax6 expressing cells which constitute the RMS in normal development. This may, in

part, explain how the GRASp53+/- mice form glial tumors or alternatively a consequence of tumor formation.

MAPK and PI3K pathways inhibitors decrease GRASp53+/- SVZ neurosphere's viability

There is no known hypothesis that explains how this potential rearrangement in differentiation programming occurs in the SVZ cells of the GRAS mice. It is well accepted that Ras oncogenicity is primarily mediated through the MAPK pathway. Mitogen-activated protein kinases (MAPKs) regulate diverse cellular programs including embryogenesis, proliferation, differentiation and apoptosis based on cues derived from the cell surface and the metabolic state and environment of the cell. The MAPK cascades consist of a core of three protein kinases- Raf, MEK, and ERK. ERK activation is entirely dependent on MEK, and ERK is the last signaling molecule in this cascade, which upon activation (phosphorylation) enters the nucleus and phosphorylates several key transcription factors such as c-fos and c-jun; activating their transcriptional inducing capabilities and controlling the important functions of proliferation and survival. However, the phosphitidylinosital 3- kinase (PI3K) pathway is also a key regulator of survival and oncogenic transformation. Since ERK activation plays an important role in early development in organisms as simple as Drosophila, and is thought to be important in maintaining the pluripotency of progenitor cells, we investigated a potential role for ERK in the oncogenic Ras mediated reprogramming of the NSCs observed in the GRAS mice, and also sought to elucidate it from the potential contribution of the PI3K pathway. Since the neurosphere assay is the hallmark assay to describe the undifferentiated,

multipotent nature of NSCs, we used this assay to determine the effect of these major signaling pathways on neurosphere formation.

PD98059 is a potent and selective inhibitor of MAP kinase kinases (MEK1 and 2). It selectively blocks the activation of MEK thereby inhibiting the phosphorylation and the activation of MAP kinase1. LY294002, 2-(4-Morpholinyl)-8-phenyl-4H-1-benzopyran-4-one hydrochloride, is a potent and selective PI3K inhibitor. Since each of these inhibitors have potent effects the individual signaling effectors that control proliferation, apoptosis, differentiation, and oncogenecity, we used these inhibitors in an in vitro assay to determine the potential contributions of these important signaling molecules in the viability (the balance of proliferation and apoptosis) of neurospheres isolated from the GRAS p53+/- mice. In this study, the neurospheres were cultured for 7-10 days and then treated with different doses of either the MEK or PI3K inhibitor for 10 days (See Figure 29). Then cell viability was measured using an MTT assay. Interestingly, there was a dose response to either inhibitor, but the ERK inhibitor had a much more pronounced effect (38 % viability for PD 1.0 versus 60% viability for LY 10). This data suggests that indeed the oncogenic Ras, signaling through the ERK pathway, is responsible for the increased neurosphere formation observed when using SVZs cultured from the p53+/- mice.

Inhibition of MAPK induces differentiation of GRASp53+/- SVZ neurospheres

Although the connection between oncogenic Ras and ERK signaling is well established; and the roles of ERK during differentiation well described, we did not know

if the change in differentiation observed in the neurospheres from the SVZ of the GRAS p53+/- mice was directly due to ERK. Having attributed the most pronounced effect on GRASp53+/- SVZ neurospheres to ERK inhibition, we investigated if ERK inhibition would affect the ability of these neurospheres to differentiate into different lineages (See Figure 30). The neurospheres were cultured as per the previously described protocols. In the presence of the mitogens FGF and EGF, the cells will remain as floating and undifferentiated spheres and few cells will differentiate and express lineage markers. Thus, control cultures (neurospheres from GRASp53+/- SVZs) demonstrate infrequent neurons. However, with the addition of the MEK inhibitor PD98059, Tuj1 and map2ap staining significantly increases. Tuj1 is a 50,432 dalton structural protein (450 amino acids) expressed in neurons of the peripheral nervous system and CNS. It contributes to microtubule stability in neuronal cell bodies and axons, and plays a role in axonal transport. Thus, it serves as a marker for mature neurons, but at less mature point than map2ab (an intermediate marker of neuronal development). However, no other lineage markers are observed. Thus, ERK inhibition in neurospheres from the control mice induces a modest lineage programming towards a greater amount of neurons. However, in the GRAS neurosphere cultures, the MEK inhibitor PD98059 caused a significantly more dramatic increase in the ratio of cells expressing the neuronal marker Map2ab (approximately 4 fold over the control cells), indicating that they were driven toward differentiating into a neuronal lineage. Along with an increase in neuronal markers, PD98059 inhibition of MEK also led to an increase in astrocytes (GFAP staining) and oligodendrocytes (GalC). Relative to controls, PI3K inhibition had a much more modest change in the percentage of differentiated cells. This data suggests that the

undifferentiated state of the NPCs in the GRAS mice is driven in part by Ras-ERK signaling.

Inhibition of MAPK reduces viability and tumor sphere formation in human primary glioblastoma cultures

Although the data generated comparing the GRAS neurospheres to the control neurospheres strongly suggested a primary role for ERK in controlling the lineage programming of the NSCs from the SVZ, it has not been established if this phenomenon is exclusive to the GRAS mice or can extend into broader models of NSC control and disease. To examine if his phenonmenon extended to human glioblastoma multiforme that were not derived from oncogenic Ras, we tested the effects of the MEK and PI3K inhibitors on the viability of human glioma cells in vitro. Both the MEK inhibitor PD98059 and PI3K inhibitor LY294002 showed a dose dependent response. Similar to the neurosphere cultures, MEK inhibition lead to significantly greater reduction in the viability of the human glioma cells in culture than did the PI3K inhibitor (See Figure 31).

Since this affected the viability of primary neurospheres from GRAS mice in the previous study, and implantation of cells from these neurospheres readily formed in vivo tumors, we sought to determine if the tumor initiating capability of these glioma cells could be affected by MEK or PI3K inhibition. As a surrogate assay for implantation, we examined the expression of CD133, since a subpopulation of cells in human gliomas are CD133+ and represent the putative cancer stem cells. This subpopulation is capable of recapitulating the tumor upon transplantation and may be responsible for the

aggressiveness of a tumor. We evaluated the effects of ERK inhibition on this population of cells and PD was able to significantly reduce the percentage of CD133+ cells, as determined by FACS analysis.

This is congruent with the in vivo studies of the GRAS mice which examined the tumor forming ability of cultured neurospheres from these mice. However, the effects of LY were divergent. LY lower dose led to an increase in CD133+ cells, and higher dose LY causes a decrease in CD133+ cells. These data are intriguing and merit further investigation in a separate study.

Inhibition of MAPK induces neuronal differentiation in human glioblastoma cells

Since ERK inhibition induced the differentiation of GRAS neurospheres in vitro, we hypothesized that human GBMs directly isolated from excised tumors would have similar effects. This study would provide significant weight to the in vivo observations in the GRAS mice, and the in vitro studies conducted using GRAS neurospheres. To perform this study, we obtained GBMs from three different patients (See Figure 34). The GBMs were dissociated and cultured to from low passage cell lines (7030, 7081, and 7192). These cells were then treated with the MAPK inhibitor PD98059 or the PI3K inhibitor LY294002. With MAPK inhibition, all three GBMs had a dramatic increase in the glial cells marker beta 3 tubulin (Tuj1) compared to untreated cells, with two of the three (7081 and 7192) GBMs expressing Tuj1 in nearly 20% of the cells. With PI3K inhibition, this effect was not observed. This observation strongly supports that in vivo and in vitro neurosphere observations using the GRAS mice where GRAS (activation of

ERK) regulating the undifferentiated state of the cells. In two of the three GBMs (7081 and 7192) ERK inhibition significantly reduced the percent of astrocytes, but PI3K inhibition had no effect. Since the presence of neurons in glial tumors is very rare in humans, the significance of this result for human tumorgenesis is unclear, however the role of MAPK in limiting neuronal differentiation will be of interest for other investigators.

DISCUSSION

Neurogenic zones and neural stem cells

The ability to produce functionally integrated neurons in the mammalian CNS was thought to only be possible during embryonic stages of life. Now neurogenic zones have been identified in mammals, including humans. These zones are comprised of various cell types, of which NSCs are the most primordial of the CNS and are the origin of more specialized cells throughout the CNS. (Alvarez-Buylla et al., 2002)

NSCs are operationally defined by their ability to: (1) differentiate into cells of all neural lineages (i.e., neurons—ideally of multiple subtypes; oligodendroglia; astroglia) in multiple regional and developmental contexts; (2) self-renew (i.e., to give rise to new NSCs with similar potential); and (3) populate developing and/or degenerating CNS.

To affirm that a single cell indeed possesses these capabilities, clonal populations (i.e., the affirmed progeny of a single cell) must be examined. While a number of antigenic markers have been proffered as distinguishing NSCs from other neural and non-neural progenitors – e.g., nestin (an intermediate filament consistent with an immature neuroectodermal lineage), musashi 1 (an RNA-binding protein), AC133 (a cell surface marker), Hoechst dye exclusion (the "side-population" after flow cytometric analysis) – none has been sufficiently specific or sensitive to supplant the above-mentioned operational definitions.

Accordingly, it is important to not define every mitotically active cell within the SVZ as a NSC. Expanding on this, the progenitor cells with the SVZ that are mitotically

active have been broadly categorized as NSCs or transit amplifying cells (TACs). SVZ astrocytes (Type B cells) function as the primary precursors of rapidly dividing transit-amplifying (Type C cells-secondary precursors), which generate neuroblasts (Type A cells) destined for the olfactory bulb. (Doetsch et al., 2002)

Similarly, the ability of a cell to form a cytosphere (a floating cluster of cells in vitro, referred to as a neurosphere when composed of neural cells) is a characteristic of *any* actively propagating cell of any lineage when maintained in serum-free medium without an adherent substrate, and hence cannot, by itself, be used to define a NSC; it simply affirms that the cell is mitotic.

With these caveats established, cells from the SVZ that remain mitotically active as neurospheres in culture can be discussed as neural progenitor cells. Their unique properties, are increasingly being investigated both to understand neurodevelopment and for their potential capacity to be exploited for therapeutic aim. In our investigation of the GRAS transgenic mouse models we realized that the SVZ has a complex cellular architecture, but the limitations of our lineage mapping technique do not allow for differentiation between NSCs and TACs. In fact, currently there is no well accepted technique (e.g, prospective isolation by flow cytometry), which allows the unambiguous separation of live NSCs and TACs in vivo. Hence, we use the term NPC, which is inclusive of both.

Identifying the glioma cell of origin

Investigation of hematopoietic stem cells and hematopoietic malignancies has led to the identification of the leukemic cell of origin. The ability to identify the cell of origin for solid organ tumors has remained elusive. Although cancer stem cells have been identified and can recapitulate primary tumors when small amounts are transplanted serially, this does not establish them as the cell or cells that acquired the original transforming event. Simply the cell of origin and cancer stem cells cannot be assumed to be the same until proven. Historically repeated references have been made based on histopathology and murine experiments with carcinogens that suggest the involvement of "embryonal" cells and the "subependyma plate." It is conceivable that the undifferentiated, mitotically active cells within the brain's neurogenic zone – the NSC— could be the glioma of origin.

Oncogenesis is assumed to require accumulation of genetic "hits." For this to occur in the brain, NPCs (either NSCs or TACs) would be the leading, but not exclusive, candidates for genetic hit accumulation. Both NSCs (Type B cells) and TACs (Type C cells) are mitotically active cells comprising the SVZ and are candidates for transformation. Although TACs do not have the longevity of NSCs, the size of the TAC compartment is at least one order of magnitude larger than that of the NSC compartment; the global number of divisions that they undergo might not be any greater than that of the transiently dividing progenitor population, which expresses its full proliferative potential over a relatively short time.

The role of transiently dividing progenitors (type C cells) as the possible source of brain tumor cell of origin is supported by the finding that in the adult subventricular zone these progenitors express EGFR. The activity of this receptor is altered in more than 50% of human gliomas and its constitutive activation can cause glioma formation in the CNS. Also, TACs may retain stem cell properties. Type C cells divide a few times in vivo, but do not function as long-term stem cells, as they can be eliminated with antimitotics without affecting SVZ regeneration. (Doetsch et al., 1999a) When C cells are exposed to high concentrations of EGF, they act as stem cells, revealing that they are not irreversibly committed to a particular differentiation pathway and may behave as a stem cell. Self-renewal and multipotency may be a property of multiple cells derived from primary stem cells. As such, the stem cell concept may be better applied to the potency of cells within the roots of a lineage rather than to a specific "rare" cell type. (Doetsch et al., 1999b)

For example recent work from the Vescovi group (Vescovi et al., 2006) demonstrated that NPCs already have activated the cellular machinery (e.g., promitotic genes, telomerase activity, and antiapoptotic genes) necessary for tumor initiation, progression, or both. Thus, neural stem cells may represent the path of least resistance in tumorigenesis, since they already have the ability to bypass apoptosis and senescence. As a result, NPCs may require less than the estimated four to seven mutations needed to effect malignant change in a differentiated cell-thereby making them the leading cellular candidates for transformation in the brain. Indeed Holland and co-workers have found that undifferentiated neural precursor cells may be more sensitive to transformation than differentiated cells. (Holland et al., 2000, Holland et al., 1998)

GRASp53+/- mice develop gliomas and allow for lineage analysis

Xenograft models from established human GBM cell lines or tumors explanted into the rodent brain do not recapitulate the hallmark histopathological features of invasion, heterogeneity, angiogenesis. These limitations apply for any investigation of therapeutic strategies against brain tumors. For the purpose of elucidating molecular and cellular mechanisms of glioma origin, xenograft models are not ideal.

With recent advances in transgenic mouse models, via a combination of approaches to activate oncogenic pathways and inactivate tumor suppressive pathways, a unique opportunity to study the neurodevelopmental biology of gliomas exists. In our experiments we exploited this opportunity to elucidate the neurodevelopmental biology of gliomas, as well as their relative relationship to the development of normal brain structures. Similar to the cell lineage mapping studies of the developing cortex, lineage mapping of brain tumors in genetically engineered mice can provide valuable insight into the origin and progression of gliomas.

Specifically, the glioma model using oncogenic Ras was selected based on the high propensity to form gliomas. Using an ES cells-based transgenic approach with in vitro selection to overexpress oncogenic V12Ha-*ras* specifically in astrocytes using the *GFAP* promoter, transgenic mice developed gliomas. When crossed on a p53+/- background, the 80% of mice developed high grade astrocytomas in 3 months. Given the greater probability of tumor occurrence, this model was used for lineage mapping. (Ding et al., 2001) Importantly, not all of these transgenic mice develop gliomas, and provided valuable controls.

Characterization of SVZ and RMS in GRASp53+/+ and GRASp53+/+ mice

The neurogenic zone hypothesized to be the origin of gliomas was first characterized in the GRASp53+/+ and GRASp53+/-. We show that the SVZ in these transgenic mice maintains the fundamental property of multipotency. Given the periventricular location of some gliomas, it is possible that in the transgenic animals the SVZ itself is transformed and the NPCs would potentially loose their multipotency. By microdissecting the SVZ of GRASp53+/+ and GRASp53+/-, and initiating neurosphere cultures the cellular composition of differentiated cells was studied. Indeed upon withdrawal of mitogens, the three neural cell types (astrocytes, oligodendrocytes, and neurons) were observed. Similar to WT SVZ, GRASp53+/+ and GRASp53+/- SVZ displayed the same characteristics of multipotency in mice with and without macroscopic tumors. This suggests that the SVZ in the GRASp53+/+ and GRASp53+/- mice and non-transgenic mice is comparable.

The GRASp53+/+ and GRASp53+/- and WT cells both possess the ability to differentiate, however their potential for neurosphere formation is different. GRASp53+/+ and GRASp53+/- SVZ neurospheres were more likely to form neurospheres, both at neurospheres size of 10um and 20um. This occurs both at plating of single SVZ cells and plating of 10 cells per well, to allow for local effects of plating density. The neurospheres are aggregates of mitotically active cells, and the GRASp53+/+ and GRASp53+/- consistently developed neurospheres at an increased rate.

The increased proliferation of the GRASp53+/+ and GRASp53+/- SVZ was also shown by increased BrdU uptake in the SVZ of P10 and P30 mice. Interestingly, when BrdU positive cells were quantified in the RMS of the same mice, at P10 the positive cells were approximately equal in number. At P30 GRASp53+/+ and GRASp53+/- mice had a significant reduction in BrdU positive cells in the RMS.

With increased proliferative capacity demonstrated by the neurosphere assay and BrdU labeled cells, we expected more cells in the SVZ of GRASp53+/+ and GRASp53+/- mice as compared to non-transgenic animals. However, this was not evident on histological brain sections. To estimate the number of apoptotic cells, we used the TUNEL assay which revealed that the increased number of BrdU cells in GRASp53+/+ and GRASp53+/- mice was paralleled by increased apoptosis. This presumably explains the normal appearance of the SVZ on routing histological sections with respect to normal size and architecture.

In seminal experiments used to identify and define brain tumor stem cells (Singh et al., 2003) malignant cells were serially transplanted to show the CD133+ cell population is able to recapitulate the primary glioma when transplanted in different animals. Also, the CD133- population was incapable of recapitulating the tumor when transplanted, demonstrating that not all cells within tumor possess the same ability to initiate, propagate, and possibly metastasize. This concept in cancer biology extends from lessons learned from the hematopoietic system and was subsequently shown to be true for solid organ malignancies as well. In all of these experiments it is a subpopulation of the tumor itself that can initiate tumors when serially transplanted.

Here we show that in tumor bearing GRASp53+/+ and GRASp53+/- mice not only can a subpopulation of glioma cells recapitulate the tumor (concordant with the literature), but also the SVZ in these tumor bearing mice can initiate gliomas after transplantation. We show for the first time that cells directly isolated from the SVZ can lead to tumor formation. These cells derived from the SVZ can also be cultured in vitro. Together with the results of other experiments it can be demonstrated that the dominant clones of gliomas originate from the SVZ. This ability of the SVZ to recapitulate tumors in not a consequence of the GRAS oncogene by itself, since the SVZ from GRASp53+/+ and GRASp53+/- mice that are not tumor bearing fail to initiate tumors. At the same time the SVZ remain mulipotent and are not fate restricted as one expects with gliomas in culture.

Lineage mapping of a glioma

We hypothesized that in the GRASp53+/-, the SVZ was the origin of malignant cancer cells. We further hypothesized that the cell was a NPC-like cell, sharing features with NSCs or TACs. Given that these tumors develop in these transgenic animals as they mature, we lineage mapped the tumor masses by labeling the SVZ in the early neonatal period before glioma formation occurs. For the lineage mapping experiments, on GRASp53+/- mice were used to the greater likelihood or tumor formation by 3 months, with some mice still available that expressed the GRAS oncogene yet without glioma formation as a control group.

Replication incompetent retroviral vectors are uniquely suited for lineage mapping and provide a genetic tool to elucidated clonal relationships. Replication incompetence is mandatory, so that the vectors cannot spread from one infected cell to another, yet they are faithfully passed on to all daughter cells of the originally infected progenitor cell, which is ideal for lineage analysis. Genomic integration of most retroviruses requires that the cell must go through an M phase, 2 and thus only mitotic cells will serve successfully as hosts for integration of most retroviruses. Lineage analysis is designed to ask about the fate of daughter cells, thus infection of postmitotic cells is not desirable. Further, since NPCs (NSCs or TACs) are only mitotically active cells in the SVZ they are selectively targeted by retroviral vectors and provide a modern molecular technique for studying their cellular fate.

The presence of helper virus is an issue of concern when using replication-incompetent viruses for lineage analysis as it can lead to horizontal spread of the marker virus, creating false lineage relationships. Accordingly we employed a third generation of "helper-free" packaging lines (Phoenix ecotropic made in 293T cells) to produce our retroviral stocks and obviate the potentially confounding effects of helper virus. Older retroviral vectors also presented risks of lumping errors are when the progeny of more than one progenitor are considered clonally related. A splitting error is made when one does not recognize siblings as being from the same progenitor and interprets them as members of different clones. Splitting errors must be addressed when a claim is made that a progenitor gives rise to a single, or very few, cell types.

To directly address this problem, we used retroviruses in which each member is both unique and identifiable. BOLAP is a degenerate oligonucleotide library that was

designed to maximize the number of unique members and to ensure their even distribution with a potential complexity of 10^8. Therefore, when sequenced from picked cells that are labeled, it allows unequivocal assignment of clonal relationships because of the insignificantly small chance of the same sequence occurring more than once. Thereby, by using the BOLAP oligonucleotide retroviral library to label progenitor cells, the risk of lumping and splitting errors is essentially eliminated, while providing the ability to generate data with strong statistical significance given the extremely high complexity of unique genetic inserts.

For accurate identification of BOLAP-retrovirus (RV) infected cells, the retrovirus was generated (Fields-Berry et al., 1992) with the placental alkaline phosphatase gene (PALP-I) because of its natural distribution being limited primarily to the placenta in humans and the great apes, (Goldstein et al., 1980a, Goldstein et al., 1980b, Goldstein et al., 1982) any potential background activity within the rodent brain can be inhibited by agents selective toward rodent AP and not PALP-I. In addition, PALP-I is 100-fold more resistant to treatment with heat than is rodent AP. (Posen et al., 1969, NEALE et al., 1965) These features made alkaline phosphatase an excellent marker for murine cells successfully infected with the BOLAP-RV.

In order to lineage map the contribution of the SVZ progenitor cells to a glioma maximal infection was required. Using a high titer and comparing labeling to BrudU in age matched pups, demonstrated that pattern, concentration, and stability of BOLAP-RV was equal to that of BrdU. This is important, because it suggests that a nearly all mitiotically active cells were successfully transfected with BOLAP-RV, thereby limiting the possibility of failing to label cells that contribute to glioma formation. Clearly a

minority of cells may not have been labeled and this is one limitation of the molecular methods, that the cell of origin may not be labeled, and subsequent lack of representation in the glioma would fail to discover a true link between one or several SVZ NPCs. Also, transgenic mice labeled with BOLAP-RV as pups, demonstrated labeling at age 14d and 28d and 60d. Importantly, the pups were injected prior to transgene activation (which in this model occurs at approximately day 6) in the pre-morbid state and labeling was persistent into adulthood, during the presumptive molecular oncogenic processes.

We demonstrate that with selective labeling of the mitotically active cells of the SVZ in the neonatal GRASp53+/- pup, the labeling persists into adulthood in the neurogenic zones. This is to be expected, since the SVZ replenishes itself as well as proving cells to the OB. In animals that form gliomas, the label is also robustly located in the tumor, whereas the cortical structures contain minimal label in concordance with the cortical findings of injected non-transgenic pups. This links the SVZ to be a major contributor to gliomas. Whether gliomas originate from the SVZ or whether the SVZ is merely a contributor to glioma growth cannot be ascertained by these experiments. The nature of the contribution however can be further characterized by having used the BOLAP oligonucletide library as the mechanism for labeling the SVZ cells when the GRASp53+/- pups were born.

We sectioned the entire brain, and with sections incorporating the AP positive glioma the tumor was laser captured and cells sequenced. In each experimental animal with a glioma, approximately 200 cells/clones were identified. The complexity of the oligonucleotide library being 10^8 and with greater than 90% of the sections with tumor analyzed for labeling, allowing us to be confident in the statistical significance of our

findings. Statistically you have a multinomial distribution for the number of viral particles with each of the 10^8 tags. This gives a 99.5% probability not infecting any of the SVZ cells with the same oligonucleotide tag, essentially removing the risk for false sibling relationships of clones.

Each tumor consists of heterogeneous clones. The great majority of clones are represented once, with some doublets as well. Interestingly, each tumor also has a dominant clone which is represented between 8-12 times, depending on the animal. With our study design, we can with confidence state that a second dominant clone is unlikely.

A confounding factor about NPC and glioma is their know property of migration toward CNS pathology (stroke, trauma, and neoplasm). It is possible that the dense and uniform labeling of the gliomas is entirely due to migration of labeled SVZ cells once the tumor has formed. We believe this to be highly unlikely given the uniform and robust nature of labeling. In experiments showing SVZ NPC migration toward implanted tumors, (Glass et al., 2005) the contribution of the SVA to gliomas is usually limited and on the periphery. Also, unlike these studies demonstrating NSC migration toward gliomas, no stream of cells linking SVZ to glioma is detectable in our experimental models. Clearly, a significant component of a glioma results from NPC migration, and we believe this to be a non-clonal contribution from the SVZ that represents the background signal of heterogeneous clones in our experiments. However, the original cell that is transformed is most likely represented by the dominant clone sequenced from the tumor.

At face value, our results suggest that the tumors in GRASp53+/- mice are polyclonal, however, always containing one clone which is on average 10 fold more abundant than the rest of the clones. This finding is intriguing and may suggest the

presence of a "master" clone, which drastically alter the proliferation potential of normal neighboring NPCs (e.g. via secreted paracrine growth factors) and accelerate the recruitment of these cells into the glioma area. It will be critical to examine if such clones can be prospectively isolated and compared with the rest of the tumor mass for their ability to induce gliomas upon transplantation into the normal mice or GRASp53+/- mice.

Also it cannot be ascertained based on these experiments whether the NSC or TAC is lineage origin for the cells within the glioma. Both are mitotically active and potential candidates for labeling and transformation. Accordingly, only the NPC at this point can be traced to be the cells of origin for gliomas in this GRAS transgenic mouse model of glioma.

Molecular mechanisms

The formation of gliomas in the GRASp53+/- mice leads to fundamental alterations in the neurobiology of the brain. In addition to the formation of a pathological structure, the glioma, the tumor bearing animals have less BOLAP infected alkaline positive cells in the olfactory bulb. The SVZ of WT, GRASp53+/- non-tumor bearing, and GRASp53+/- tumor bearing mice remain histologically similar and have similar patterns of BrdU uptake. However, the RMS in non-transgenic mice and GRASp53+/- mice without tumors versus GRASp53+/- tumor bearing mice is dramatically different, with the latter having a disruption of the RMS. This disruption of the RMS is not seen in p53+/- mice without expression of the GRAS oncogene, but p53+/- mice do not form

gliomas so it remains possible that the disrupted genesis is secondary to glioma formation and not simply the GRAS oncogene.

The RMS is the migratory path of ongoing neurogenesis in adult animals and its disruption was further delineated by immunofluroscense of markers characteristic of neuronal progenitors and migratory neuroblasts. In WT animals the percentage of BrdU cells in the SVZ and RMS that co-localize with DCX is approximately 18% and 25% respectively. DCX is maker for immature neurons and migratory neuroblasts which comprise part of the SVZ to RMS to olfactory bulb axis for generating neurons. In GRASp53+/- tumor bearing mice the amount of DCX labeling is significantly reduced, consistent with the histologically observed disrupted RMS and altered neurogenesis.

We also show that in the GRASp53+/- tumor bearing mice there is a loss of Pax6 expression. This suggests that the in the SVZ to RMS transition, the neuronal committed progenitors that label with Pax6 are reduced in concordance with the disrupted RMS. These findings are in agreement with the fact that Pax6 overexpression is sufficient to direct almost all neurosphere-derived cells towards neurogenesis. (Hack et al., 2004) The RMS disruption is characterized with decreased DCX and Pax6 labeling which represent the migratory neuroblasts and committed progenitors toward the neuronal lineage, respectively.

MAPK inhibition decreases GRASp53+/- SVZ neurosphere viability as well as, decreases human GBM in vitro viability and tumorsphere formation. This mechanism is expected with oncogenic Ras activation in the transgenic mice, and we show that in human GBM cells, MAPK inhibition is able to reduce the viability and proliferation (tumorsphere formation) of these malignant cells.

MAPK inhibition was shown to increase neuronal differentiation of GRASp53+/- SVZ neurospheres and human GBM cells in vitro. These data suggest that the observed decrease in GRASp53+/- SVZ and human GBM viability may be due to a switch in differentiation. MAPK may be a molecular switch that limits neuronal differentiation in vivo in these GRASp53+/- animals and with inhibition leads to greater neuronal cell population in vitro with human GBM lines. It is also possible that the oncogenic event occurred originally in a NSC with a subsequent block in differentiation (Pereira et al., 1998) that allows the transformed cell to differentiate down glial lineages but not neuronal.

CONCLUSION

The stem-cell origin hypothesis still accepts the contribution of genetic instabilities and epigenetic factors to the evolution of heterogeneity in a malignancy. (Fidler and Hart, 1982, Pathak, 1990, Chow and Greenberg, 1980) Only in this instance, it is the stem cell that is the target of the genetic or epigenetic effects. Further, the stem-cell view also accommodates Knudson's (Knudson, 1977) and Volgelstein and colleagues' (Vogelstein et al., 1988) concept of initiation and promotion in the development of a neoplasia, provided that the mutations leading to clonal expansion originate in a stem cell.

However, this concept should be viewed as distinct from to the long standing "monoclonal" cancer hypothesis, which indicates that a tumor arises from a single cell that has acquired the necessary mutations to dsyregulate growth and dedifferentiation, leading to a tumor. The explosion of modern day epigenetic studies points away from a reliance on this concept, demonstrating that the classic Volgelstein tumor progression hypothesis is not a discrete set of stepwise changes but rather the natural selection of heterogeneous populations within a tumor. In this sense, the stem-cell origin hypothesis can be thought to integrate the concept of tumor heterogeneity with the "cancer stem cell hypothesis", where the self-renewing population within a tumor is due to a minor population of cells with the tumors. Just as the neural stem cell is the self-renewing component in normal neurobiology, it could be a driving force behind the formation of brain tumors. Indeed, the self-renewing, or "cancer stem cell" component of brain tumors is much higher than other types of cancer. These "cancer stem cells" possess all

the key properties ascribed to a neural stem cell. These types of observations due not prove that cancer stem cells in brain tumors are derived from neural stem cells. However, they do suggest that brain cancer should not be viewed as a tumor mass comprised of undifferentiated cells, but rather a group of cells which exhibit patterns of abnormal differentiation. The initiation and promotion of malignancy, in the hematopoietic system, leads to blocked differentiation of stem cells rather than dedifferentiation of mature cells, and this may apply to brain tumors as well. So whether the cancer-initiating event occurs in a normal stem cell or in normal progenitor cell or differentiated cells that have reacquired stem cell properties, the driving force of the tumor is comprised of a self-renewing population of cells with stem cell-like qualities.

This study sought out to determine if indeed the cells in spontaneous gliomas are derived from the neural stem cells that have acquired the necessary genetic and epigenetic changes to form a malignancy. Utilizing the GRAS background to drive tumor formation, we used a system of SVZ retroviral tagging and lineage mapping to definitively determine this. As such, the **c**urrent study is the first attempt to rigorously analyze the clonality and lineage relationship of brain tumors using a genetic model. Although we did not demonstrate that the tumor originated entirely from SVZ cells, we did identify a large constituency of cells derived from the SVZ that comprise a significant bulk of the tumor. We determined that the SVZ cells in the GRAS mice are phenotypically different, showing increased proliferation and neurosphere forming ability, similar to the "cancer stem cell" components of human gliomas that were subjected to the same assays. GRAS SVZ cells also showed aberrations in differentiation by lineage markers and atypical RMS migration, mimicking the phenotypic behavior of

glioma cells that have lost the ability to maintain the appropriate lineage path and phenotypic behavior. We demonstrated that the oncogenic RAS was indeed the driving force behind these changes, by regulation of the ERK pathway. It could also be that the GRAS SVZ cells indeed have an abnormal karyotype and aneusomy pattern characteristic of the genetic instability seen in human gliomas; as deletion of p53 alleles increased the incidence of tumor formation in a dose-dependant fashion. Thus, these observations better fit the cancer hypothesis that requires heterogeneity as the driving force of tumors, rather than a monoclonal origin of tumor initiating cells progressing stepwise through tumor progression events.

Although our observation that the cells in the glioma areas appeared to originate from different clones supports the conclusion that brain tumors do not originate from neural stem cells, there was always a clearly identifiable "master" clone, on average overrepresented 10 times compared to any other clones. This raises intriguing possibility that the master clones may orchestrate the over-proliferation / transformation of normal neighboring neural progenitors. Also, the abundance of a "master clone" fits with the hypothesis that tumor heterogeneity is the driving force behind tumor progression- the selection of one SVZ clone over another is determined by its natural advantages in the tumor environment. The specific factors that determine this selection are unknown, but it suggests that epigenetic changes apart from the Ras oncogene or differential p53 status are what distinguish the prevalence of one clone over another in the tumor. Thus, what we have observed in these studies better fit with the modern day concept of tumor initiation and progression as a dynamic selection of natural heterogeneity, rather than a single tumor initiating cell determining the makeup of the tumor from start to finish. It is

unclear exactly what role the neural stem cells have in this process, but their uneven selection and gross representation within the tumor indicates for the first time in any study that there is an important contribution of the SVZ to the formation and development of tumors. Furthermore, this study identified the key regulatory pathway that is regulated by Ras in this model, and suggests that this paradigm may important to the differentiation and proliferation of not only neural stem cells proper, but potentially putative cancer stem cells. It will be important to develop the experimental strategies allowing direct comparing on tumor initiation capacity of the master clone and the rest of cells in the tumor.

Although it remains controversial whether malignancy originates from a stem cell or arises from the dedifferentiation of a somatic cell, this study has taken the first steps to identify the origins of those cells that ultimately form a tumor. We believe our model demonstrates altered neuronal differentiation in the setting of a brain tumor. Undoubtedly, this type of dysregulation is an essential element of the cells which form a brain tumor. It is intriguing to consider that the neurogenic SVZ, which already compromises the fundamental neurophysiology of brain tumor formation, can demonstrate the type of altered neurogenesis we observed, which is typical of malignant cells in brain tumors. It is also intriguing that there was a significant non-random presence of clonal SVZ derived cells constituting part of the tumor, akin to the identification of a discrete population of self-renewing cells now thought to be the putative cancer stem cells. It may be that the exact same aberrant behaviors exhibited by the neural stem cells in the GRAS mice are a hallmark of the cells which initiate brain tumors, even though in these mice, they were not clearly one in the same.

Identifying the cells that originate brain tumors will allow an entirely new field of investigation of chemoprevention and an effort to target the cell or cells fated for malignancy in their pre-morbid state. The phenotype of the GRAS SVZ cells and the observed parallels to tumor initiating cells points towards the utilization of identical or at least congruent mechanisms by the tumor initiating cells, thereby identifying new mechanisms to help understand the origins of brain tumors. Since the SVZ also provides a uniquely accessible location for therapeutic delivery by neurosurgeons, as it surrounds the ventricular system which is routinely and safely entered for numerous CNS diseases, continued work understanding SVZ derived cells in the processes in tumor development and progression will help in exploiting the accessibility of these cells to be used as means to treat or prevent brain tumors.

FIGURES

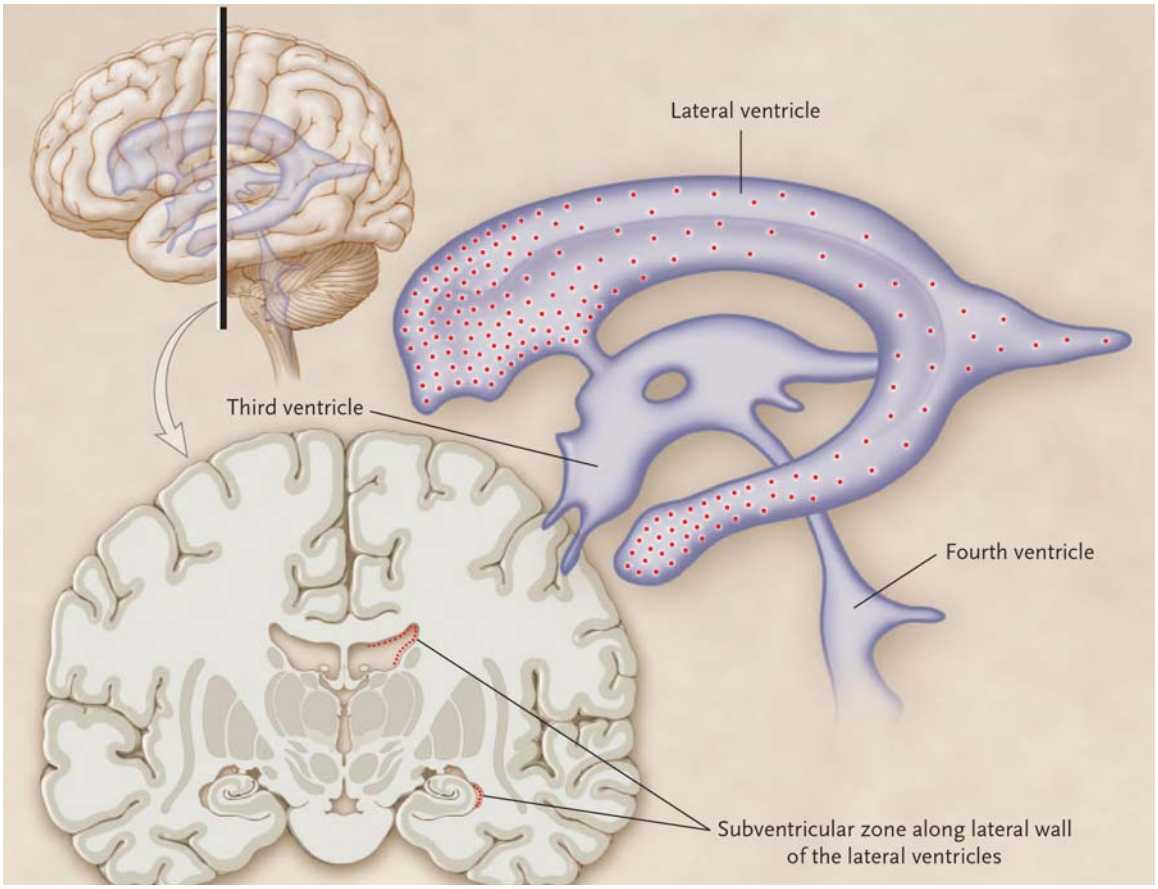


Figure 1. Location of the SVZ in the adult human brain. This schema shows the SVZ exists on the lateral aspect of lateral ventricles. Greatest density is on the lateral aspect of the frontal and temporal horns of the lateral ventricular system. (Sanai et al., 2005)

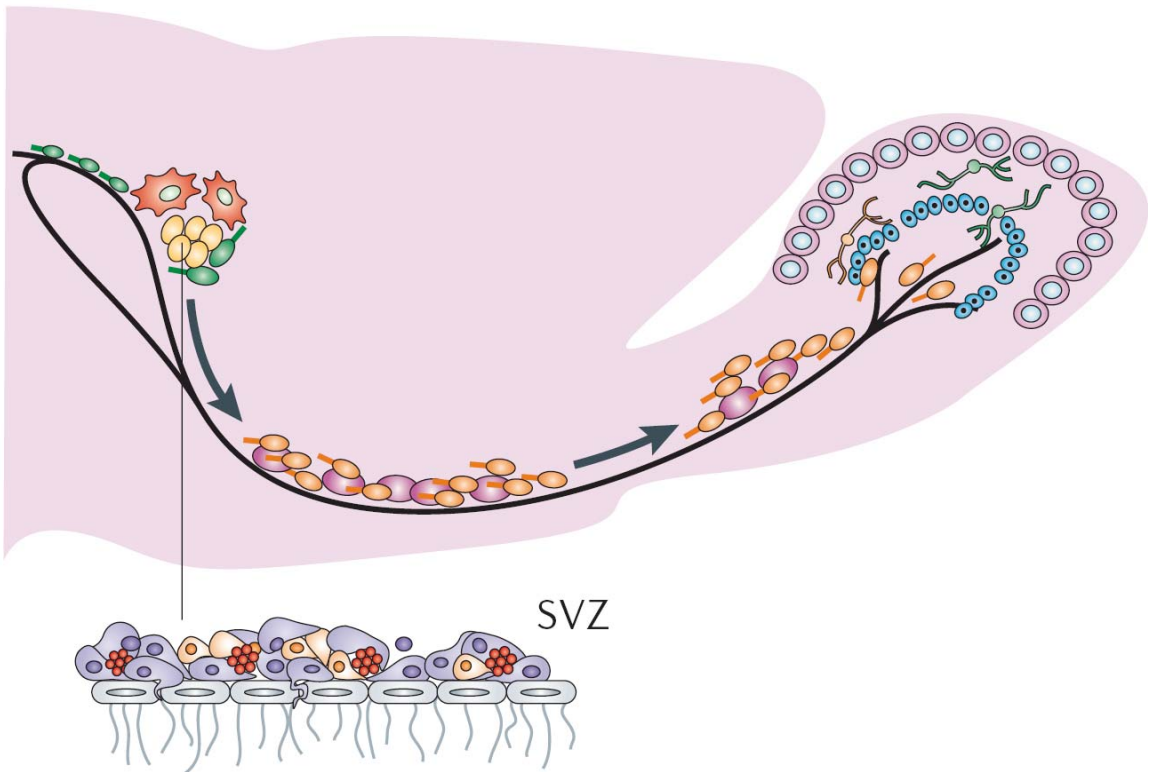


Figure 2. Sagittal section of the rodent SVZ and RMS to the olfactory bulb. A sagittal section through the lateral ventricle that shows the larger area of adult neurogenesis; that is, the subventricular zone (SVZ). This region lines the lateral ventricles of the forebrain and is comprised of three main cell types. The multipotent, type B astrocytes, that have been identified as the bona fide SVZ stem cells, give rise to fast-cycling transiently proliferating precursor cells that are called type C precursors and that, in turn, generate mitotically active type A neuroblasts. The type A cells, while dividing, migrate tangentially towards the olfactory bulbs where they integrate as new interneurons. (Vescovi et al., 2006)

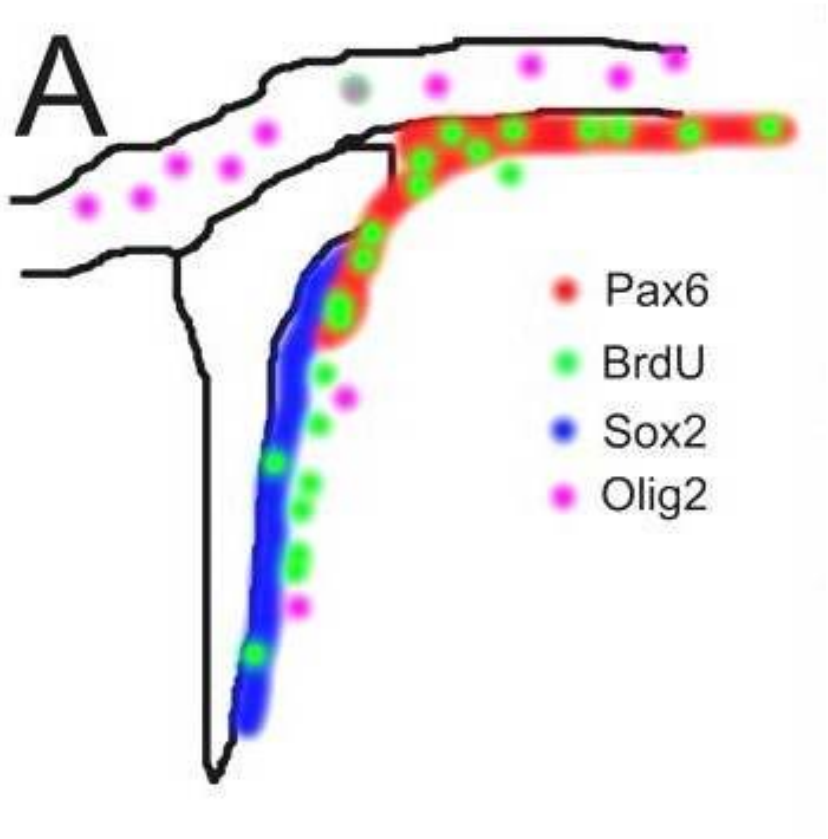


Figure 3. Neurogenic zone transcription factors. (A) Schema showing normal regions of transcription factor staining in relation to BrdU positive cells to identify stem cel, glial and neuronal lineages.

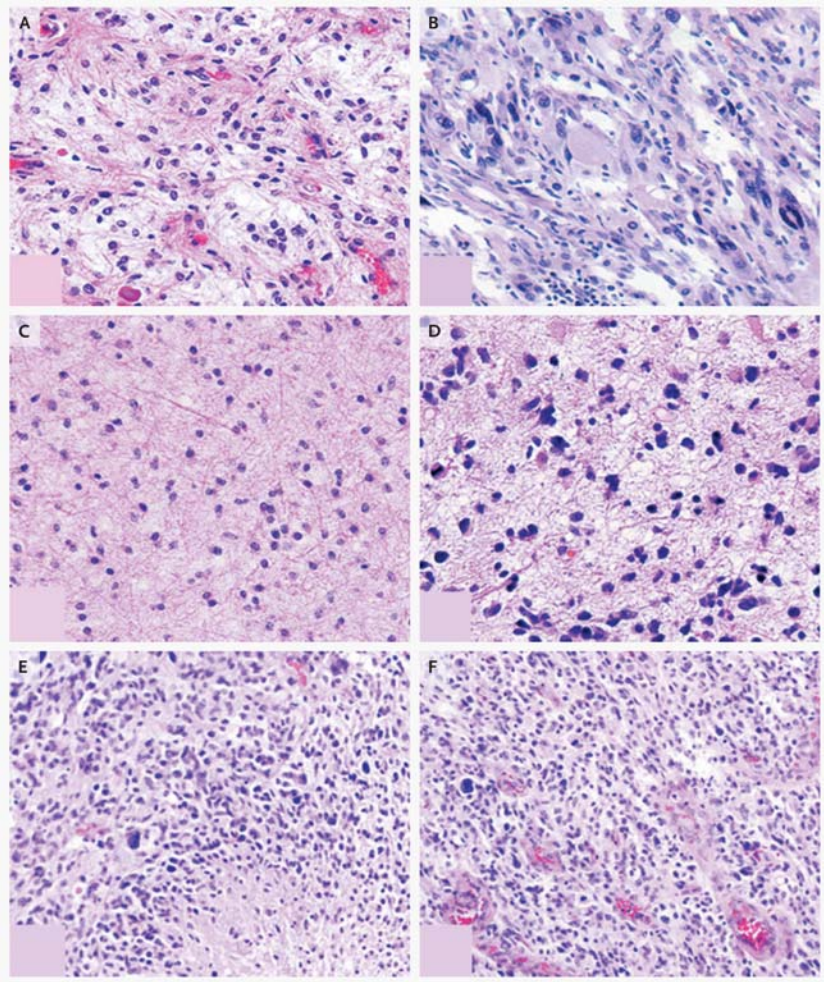


Figure 4. Grades I to IV (World Health Organization) Astrocytic Tumors. Panels A and B show circumscribed astrocytomas. Pilocytic astrocytomas (Panel A) are typically indolent, have a limited invasive capacity, and rarely undergo anaplastic progression. These tumors may have microvascular hyperplasia and cellular pleomorphism despite their designation as grade I tumors. Pleomorphic xanthoastrocytomas (Panel B) are also relatively circumscribed and, despite their distinct, conspicuous cellular pleomorphism, tend to be low-grade (grade II) tumors with limited capacity for brain invasion. Panels C through F show diffuse-type astrocytomas, which have the capacity for dispersion into the surrounding brain and a high frequency of anaplastic progression. A grade II astrocytoma (Panel C) is well-differentiated, with mild-to-moderate nuclear pleomorphism. A grade III astrocytoma (Panel D) has a high rate of cell proliferation, as indicated by the mitotic figures. These tumors commonly have a moderate degree of cellular pleomorphism and more heterogeneous cellularity. Glioblastoma multiforme, grade IV, is the most aggressive glial tumor and has the distinctive features of palisading or geographic necrosis (Panel E) and conspicuous microvascular hyperplasia (Panel F) in addition to marked cellular pleomorphism. (Sanai et al., 2005)

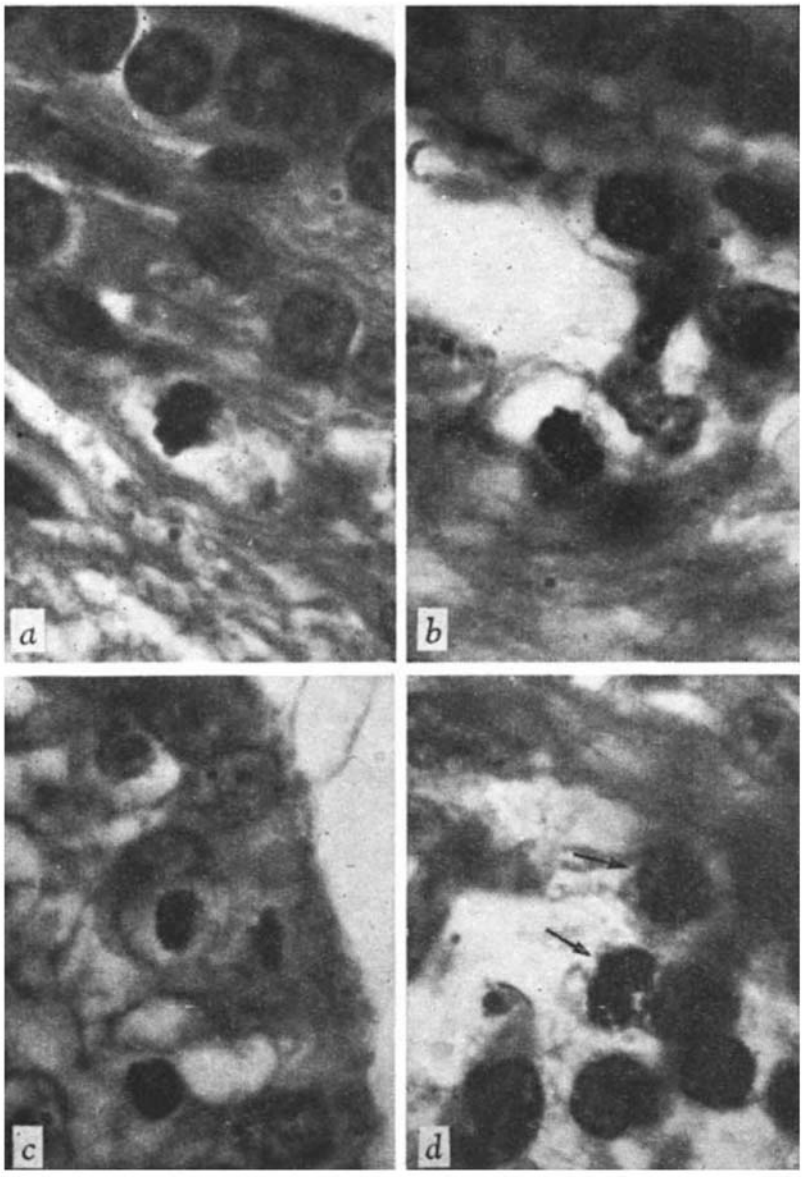


Figure 5. Subependymal plate mitoses. Haematoxylin and eosin image demonstrating mitoses in the subependymal layer. A) Metaphase, B) Metaphase, C) Anaphase, and D) Telophase. (Lewis, 1968)

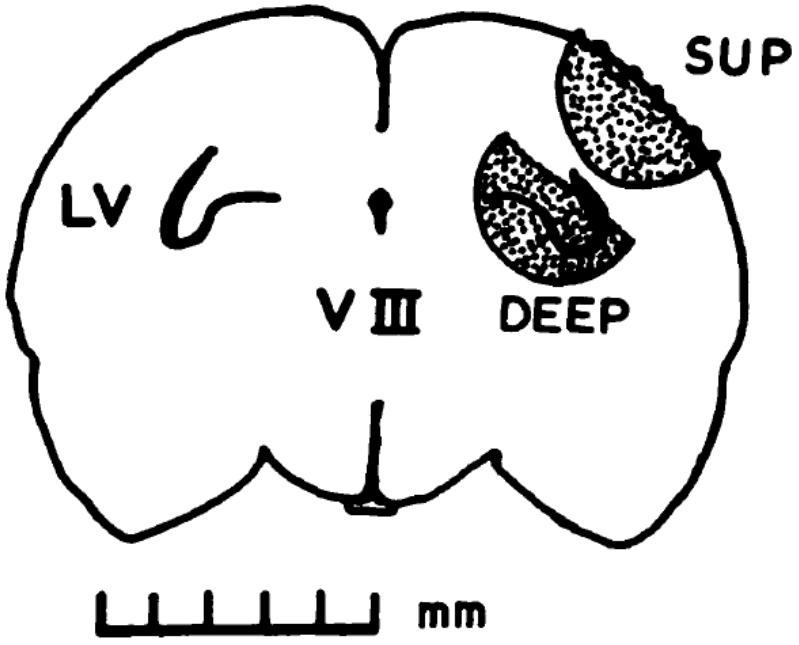


Figure 6. Diagram of carcinogenic implants. Diagram of rat brain showing the position of deep and superficial carcinogenic implants in their experiments, superficial (SUP), lateral ventricle (LV), third ventricle (VIII). (Hopewell and Wright, 1969)

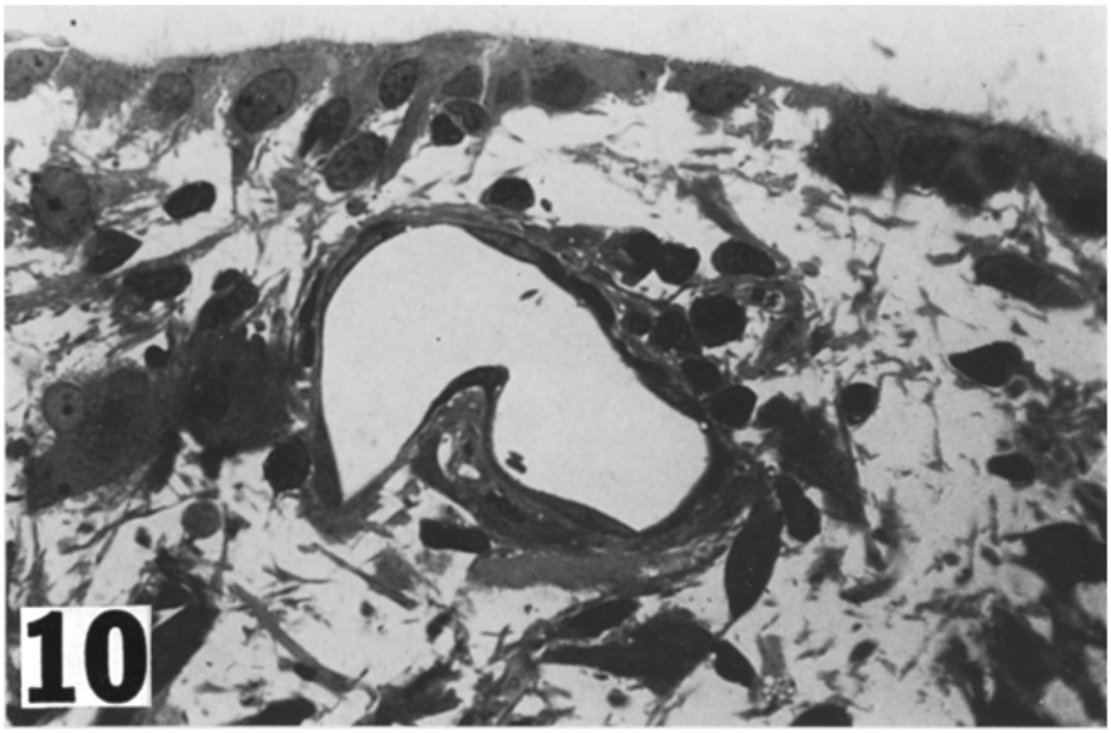


Figure 7. Periventricular glioma. Periventricular glioma at 4 weeks after inoculation. The lesion is covered at ventricular surface by ependyma. (Vick et al., 1977)

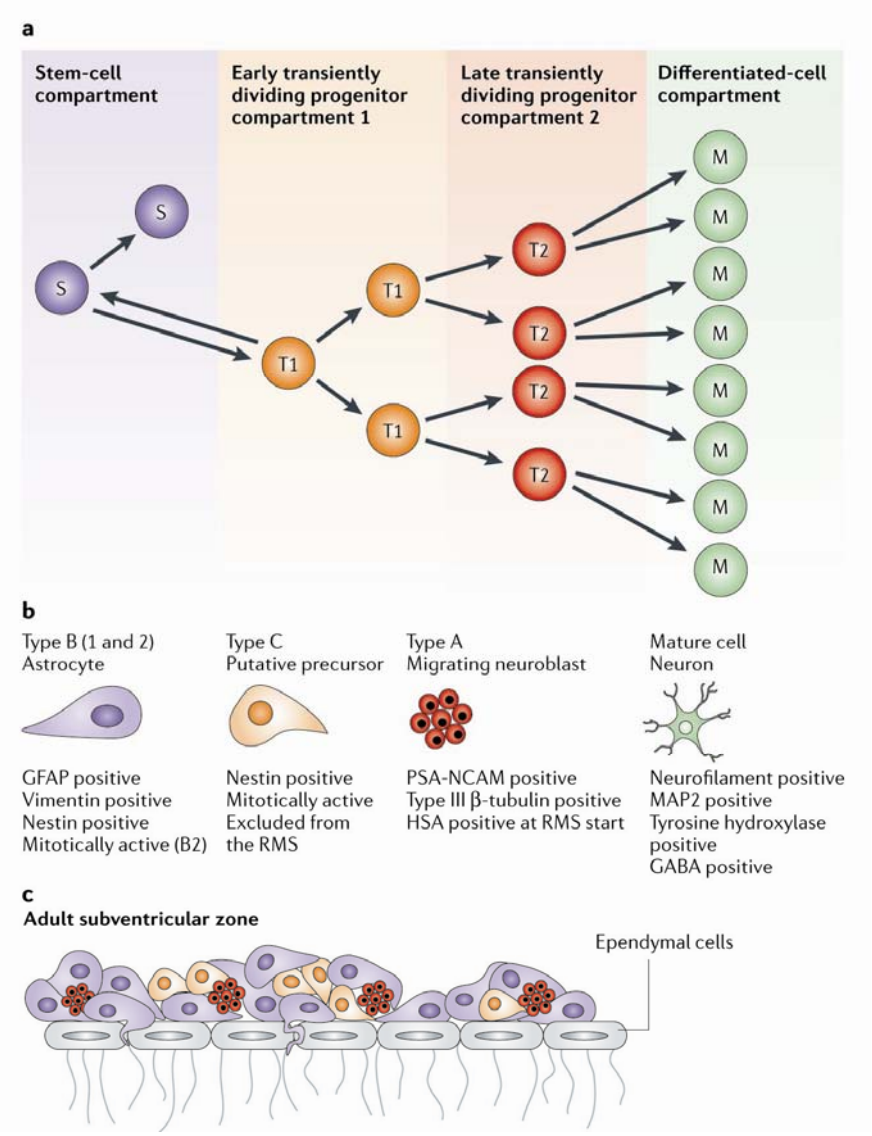


Figure 8. Hierarchical organization of the functional compartments in renewing tissues. (A) The stem-cell compartment (purple), early transiently dividing progenitor compartment (orange), late transiently dividing progenitor compartment (red) and differentiated-cell compartment (green) are schematically described. Cells in the stem-cell and transiently dividing progenitor compartments could be the target of the onco-transformation that leads to the formation of tumour stem cells. (B) The neural precursors that make up similar functional compartments in the neurogenetic regions of the adult brain and that might be the source of brain tumour stem cells. (C) The structure of the subventricular zone, showing how these precursors fit and are organized in the germinal neuroepithelium of the largest neurogenetic region of the adult brain. GABA, y - aminobutyric acid; GFAP, glial fibrillary acid protein; HSA, heat-stable antigen; MAP2, microtubule-associated protein 2; NCAM1, neural cell adhesion molecule 1; PSA polysialic acid; RMS, rostral migratory stream. (Vescovi et al., 2006)

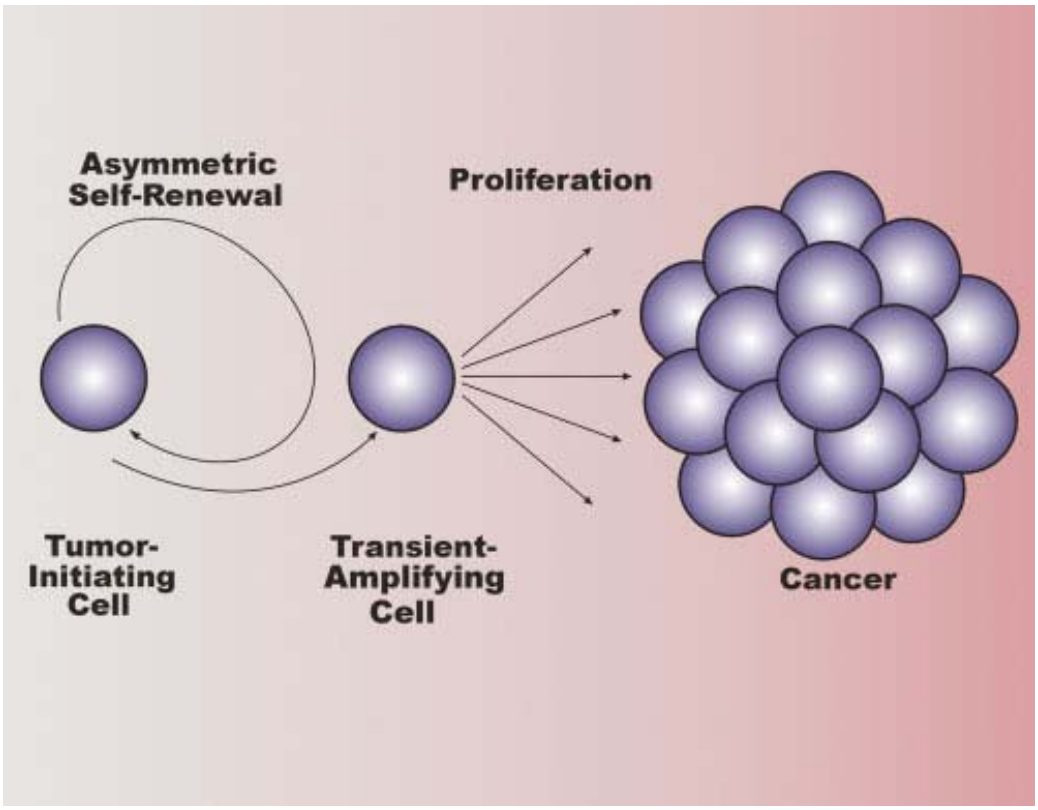


Figure 9. Overview of tumor stem cells in cancer. Cancer stem cells (tumor-initiating cells) divide asymmetrically, resulting in self-renewal of the tumor-initiating cell and production of a daughter cell known as a transient-amplifying cell (progenitor cell). The transient-amplifying cell is not thought to possess self-renewing capabilities, but can proliferate and contribute to cancer progression. (Lee and Herlyn, 2007)

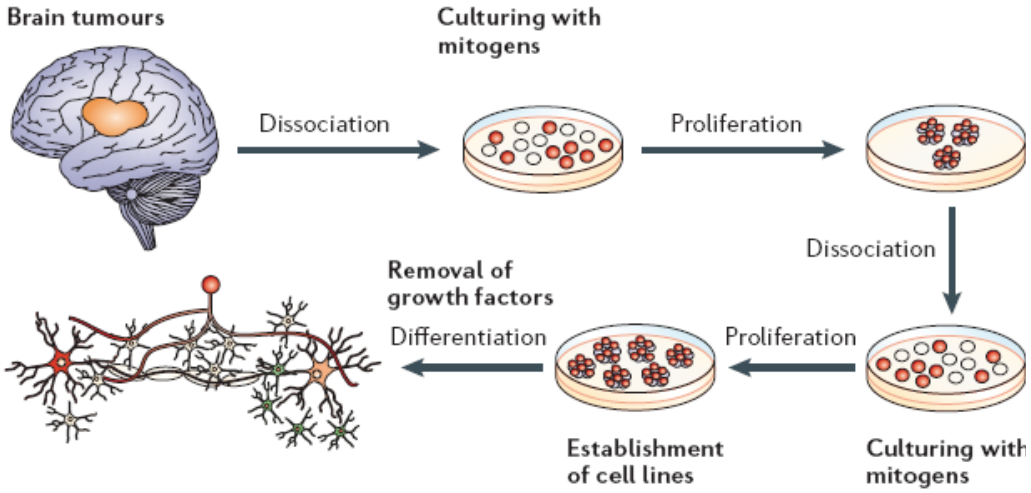


Figure 10. Isolation and perpetuation of brain tumor stem cells in culture. The neurosphere assay is a defined serum-free culture system that allows the isolation and propagation of CNS-derived stem cells. Adult precursors are dissociated and plated in a liquid growth medium that contains the stem-cell mitogens epidermal growth factor and/or fibroblast growth factor 2. Because of the lack of serum and the low plating density, most cells die, except those that divide in response to the stem-cell mitogens. The growth-factor- responsive cells proliferate to form floating clusters of cells that are referred to as neurospheres. These can be further dissociated into a single-cell suspension and then re-plated in fresh medium to produce secondary neurospheres. The process can be repeated, resulting in a geometric expansion in the number of cells that are generated at each passage. Upon mitogen removal, the progeny of the proliferating precursors can be differentiated into neurons, astrocytes and oligodendrocytes, which are the three primary cell types that are found in the adult mammalian CNS. Under these conditions, the growth-factor-responsive precursors can be expanded indefinitely with little change in their growth or differentiation characteristics. These results indicate the existence of an adult neural stem cell as these cells possess the fundamental stem-cell features of extensive self-renewal, generation of many progeny and the ability to give rise to the primary cell types of the tissue from which they were obtained. (Vescovi et al., 2006)

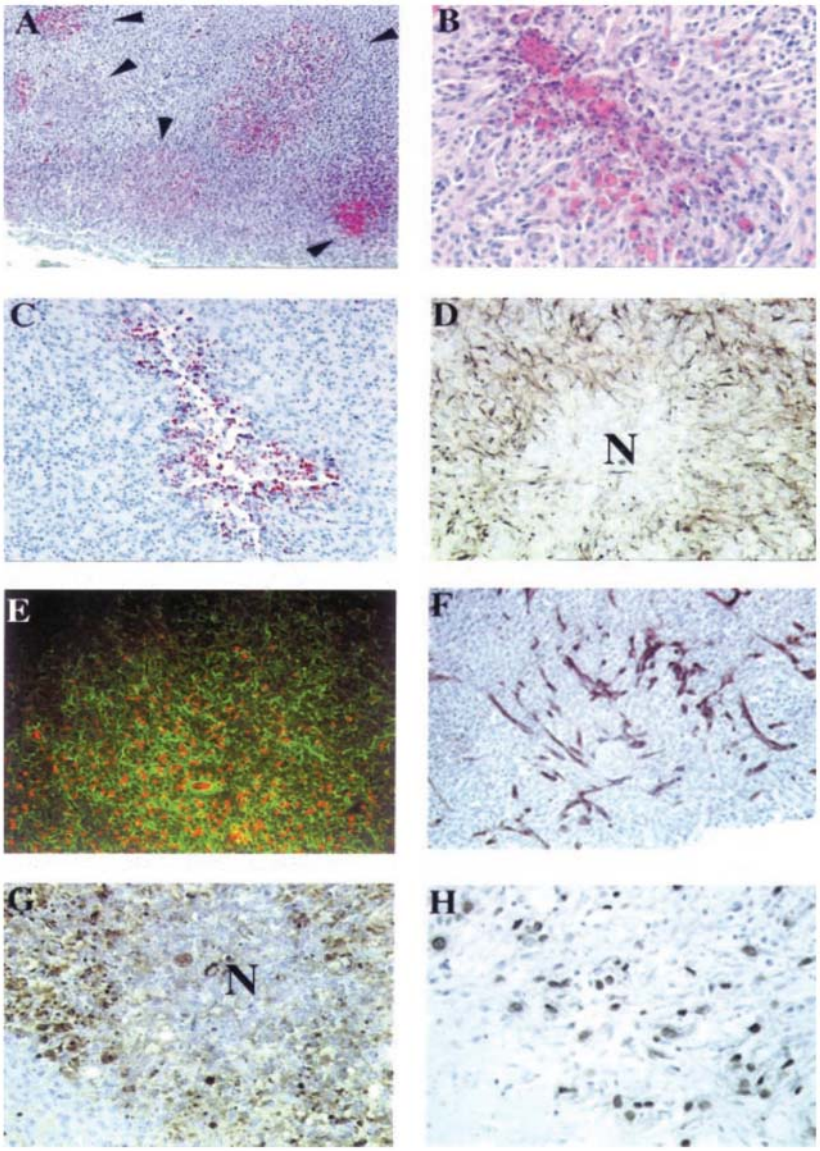


Figure 11. Histopathology of astrocytomas from transgenic mice. Tumors from RasD7 chimeric mice 2 weeks of age that are similar to human GBMs. A) H&E staining (350), illustrating diffusely hypercellular brain, with multiple astrocytoma-like foci (*arrowheads*). B) H&E staining (3200), demonstrating a spindled-cell morphology, nuclear pleomorphism, and numerous mitotic figures in the hypercellular aggregates, with an area of intratumoral hemorrhage and necrosis. C) CD45 immunostaining, demonstrating positively stained macrophages inside zones of necrosis. D) pseudopalisading GFAP positive hypercellular astrocytoma cells around regions of central necrosis (*N*). E) immunofluorescence double-staining for GFAP (*green*) and nuclear localized LacZ (*red*). F) increased vascularity as demonstrated by FactorVIII-positive microvessels. G) increased expression of VEGF by astrocytoma cells around perinecrotic regions. H) increased PCNA immunostaining in astrocytoma regions, demonstrating, proliferating, and infiltrating astrocytoma cells. (Ding et al., 2001)

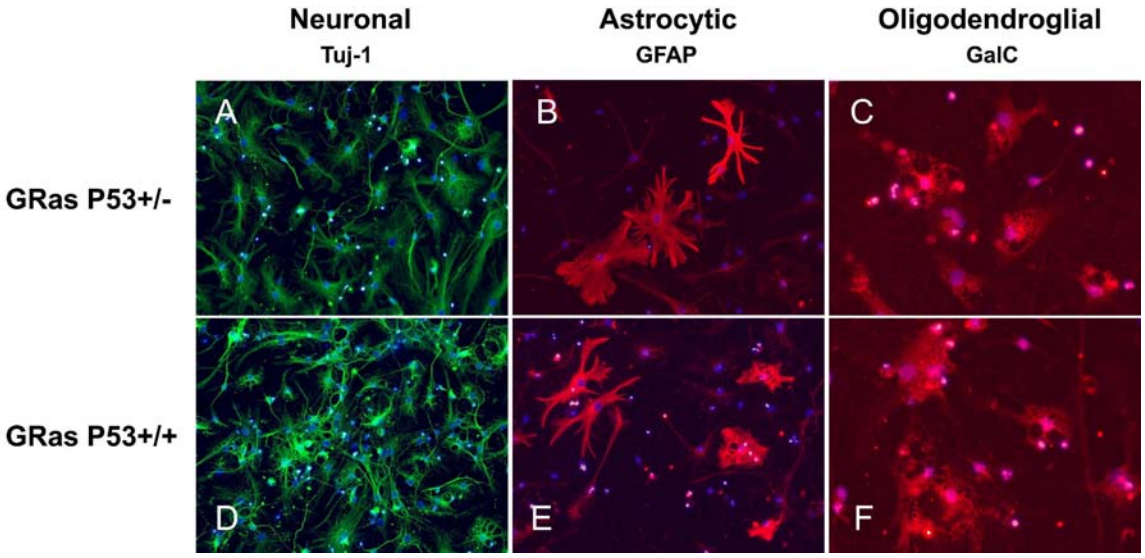


Figure 12. Differentiation of multipotent SVZ cells in GRASp53+/+ and GRASp53+/- mice age P30. (A) Tuj-1 staining of differentiated GRAS P53+/- cells grown in culture demonstrating neuronal differentiation. (B) GFAP staining of differentiated GRAS P53+/- cells grown in culture demonstrating astrocytic differentiation. (C) GalC staining of differentiated GRAS P53+/- cells grown in culture demonstrating oligodendroglial differentiation. (D) Tuj-1 staining of differentiated GRAS P53+/+ cells grown in culture demonstrating neuron nal differentiation. (E) GFAP staining of differentiated GRAS P53+/+ cells grown in culture demonstrating astrocytic differentiation. (F) GalC staining of differentiated GRAS P53+/+ cells grown in culture demonstrating oligodendroglial differentiation. (A-F) Cells are co-stained blue with DAPI nuclear stain.

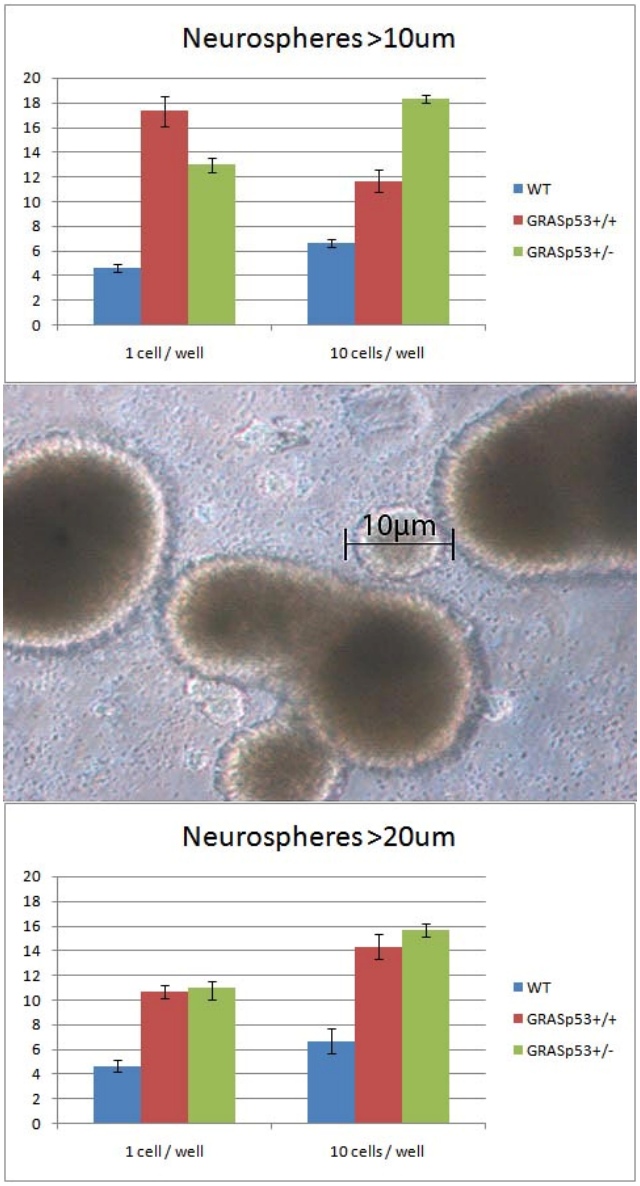


Figure 13. SVZ neurosphere formation in GRAS P53+/+ and GRAS P53+/- mice age P30. Graph Neurospheres>10um displays the number of neurospheres isolated from P30 GRAS P53+/+ and GRas P53+/- SVZs larger than 10 micrometers found in vitro plated at a density of one cell per well and ten cells per well on a 96-well plate. Graph Neurospheres>20um displays the number of neurospheres isolated from P30 GRAS P53+/+ and GRAS P53+/- SVZs larger than 20 micrometers found in vitro plated at a density of one cell per well and ten cells per well on a 96-well plate. The middle image shows neurospheres isolated from P30 GRAS P53+/- SVZ smaller than 10 and larger than 20 micrometers.

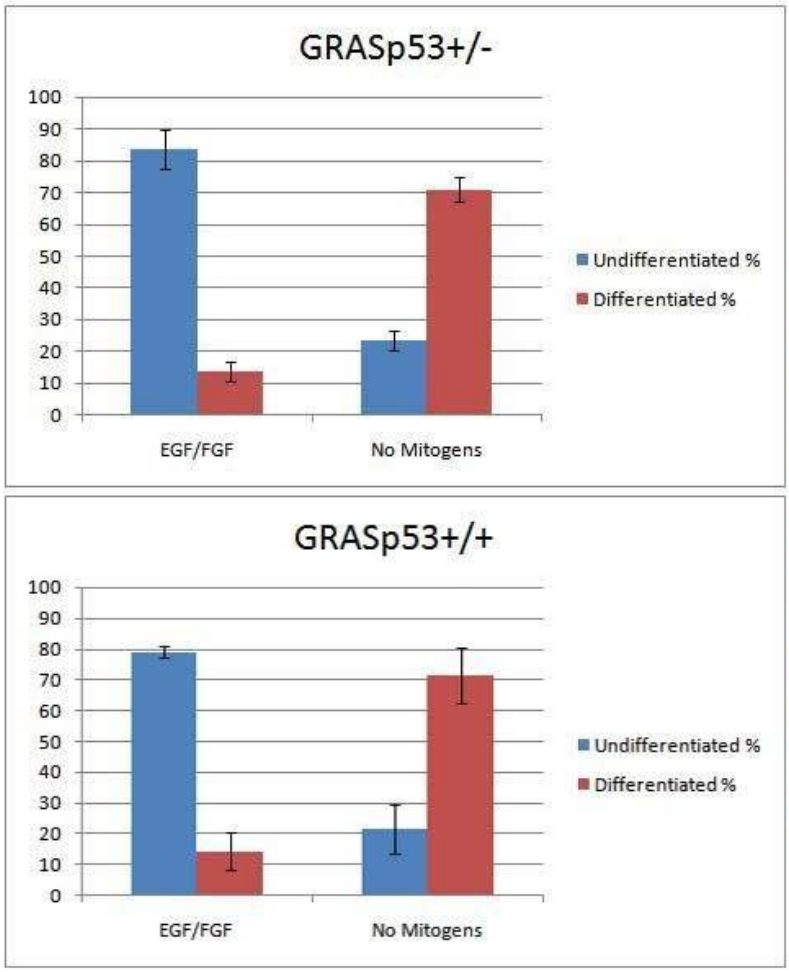


Figure 14. Differentiation or tumor cells from adult (P45) GRASp53+/+ and GRASp53+/- mice. The two graphs to the left show the percentage of tumor cells isolated from adult (P45) GRAS P53+/+ and GRAS P53+/- that differentiate and remain undifferentiated when propagated in culture with mitogens EGF/FGF and without.

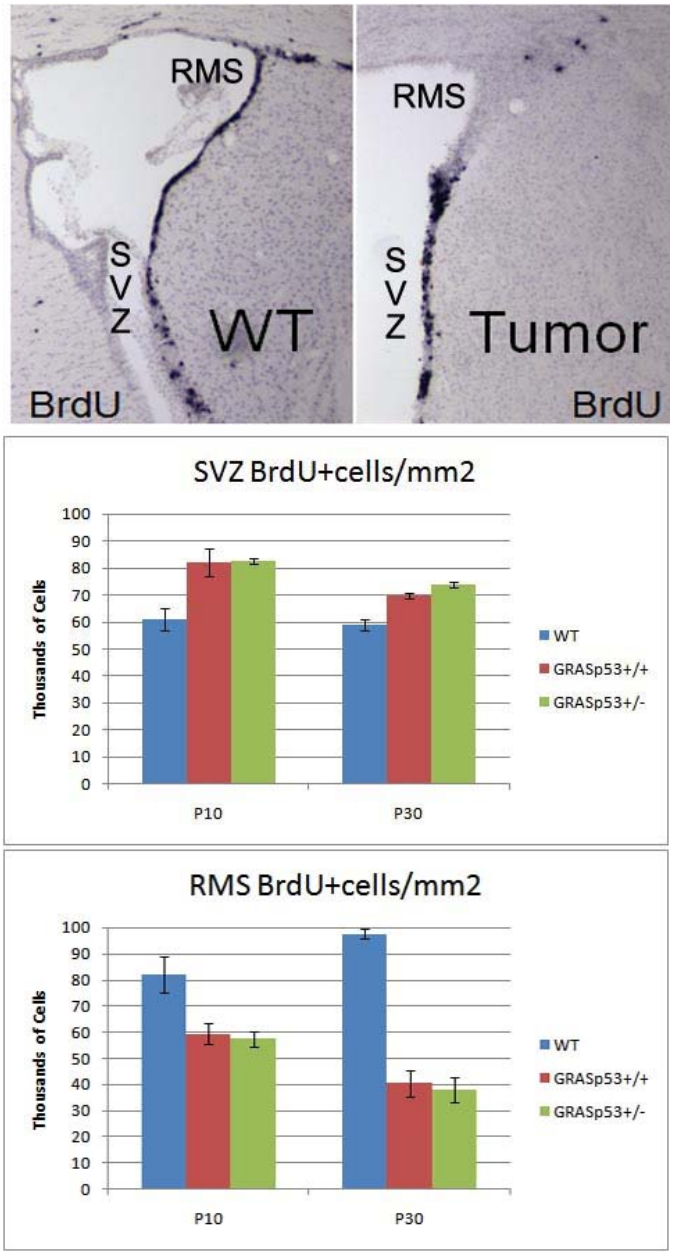


Figure 15. SVZ and early RMS BrdU labeling in P10 and P30 GRAS P53+/+ and GRAS P53+/- mice. The top two images are BrdU stainings of the SVZs and RMSs of a P30 wild type and a P30 tumor bearing GRAS P53+/- mouse, respectively. The bottom two graphs quantify the number of BrdU positive cells found in the SVZ and RMS of P10 and P30 wild type, GRAS P53+/-, and GRAS P53+/+. Note the increase in BrdU staining of the SVZ, and the absence of staining in the RMS of the tumor bearing animals in the images and graphs pointing towards an increase in proliferative activity, but also a disruption of neurogenesis in these animals.

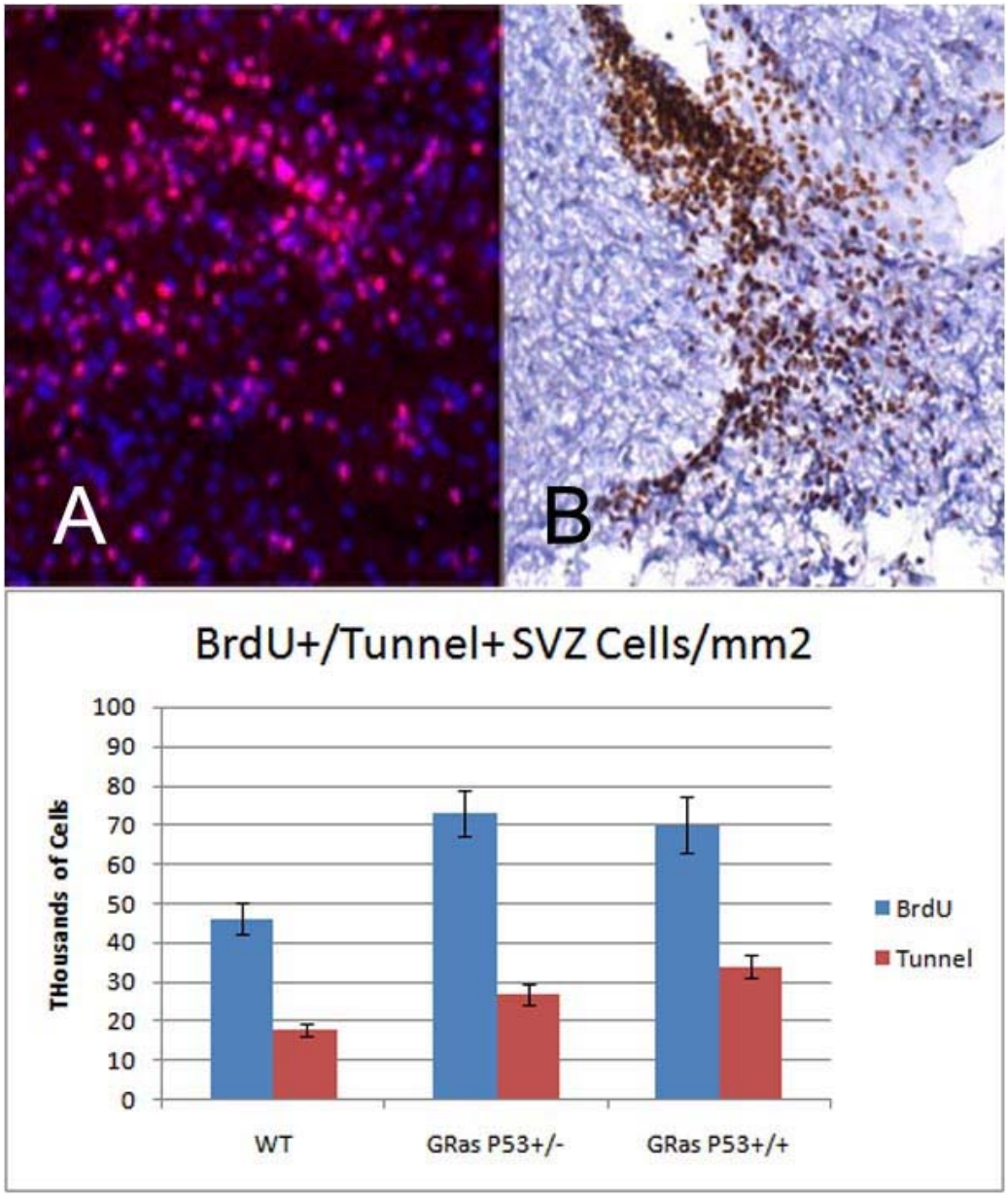


Figure 16. In vivo apoptosis assay in GRAS P53+/+ and GRAS P53+/- P30 SVZ. The graph in this figure quantifies the amount of in vivo BrdU and TUNEL staining in the SVZ of wild type, GRAS P53+/-, and GRASP53+/+ animals. Note the increased proliferation (BrdU), but also the increased cell death (Tunnel) in tumor bearing mice. The difference between TUNEL and BrdU labeling does increase between WT and GRAS P53+/-, and GRASP53+/+ animals. (A) In vivo BrdU staining of proliferative cells in red and DAPI nuclear stain in blue of SVZ cells in a GRAS P53+/- mouse. (B) In vivo Tunnel stain in brown of apoptotic SVZ cells in a GRAS P53+/- mouse.

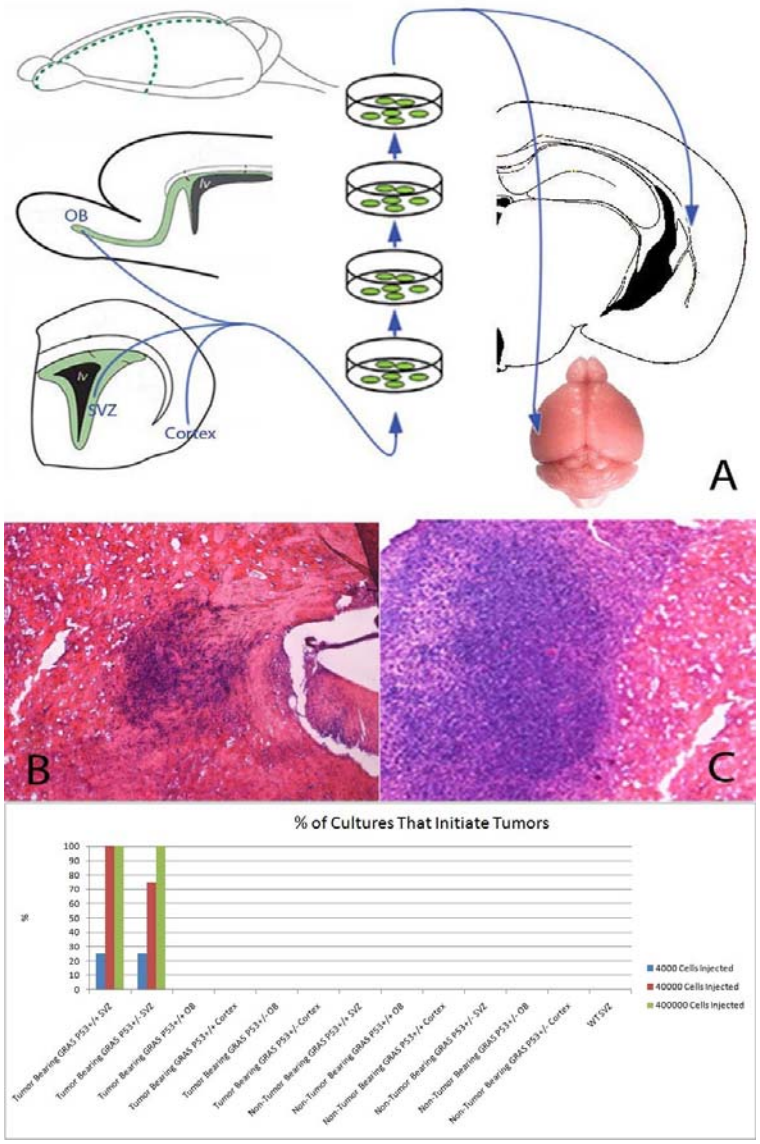


Figure 17. SVZ cultures from tumor bearing GRAS P53+/+ and GRAS P53+/- mice initiate tumors in syngeneic mice. (A) Schema of the design of the transplantation experiment. Cells were isolated separately from the olfactory bulb, SVZ, and cortex of tumor bearing animals and each group was grafted separately into the cortex of different wild type animals to see if they would recapitulate the tumor. In the graph below, only the SVZ cells isolated from the tumor bearing GRAS animals were able to recapitulate tumor after transplantation, and the tumor initiating efficiency increased with the number of cells injected. (B) H&E stain of an original tumor from the cortex of a GRAS P53+/- animal. Cells were isolated from animals with tumors like these for transplantation. (C) H&E stain of the recapitulated tumor in the cortex of a wild type animal following transplantation of SVZ cells from a tumor bearing animal.

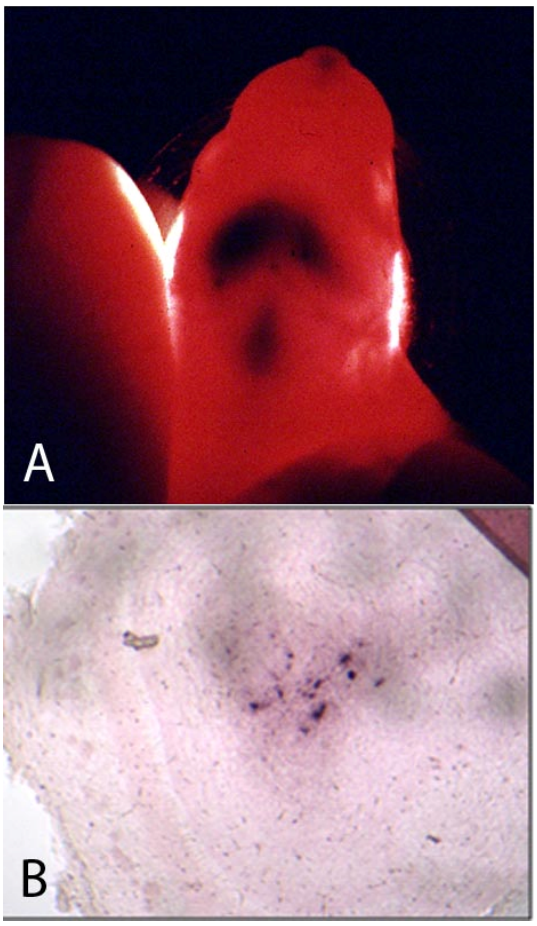


Figure 18. Intraventricular injection of BOLAP retrovirus successfully infects the SVZ. (A) Image is the transillumination of a P2 pup after BOLAP retroviral injection, and shows the encasement of the entire ventricular system after injecting the retrovirus with dye into one lateral ventricle. (B) A BOLAP transfected SVZ would lead to transfected cells migrating to the olfactory bulb, and this figure demonstrates alkaline-phosphatase staining of cells transfected with the BOLAP retrovirus in the olfactory bulb.

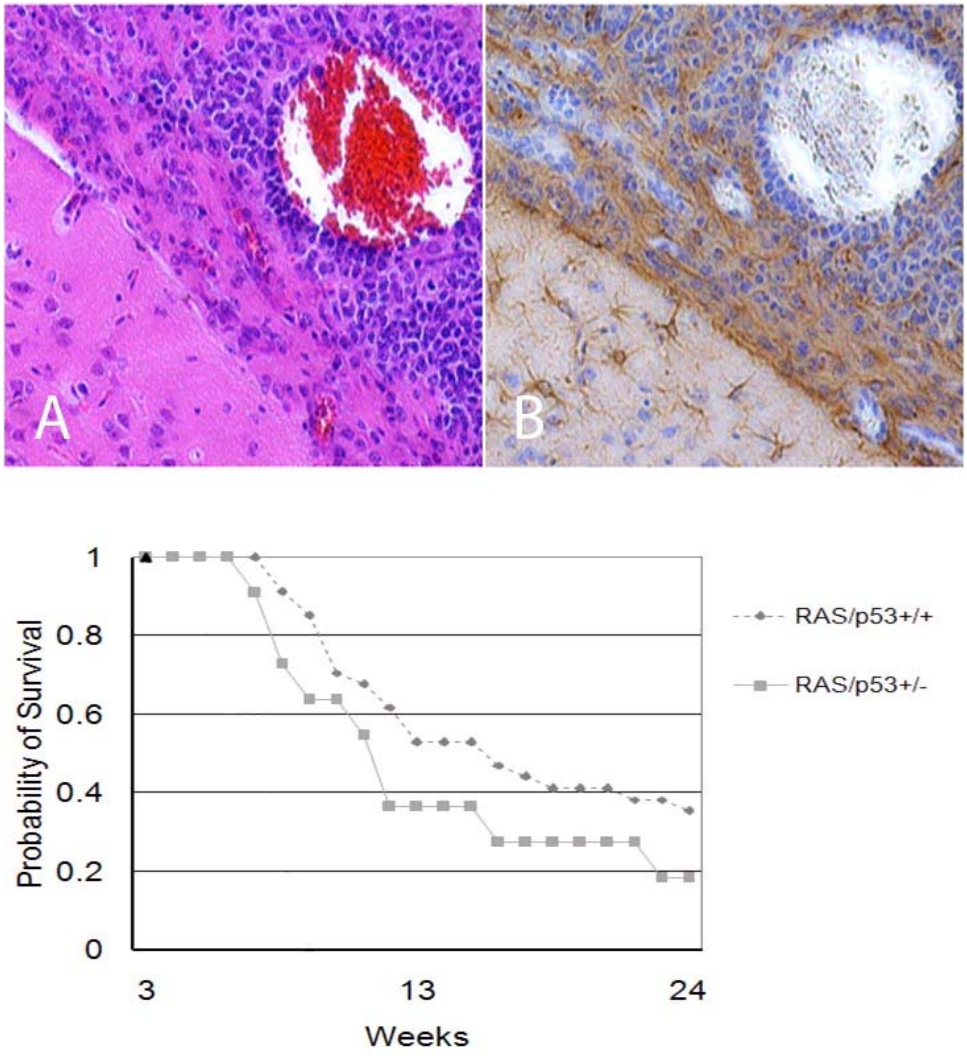


Figure 19. Oncogenic H-Ras in GFAP-positive glial cells induces gliomas in mice. The bottom graph is a survival curve of the GRAS P53+/+ and GRAS P53+/- animals, respectively. (A) H&E staining of a tumor from a Gras P53+/- animal. (B) GFAP staining in brown of the same tumor from A.

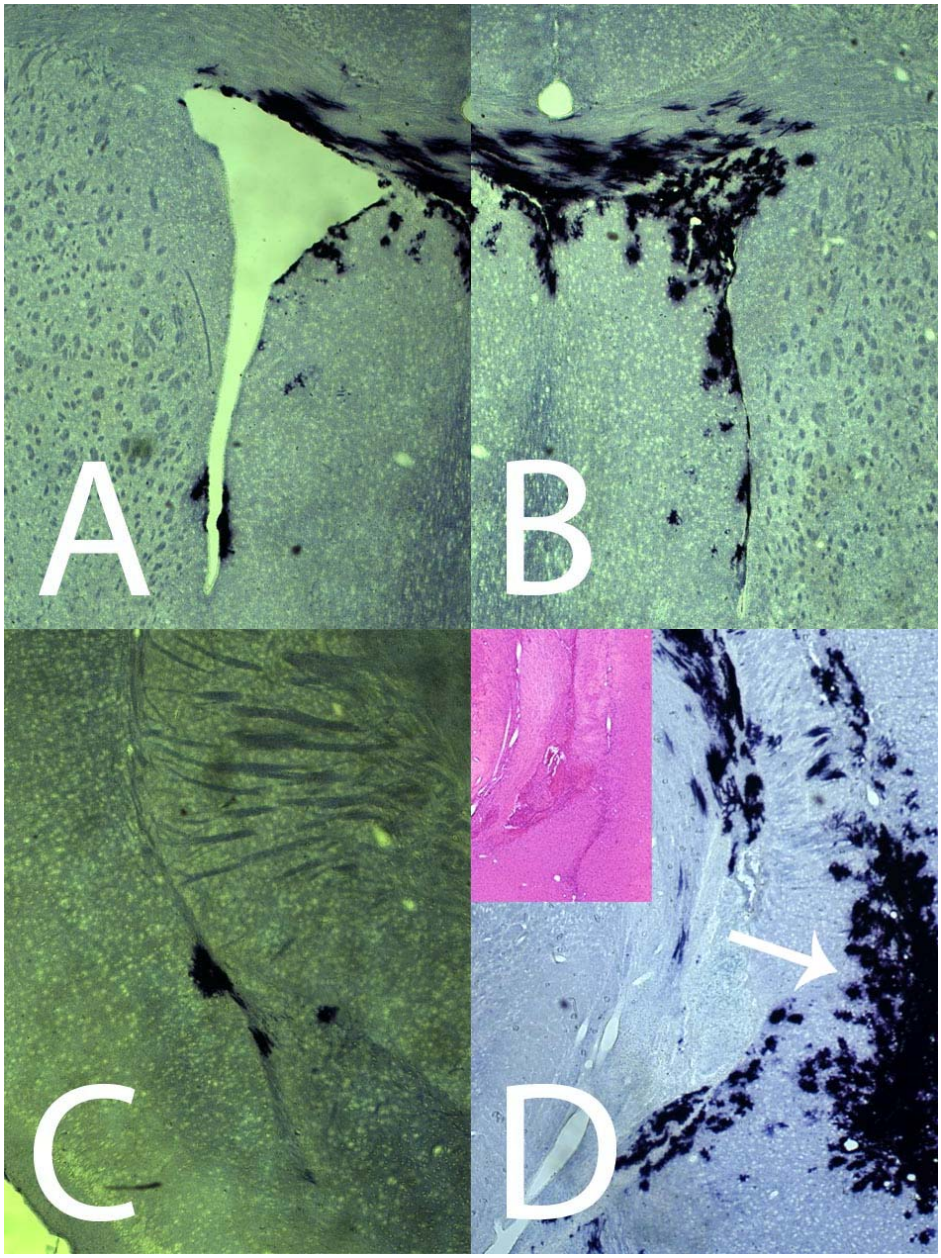


Figure 20. BOLAP injected GRAS P53+/- mice evince robust AP positivity in SVZ and glioma as adult mice (P45). (A) Contra-lateral SVZ stained with alkaline-phosphatase of a GRAS P53+/- mouse injected with the BOLAP retrovirus. (B) Ipsi-lateral SVZ stained with alkaline-phosphatase of a GRAS P53+/- mouse. Note the increased AP staining in this side versus A. (C) Contra-lateral cortex stained with alkaline-phosphotase of the same animal from A and B demonstrating no significant staining and the absence of tumor. (D) Ipsi-lateral cortex stained with alkapline-phosphatase of the same animal from A and B demonstrating significant alkaline-phosphatase staining of the tumor. Inset image is the H&E stain of this same tumor.

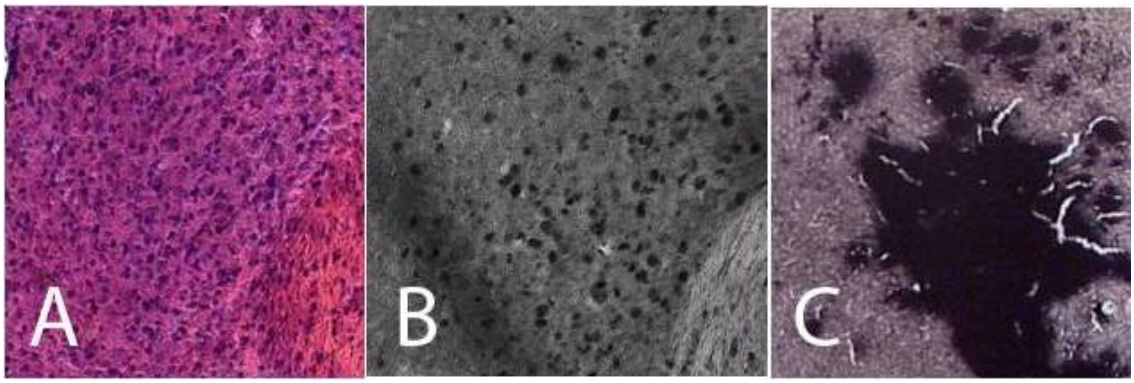


Figure 21. Verification of alkaline phosphatase labeled regions as gliomas in GRAS P53+/- mice serial sections. (A) H&E stain in a serial section of a glioma in a GRAS P53+/- mouse. (B) Ki-67 stain in a serial section of the same glioma and mouse from A. (C) Alkaline-phosphotase stain of a the same glioma and mouse from A.

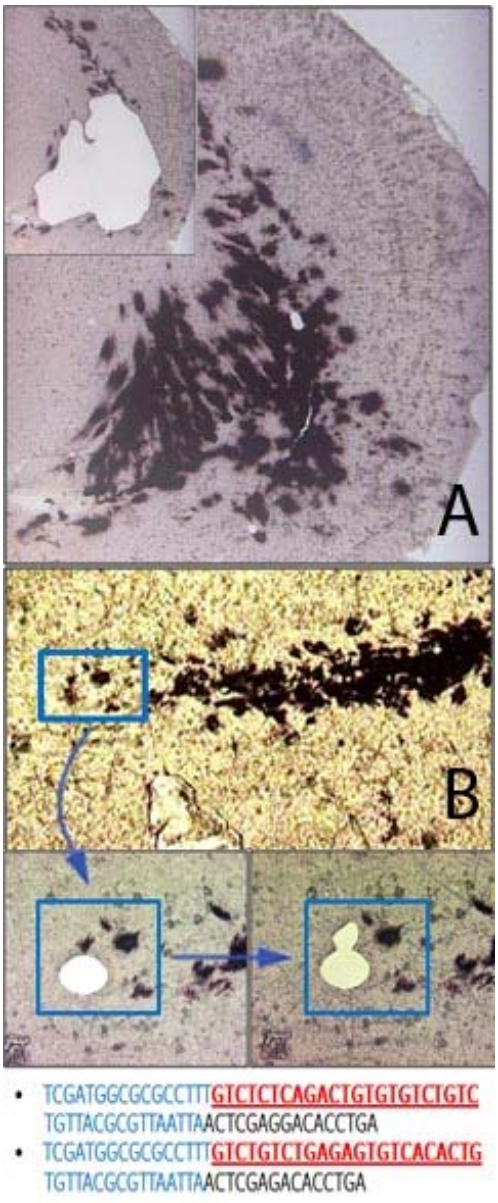


Figure 22. Laser capture microdissection & sequencing of AP+ cells in GRAS P53+/- mice. (A) AP stained tumor from a GRAS P53+/- mouse before laser capture. Inset image shows the same section after laser capture microdissection of the tumor. (B) This figure demonstrates the laser capture microdissection of single cells. The first image is of a AP stained tumor from a GRAS P53+/- mouse before laser capture. The following figures below are magnified images of the blue box in B, and show the single cell laser capture of two single cells from that same sample. The two DNA sequences below are the retroviral tags retrieved from those two single cell samples., with the base pairs in red being the unique BOLAP oligonucleotide library region.

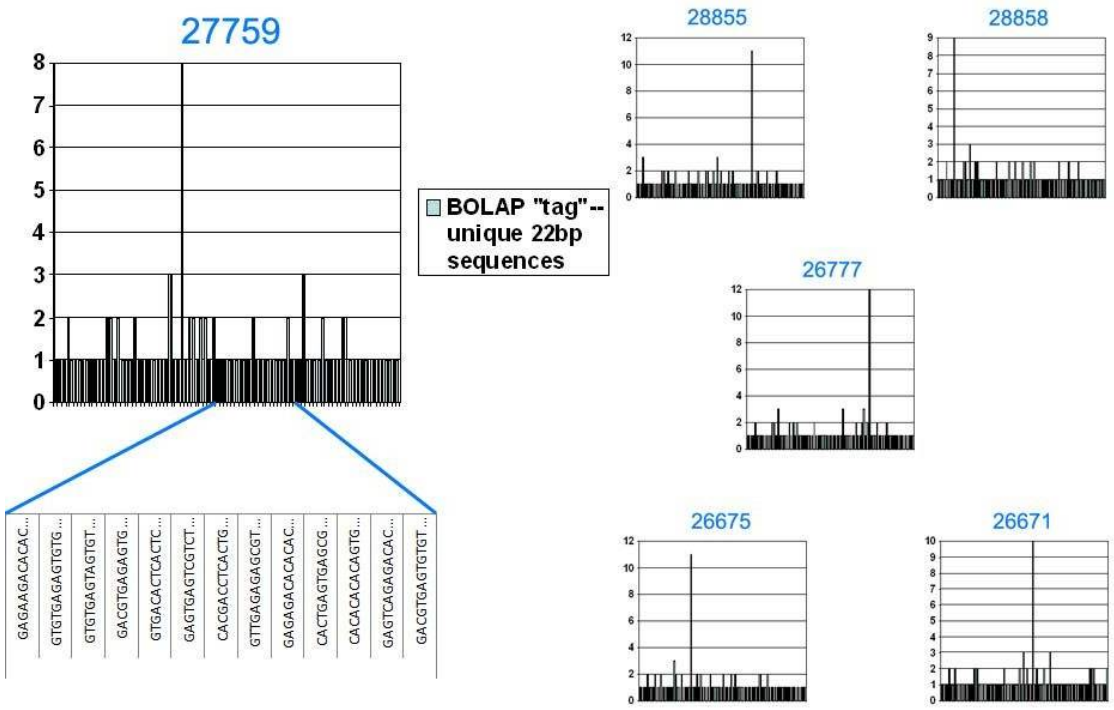


Figure 23. Gliomas are comprised of heterogeneous tumor clones and dominant clone. Figure is of the tumor clone quantification of six tumor bearing GRAS P53+/- mice. The enlarged graph to the left demonstrates that each value on the horizontal axis represents one unique BOLAP 22bp sequence. The number of clones of each 'tag' is plotted on the vertical axis.

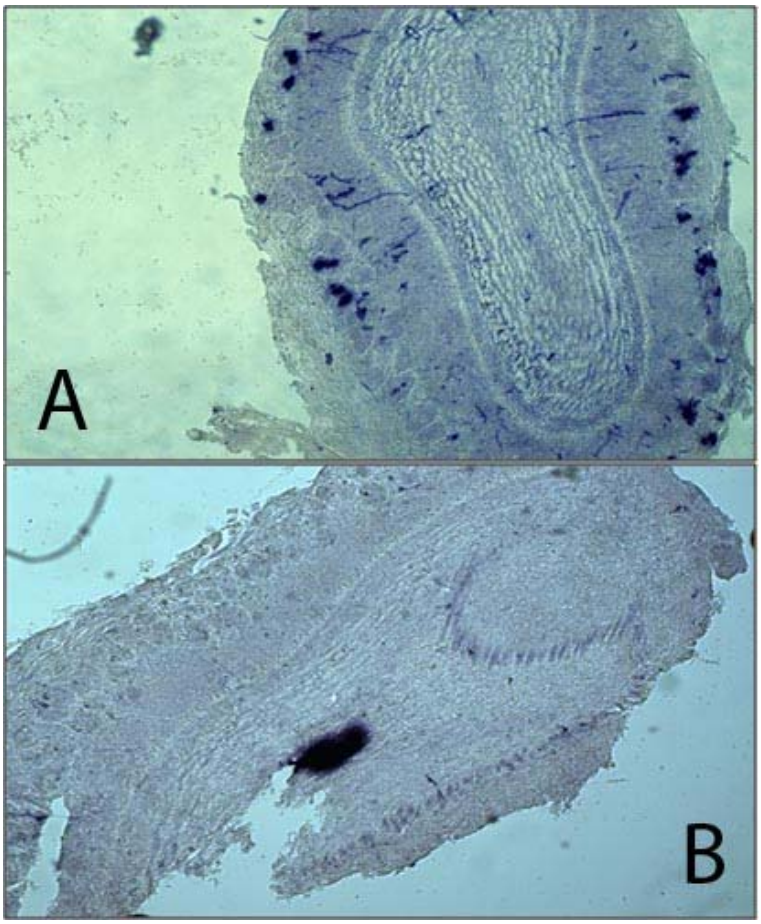


Figure 24. BOLAP-RV staining of GRAS P53+/- olfactory bulb. (A) AP staining of an olfactory bulb from a wild type animal injected with the BOLAP retrovirus. Labeled cells from the SVZ have integrated into the bulb and exhibit neuronal differentiation. (B) AP staining of an olfactory bulb from a GRAS P53+/- animal injected with the BOLAP retrovirus. Fewer labeled cells from the SVZ have integrated into the bulb.

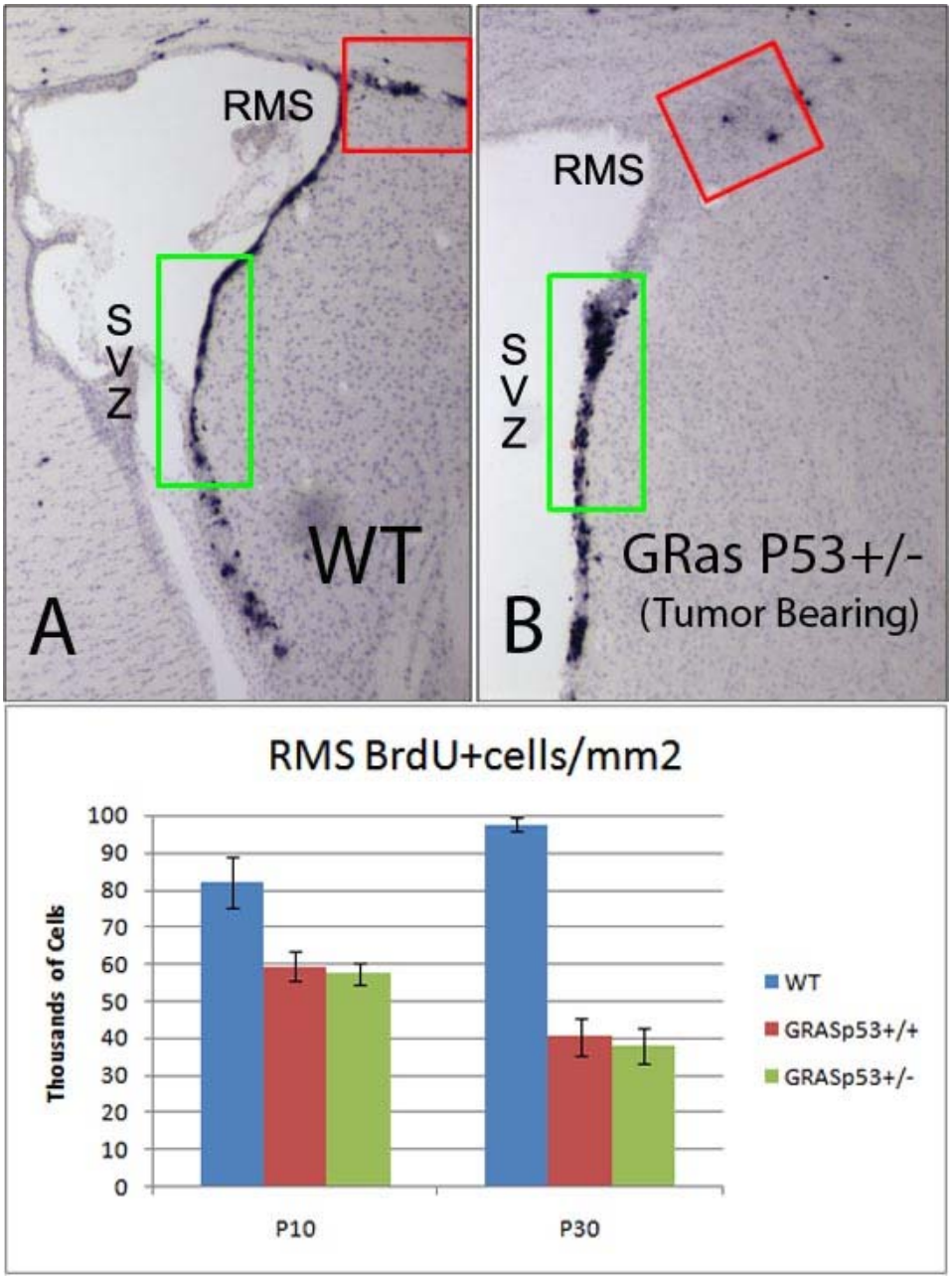


Figure 25. Disrupted RMS in GRAS P53+/- mice. (A) BrdU staining of the SVZ of a wild type mouse. The green and red boxes display an intact SVZ and RMS, respectively. (B) BrdU staining of the SVZ of a tumor bearing GRAS P53+/- mouse. The green and red boxes display a disrupted SVZ and RMS, respectively, when contrasted with the wild type. The early RMS is nearly absent in B suggesting that the RMS has been disrupted.

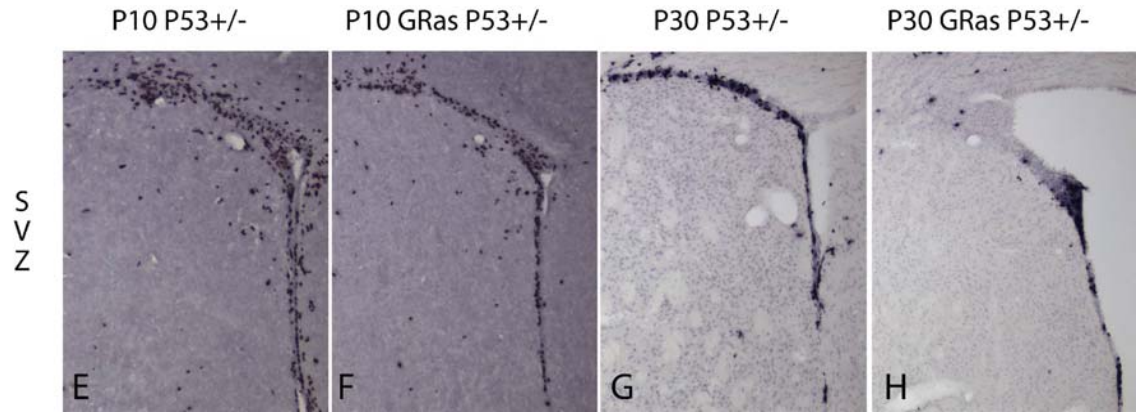


Figure 26. RMS disruption requires oncogenic RAS. (E) BrdU stained SVZ and RMS of a P10 P53+/- animal. (F) Similar BrdU staining in the SVZ and RMS of a P10 GRAS P53+/- when contrasted with a non-tumor bearing animal E. (G) BrdU stained SVZ of a P30 P53+/- animal. (H) Decreased BrdU staining, with near absence of proliferative cells within the RMS, in the SVZ of a P30 GRAS P53+/- tumor bearing with near absence of proliferative cells within the RMS.

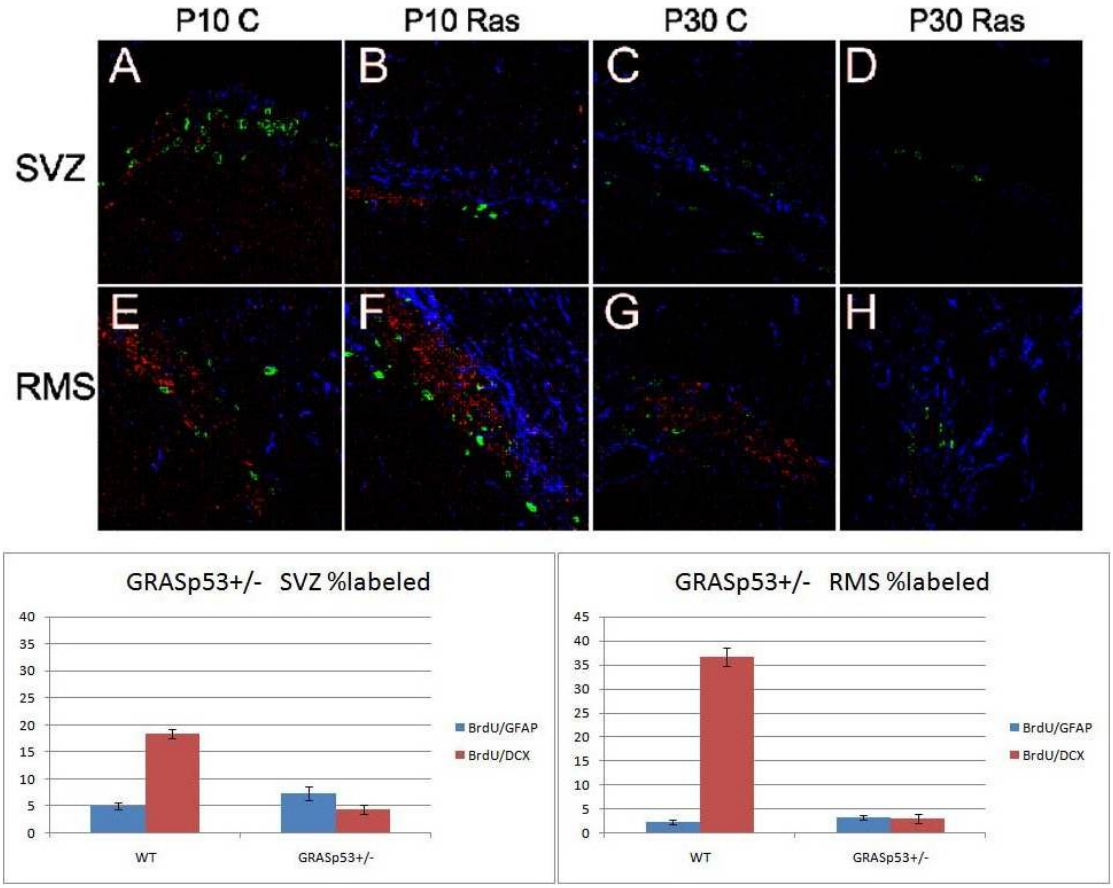


Figure 27. Reduced doublecortin positive cells in SVZ and RMS of GRASp53+/- mice. Graphs chart the percentage of cells (double labeled with BrdU and DCX) and cells (double labeled with BrdU and GFAP) found in the SVZ and RMS of wild type and GRas P53+/- mice. Doublecortin labels type I and type II neuroblasts, immature neurons, and granule cells. The SVZ of the tumor bearing mice display a marked decrease in neuronally committed cells, and a small increase in glial precursors when contrasted with the wild type mice. The RMS of the tumor bearing mice display a marked decrease in neural precursors when contrasted with wild type mice. All images in this figure are stained for DCX in red, GFAP in blue, and BrdU in green. (A) Image is of a P10 wild type control SVZ. (B) Image is of a P10 GRAS P53+/- SVZ. (C) Image is of a P30 wild type control SVZ. (D) Image is of a P30 GRAS P53+/- SVZ. (E) Image is of the RMS of the same animal from A. (F) Image is of the RMS of the same animal from B. (G) Image is of the RMS of the same animal from C. (H) Image is of RMS of the same animal from D with marked loss of DCX labeling, and absent neurogenesis when compared to control.

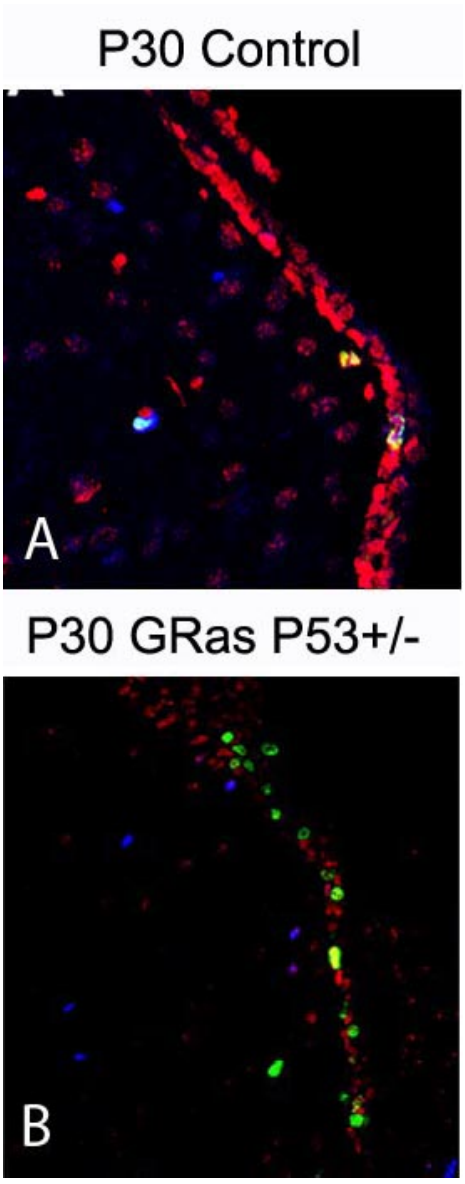


Figure 28. Decreased Pax6 expression in GRAS P53+/- SVZ & RMS. All images are stained for Pax6 in red, Olig2 in blue, and BrdU in green. Pax6 labels neural precursors and immature neurons. Olig2 labels glial progenitors and immature oligodendrocytes. (A) Image of the early RMS and SVZ of a P30 wild type control animal displaying normal neurogenesis through the presence of Pax6 positive neural precursor cells. (B) Image of the SVZ of a P30 GRAS P53+/- animal displaying decreased Pax6 expression and hence, decreased neurogenesis.

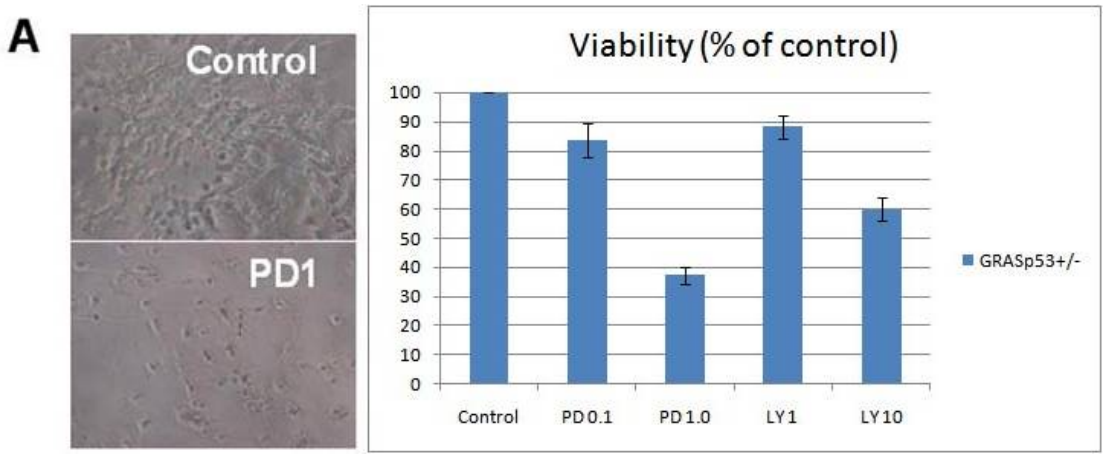


Figure 29. In vitro effects of MAPK and PI3K inhibition on GRAS P53+/- SVZ neurosphere viability. The graph to the right quantifies the percentage of GRAS P53+/- SVZ cell viability in vitro after MAPK and PI3K inhibition with drugs PD and LY, respectively, at different dosages compared to control. All drugs seem to have a dampening effect on cell viability, but the severe effect of PD indicates that blocking MAPK is the most efficient method to reduce viability. (A) Top image display normal control GRAS P53+/- SVZ cells, and bottom image shows the effect of PD on these same cells.

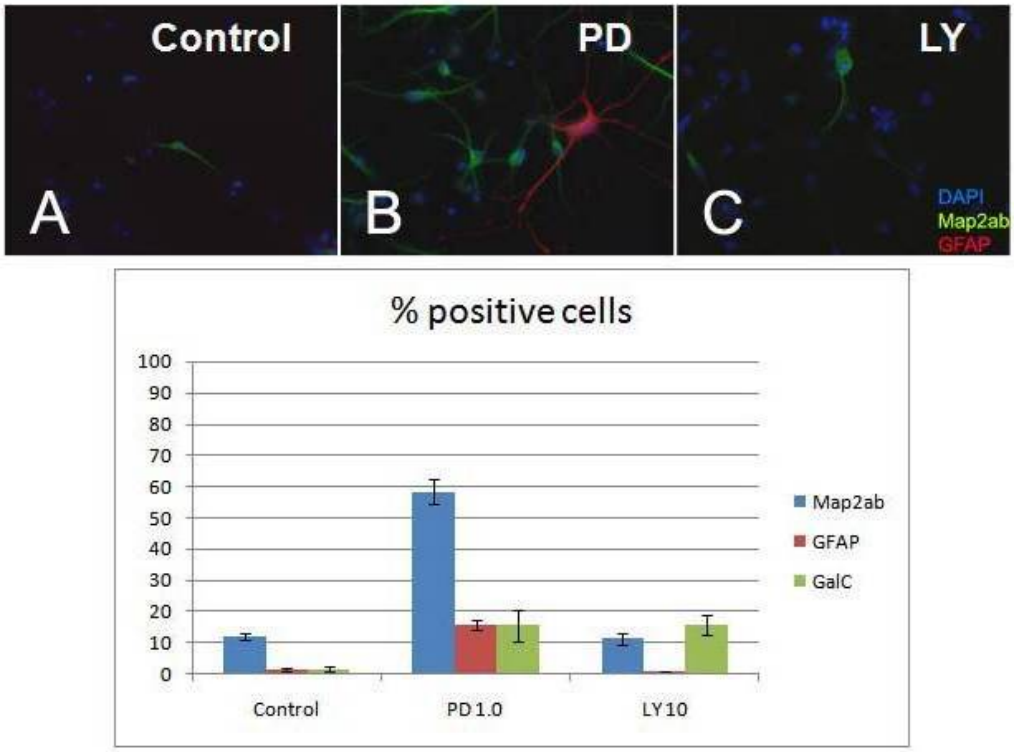


Figure 30. Inhibition of MAPK induces differentiation of GRAS P53+/- SVZ neurospheres. The bottom graph quantifies the percentage of cells positive for markers of neuronal (Map2ab), astrocytic (GFAP), and oligodendroglial (GalC) differentiation in cultures of GRAS P53+/- SVZ cells after administration of PD and LY compared to control. MAPK inhibition via PD induces differentiation of these SVZ neurospheres, increasing the percentage of all markers of differentiation. (A) Image of control cells in vitro with minimal differentiation. (B) Image shows the differentiating effect of PD on SVZ neurospheres with an increase in Map2ab, GFAP, and GalC cells when compared to control (C) Image shows the effect of LY on SVZ neurospheres with an increase in Map2ab, and GalC cells when compared to control.

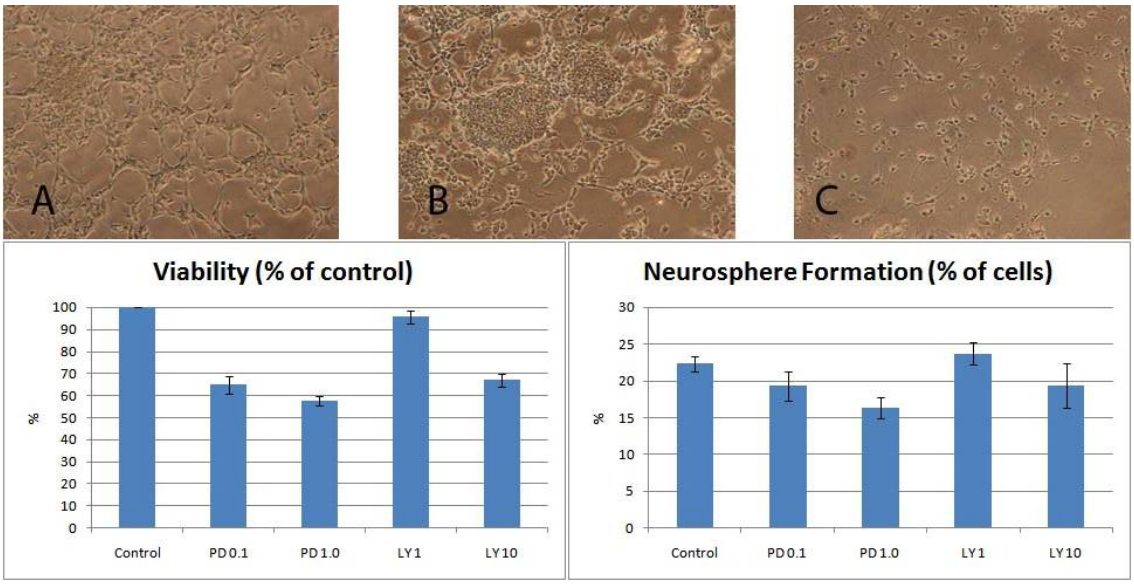


Figure 31. Inhibition of MAPK reduces viability and tumor sphere formation in human primary glioblastoma cultures. The bottom left graph displays the viability of primary human glioblastoma cells after treatments of PD and LY as a percentage of the control sample. The dampening effect on viability of MAPK inhibition via PD in primary human gliobastoma cells. The bottom right graph displays Note the dampening effect on neurosphere formation of MAPK inhibition via PD in primary human glioblastoma cultures. (A) Control sample of human glioblastoma cells without drug administration. (B) Human glioblastoma cells after LY administration. Note that LY seems to increase the amount of neurosphere formation when compared to control A. (C) Human glioblastoma cells after PD administration. Note the reduction in sphere formation and the increase in neuronal differentiation when compared to control.

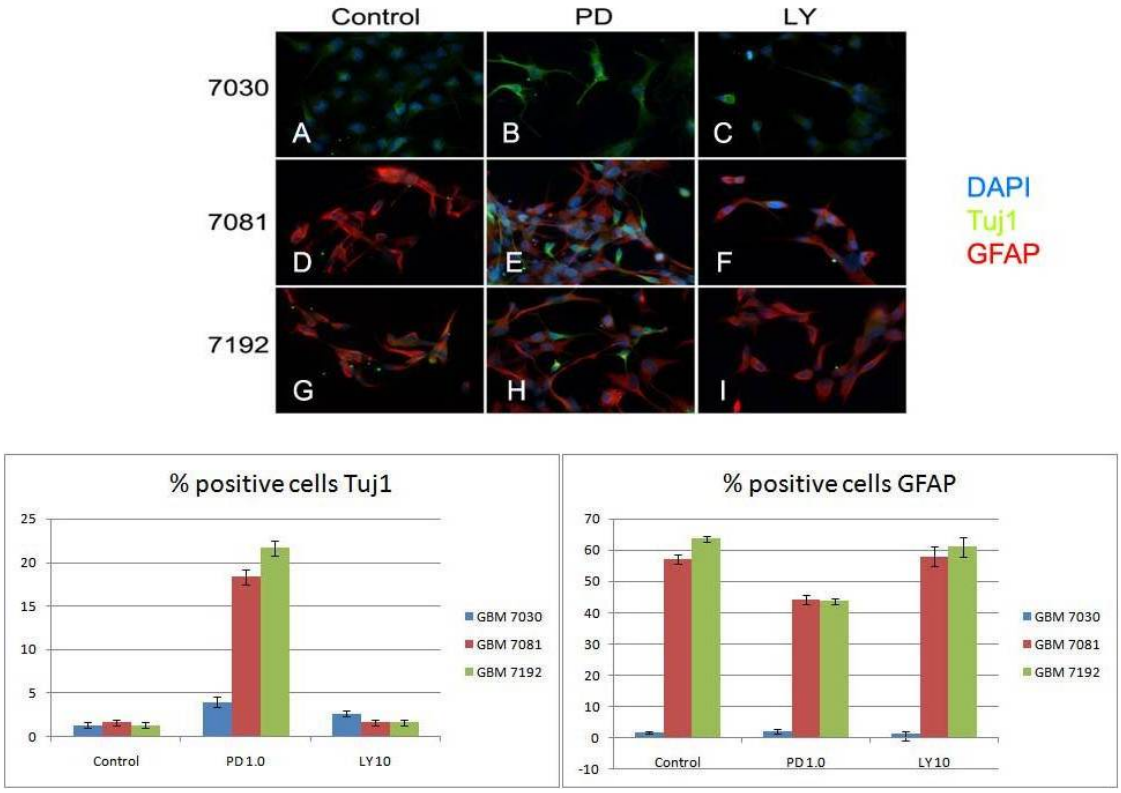


Figure 32. Inhibition of MAPK induces neuronal differentiation in human glioblastoma cells. Bottom left graph quantifies the percentage of Tuj-1 positive cells in three samples of human glioblastoma after PD and LY administration compared to control. Inhibition of MAPK via PD greatly increases the percentage of neuronal differentiated cells (Tuj-1 positive). The graph to the bottom right quantifies the percentage of GFAP positive cells in three samples of human glioblastoma after PD and LY treatments compared to control. Inhibition of MAPK via PD decreases the percentage of glial differentiation (GFAP positive). All images display GFAP staining in red and Tuj-1 staining in green. (A) GBM sample 7030 cells without PD or LY administration. (B) GBM sample 7030 cells after PD administration with a increase in Tuj-1 staining and neuronal differentiation compared to control A. (C) GBM sample 7030 cells after LY administration with little change when compared to control A. (D) GBM sample 7081 cells without PD or LY administration. (E) GBM sample 7081 cells after PD administration with a increase in Tuj-1 staining and neuronal differentiation compared to control D. (F) GBM sample 7081 cells after LY administration with little change when compared to control D. (G) GBM sample 7192 cells without PD or LY administration. (H) GBM sample 7192 cells after PD administration with a increase in Tuj-1 staining and neuronal differentiation compared to control G. (I) GBM sample 7192 cells after LY administration with little change when compared to control G.

REFERENCES

AL-HAJJ, M., WICHA, M., BENITO-HERNANDEZ, A., MORRISON, S. & CLARKE, M. (2003) Prospective identification of tumorigenic breast cancer cells. *Proc Natl Acad Sci U S A,* 100**,** 3983-8.

ALLEN, E. (1912) The cessation of mitosis in the central nervous system of albino rat. *J. Comp. Neurol.***,** 547–68.

ALTMAN, J. (1969) Autoradiographic and histological studies of postnatal neurogenesis. IV. Cell proliferation and migration in the anterior forebrain, with special reference to persisting neurogenesis in the olfactory bulb. *J Comp Neurol,* 137**,** 433-57.

ALTMAN, J. & DAS, G. (1965) Autoradiographic and histological evidence of postnatal hippocampal neurogenesis in rats. *J Comp Neurol,* 124**,** 319-35.

ALTMAN, J. & DAS, G. (1966) Autoradiographic and histological studies of postnatal neurogenesis. I. A longitudinal investigation of the kinetics, migration and transformation of cells incorporating tritiated thymidine in neonate rats, with special reference to postnatal neurogenesis in some brain regions. *J Comp Neurol,* 126**,** 337-89.

ALVAREZ-BUYLLA, A. & LIM, D. (2004) For the long run: maintaining germinal niches in the adult brain. *Neuron,* 41**,** 683-6.

ALVAREZ-BUYLLA, A., SERI, B. & DOETSCH, F. (2002) Identification of neural stem cells in the adult vertebrate brain. *Brain Res Bull,* 57**,** 751-8.

AUGUSTE, P., GÜRSEL, D., LEMIÈRE, S., REIMERS, D., CUEVAS, P., CARCELLER, F., DI SANTO, J. & BIKFALVI, A. (2001) Inhibition of fibroblast growth factor/fibroblast growth factor receptor activity in glioma cells impedes tumor growth by both angiogenesis-dependent and -independent mechanisms. *Cancer Res,* 61**,** 1717-26.

BACHOO, R., MAHER, E., LIGON, K., SHARPLESS, N., CHAN, S., YOU, M., TANG, Y., DEFRANCES, J., STOVER, E., WEISSLEDER, R., ROWITCH, D., LOUIS, D. & DEPINHO, R. (2002) Epidermal growth factor receptor and Ink4a/Arf: convergent mechanisms governing terminal differentiation and transformation along the neural stem cell to astrocyte axis. *Cancer Cell,* 1**,** 269-77.

BAILEY, P. & CUSHING, H. (1926) *A classification of the tumors of the glioma group on a histogenetic basis with a correlated study of prognosis,* Philadelphia, London, J. B. Lippincott Company.

BAKER, S. & MCKINNON, P. (2004) Tumour-suppressor function in the nervous system. *Nat Rev Cancer,* 4**,** 184-96.

BELLUZZI, O., BENEDUSI, M., ACKMAN, J. & LOTURCO, J. (2003) Electrophysiological differentiation of new neurons in the olfactory bulb. *J Neurosci,* 23**,** 10411-8.

BERGER, F., GAY, E., PELLETIER, L., TROPEL, P. & WION, D. (2004) Development of gliomas: potential role of asymmetrical cell division of neural stem cells. *Lancet Oncol,* 5**,** 511-4.

BOLTEUS, A. & BORDEY, A. (2004) GABA release and uptake regulate neuronal precursor migration in the postnatal subventricular zone. *J Neurosci,* 24**,** 7623-31.

BOS, J. (1989) ras oncogenes in human cancer: a review. *Cancer Res,* 49**,** 4682-9.

BRUNJES, P. & FRAZIER, L. (1986) Maturation and plasticity in the olfactory system of vertebrates. *Brain Res,* 396**,** 1-45.

BRYANS, W. (1959) Mitotic Activity in the Brain of the Albino Rat. *Anat. Record***,** 65-73.

BUZZEO, M., SCOTT, E. & COGLE, C. (2007) The hunt for cancer-initiating cells: a history stemming from leukemia. *Leukemia,* 21**,** 1619-27.

CAJAL, S. (1955) Studies on the Cerebral Cortex. Chicago, Year Book Publishers.

CARLETON, A., PETREANU, L., LANSFORD, R., ALVAREZ-BUYLLA, A. & LLEDO, P. (2003) Becoming a new neuron in the adult olfactory bulb. *Nat Neurosci,* 6**,** 507-18.

CEPKO, C., FIELDS-BERRY, S., RYDER, E., AUSTIN, C. & GOLDEN, J. (1998) Lineage analysis using retroviral vectors. *Curr Top Dev Biol,* 36**,** 51-74.

CHEKENYA, M. & PILKINGTON, G. (2002) NG2 precursor cells in neoplasia: functional, histogenesis and therapeutic implications for malignant brain tumours. *J Neurocytol,* 31**,** 507-21.

CHENN, A. & WALSH, C. (2003) Increased neuronal production, enlarged forebrains and cytoarchitectural distortions in beta-catenin overexpressing transgenic mice. *Cereb Cortex,* 13**,** 599-606.

CHOW, D. & GREENBERG, A. (1980) The generation of tumor heterogeneity in vivo. *Int J Cancer,* 25**,** 261-5.

CLARKE, M., DICK, J., DIRKS, P., EAVES, C., JAMIESON, C., JONES, D., VISVADER, J., WEISSMAN, I. & WAHL, G. (2006) Cancer stem cells--perspectives on current status and future directions: AACR Workshop on cancer stem cells. *Cancer Res,* 66**,** 9339-44.

COPELAND, D. & BIGNER, D. (1977) The role of the subependymal plate in avian sarcoma virus brain tumor induction: comparison of incipient tumors in neonatal and adult rats. *Acta Neuropathol (Berl),* 38**,** 1-6.

COPELAND, D., VOGEL, F. & BIGNER, D. (1975) The induction of intractranial neoplasms by the inoculation of avian sarcoma virus in perinatal and adult rats. *J Neuropathol Exp Neurol,* 34**,** 340-58.

CURTIS, M., KAM, M., NANNMARK, U., ANDERSON, M., AXELL, M., WIKKELSO, C., HOLTÅS, S., VAN ROON-MOM, W., BJÖRK-ERIKSSON, T., NORDBORG, C., FRISÉN, J., DRAGUNOW, M., FAULL, R. & ERIKSSON, P. (2007) Human neuroblasts migrate to the olfactory bulb via a lateral ventricular extension. *Science,* 315**,** 1243-9.

DAHLSTRAND, J., COLLINS, V. & LENDAHL, U. (1992) Expression of the class VI intermediate filament nestin in human central nervous system tumors. *Cancer Res,* 52**,** 5334-41.

DAI, C., CELESTINO, J., OKADA, Y., LOUIS, D., FULLER, G. & HOLLAND, E. (2001) PDGF autocrine stimulation dedifferentiates cultured astrocytes and induces oligodendrogliomas and oligoastrocytomas from neural progenitors and astrocytes in vivo. *Genes Dev,* 15**,** 1913-25.

DEISSEROTH, K., SINGLA, S., TODA, H., MONJE, M., PALMER, T. & MALENKA, R. (2004) Excitation-neurogenesis coupling in adult neural stem/progenitor cells. *Neuron,* 42**,** 535-52.

DING, H., RONCARI, L., SHANNON, P., WU, X., LAU, N., KARASKOVA, J., GUTMANN, D., SQUIRE, J., NAGY, A. & GUHA, A. (2001) Astrocyte-specific expression of activated p21-ras results in malignant astrocytoma formation in a transgenic mouse model of human gliomas. *Cancer Res,* 61**,** 3826-36.

DOETSCH, F. (2003) A niche for adult neural stem cells. *Curr Opin Genet Dev,* 13**,** 543-50.

DOETSCH, F., CAILLÉ, I., LIM, D., GARCÍA-VERDUGO, J. & ALVAREZ-BUYLLA, A. (1999a) Subventricular zone astrocytes are neural stem cells in the adult mammalian brain. *Cell,* 97**,** 703-16.

DOETSCH, F., GARCÍA-VERDUGO, J. & ALVAREZ-BUYLLA, A. (1999b) Regeneration of a germinal layer in the adult mammalian brain. *Proc Natl Acad Sci U S A,* 96**,** 11619-24.

DOETSCH, F., PETREANU, L., CAILLE, I., GARCIA-VERDUGO, J. & ALVAREZ-BUYLLA, A. (2002) EGF converts transit-amplifying neurogenic precursors in the adult brain into multipotent stem cells. *Neuron,* 36**,** 1021-34.

ERIKSSON, P., PERFILIEVA, E., BJÖRK-ERIKSSON, T., ALBORN, A., NORDBORG, C., PETERSON, D. & GAGE, F. (1998) Neurogenesis in the adult human hippocampus. *Nat Med,* 4**,** 1313-7.

FELDKAMP, M., LAU, N., RAK, J., KERBEL, R. & GUHA, A. (1999) Normoxic and hypoxic regulation of vascular endothelial growth factor (VEGF) by astrocytoma cells is mediated by Ras. *Int J Cancer,* 81**,** 118-24.

FIDLER, I. & HART, I. (1982) Biological diversity in metastatic neoplasms: origins and implications. *Science,* 217**,** 998-1003.

FIELDS-BERRY, S., HALLIDAY, A. & CEPKO, C. (1992) A recombinant retrovirus encoding alkaline phosphatase confirms clonal boundary assignment in lineage analysis of murine retina. *Proc Natl Acad Sci U S A,* 89**,** 693-7.

FULCI, G., LABUHN, M., MAIER, D., LACHAT, Y., HAUSMANN, O., HEGI, M., JANZER, R., MERLO, A. & VAN MEIR, E. (2000) p53 gene mutation and ink4a-arf deletion appear to be two mutually exclusive events in human glioblastoma. *Oncogene,* 19**,** 3816-22.

GLASS, R., SYNOWITZ, M., KRONENBERG, G., WALZLEIN, J., MARKOVIC, D., WANG, L., GAST, D., KIWIT, J., KEMPERMANN, G. & KETTENMANN, H. (2005) Glioblastoma-induced attraction of endogenous neural precursor cells is associated with improved survival. *J Neurosci,* 25**,** 2637-46.

GLOBUS, J. & KUHLENBECK, H. (1942) Tumors of the Striaticthalamic and Related Regions. Their Probable Source of Origin and More Common Forms. *Arch. Pathol.,* 34.

GLOBUS, J. H., KUHLENBECK, H (1944) The subependymal plate (matrix) and its relationship to brain tumors of the ependymal type. J. Neuropathol. Exp. Neurol.

GOLDEN, J. & CEPKO, C. (1996) Clones in the chick diencephalon contain multiple cell types and siblings are widely dispersed. *Development,* 122**,** 65-78.

GOLDSTEIN, D., BLASCO, L. & HARRIS, H. (1980a) Placental alkaline phosphatase in nonmalignant human cervix. *Proc Natl Acad Sci U S A,* 77**,** 4226-8.

GOLDSTEIN, D., ROGERS, C. & HARRIS, H. (1980b) Expression of alkaline phosphatase loci in mammalian tissues. *Proc Natl Acad Sci U S A,* 77**,** 2857-60.

GOLDSTEIN, D., ROGERS, C. & HARRIS, H. (1982) Evolution of alkaline phosphatases in primates. *Proc Natl Acad Sci U S A,* 79**,** 879-83.

GOTTLIEB, D. (2002) Large-scale sources of neural stem cells. *Annu Rev Neurosci,* 25**,** 381-407.

GOULD, V., LEE, I., WIEDENMANN, B., MOLL, R., CHEJFEC, G. & FRANKE, W. (1986) Synaptophysin: a novel marker for neurons, certain neuroendocrine cells, and their neoplasms. *Hum Pathol,* 17**,** 979-83.

GRITTI, A., PARATI, E., COVA, L., FROLICHSTHAL, P., GALLI, R., WANKE, E., FARAVELLI, L., MORASSUTTI, D., ROISEN, F., NICKEL, D. & VESCOVI, A. (1996) Multipotential stem cells from the adult mouse brain proliferate and self-renew in response to basic fibroblast growth factor. *J Neurosci,* 16**,** 1091-100.

GROSS, C. (2000) Neurogenesis in the adult brain: death of a dogma. *Nat Rev Neurosci,* 1**,** 67-73.

GROSZER, M., ERICKSON, R., SCRIPTURE-ADAMS, D., LESCHE, R., TRUMPP, A., ZACK, J., KORNBLUM, H., LIU, X. & WU, H. (2001) Negative regulation of neural stem/progenitor cell proliferation by the Pten tumor suppressor gene in vivo. *Science,* 294**,** 2186-9.

GUHA, A., FELDKAMP, M., LAU, N., BOSS, G. & PAWSON, A. (1997) Proliferation of human malignant astrocytomas is dependent on Ras activation. *Oncogene,* 15**,** 2755-65.

HACK, M., SUGIMORI, M., LUNDBERG, C., NAKAFUKU, M. & GÖTZ, M. (2004) Regionalization and fate specification in neurospheres: the role of Olig2 and Pax6. *Mol Cell Neurosci,* 25**,** 664-78.

HAMILTON, A. (1901) The division of differentiated cells in the central nervous system of the white rat. *J. Comp. Neurol.***,** 297–320.

HITOSHI, S., ALEXSON, T., TROPEPE, V., DONOVIEL, D., ELIA, A., NYE, J., CONLON, R., MAK, T., BERNSTEIN, A. & VAN DER KOOY, D. (2002)

Notch pathway molecules are essential for the maintenance, but not the generation, of mammalian neural stem cells. *Genes Dev,* 16**,** 846-58.

HOLLAND, E., CELESTINO, J., DAI, C., SCHAEFER, L., SAWAYA, R. & FULLER, G. (2000) Combined activation of Ras and Akt in neural progenitors induces glioblastoma formation in mice. *Nat Genet,* 25**,** 55-7.

HOLLAND, E., HIVELY, W., GALLO, V. & VARMUS, H. (1998) Modeling mutations in the G1 arrest pathway in human gliomas: overexpression of CDK4 but not loss of INK4a-ARF induces hyperploidy in cultured mouse astrocytes. *Genes Dev,* 12**,** 3644-9.

HOPEWELL, J. & WRIGHT, E. (1969) The importance of implantation site in cerebral carcinogenesis in rats. *Cancer Res,* 29**,** 1927-31.

HUNTLY, B. & GILLILAND, D. (2005) Leukaemia stem cells and the evolution of cancer-stem-cell research. *Nat Rev Cancer,* 5**,** 311-21.

ICHIMURA, K., BOLIN, M., GOIKE, H., SCHMIDT, E., MOSHREF, A. & COLLINS, V. (2000) Deregulation of the p14ARF/MDM2/p53 pathway is a prerequisite for human astrocytic gliomas with G1-S transition control gene abnormalities. *Cancer Res,* 60**,** 417-24.

IGNATOVA, T., KUKEKOV, V., LAYWELL, E., SUSLOV, O., VRIONIS, F. & STEINDLER, D. (2002) Human cortical glial tumors contain neural stem-like cells expressing astroglial and neuronal markers in vitro. *Glia,* 39**,** 193-206.

JACKSON, E. & ALVAREZ-BUYLLA, A. (2008) Characterization of Adult Neural Stem Cells and Their Relation to Brain Tumors. *Cells Tissues Organs*.

JANECZKO, K. (1989) Spatiotemporal patterns of the astroglial proliferation in rat brain injured at the postmitotic stage of postnatal development: a combined immunocytochemical and autoradiographic study. *Brain Res,* 485**,** 236-43.

JOHANSSON, C., SVENSSON, M., WALLSTEDT, L., JANSON, A. & FRISÉN, J. (1999) Neural stem cells in the adult human brain. *Exp Cell Res,* 253**,** 733-6.

JOY, A., MOFFETT, J., NEARY, K., MORDECHAI, E., STACHOWIAK, E., COONS, S., RANKIN-SHAPIRO, J., FLORKIEWICZ, R. & STACHOWIAK, M. (1997) Nuclear accumulation of FGF-2 is associated with proliferation of human astrocytes and glioma cells. *Oncogene,* 14**,** 171-83.

KAPLAN, M. & BELL, D. (1983) Neuronal proliferation in the 9-month-old rodent-radioautographic study of granule cells in the hippocampus. *Exp Brain Res,* 52**,** 1-5.

KEMPERMANN, G. & GAGE, F. (1999) New nerve cells for the adult brain. *Sci Am,* 280**,** 48-53.

KEMPERMANN, G., JESSBERGER, S., STEINER, B. & KRONENBERG, G. (2004) Milestones of neuronal development in the adult hippocampus. *Trends Neurosci,* 27**,** 447-52.

KEMPERMANN, G., KUHN, H. & GAGE, F. (1997) More hippocampal neurons in adult mice living in an enriched environment. *Nature,* 386**,** 493-5.

KLEIHUES, P. & CAVENEE, W. (1997) Pathology and Genetics of Tumours of the Nervous System. Lyon, International Agency for Research on Cancer.

KLEIHUES, P., SCHÄUBLE, B., ZUR HAUSEN, A., ESTÈVE, J. & OHGAKI, H. (1997) Tumors associated with p53 germline mutations: a synopsis of 91 families. *Am J Pathol,* 150**,** 1-13.

KNUDSON, A. J. (1977) Mutation and cancer in man. *Cancer,* 39**,** 1882-6.

KOESTNER, A., SWENBERG, J. & WECHSLER, W. (1971) Transplacental production with ethylnitrosourea of neoplasms of the nervous system in Sprague-Dawley rats. *Am J Pathol,* 63**,** 37-56.

KRAUS, J., KOOPMANN, J., KASKEL, P., MAINTZ, D., BRANDNER, S., SCHRAMM, J., LOUIS, D., WIESTLER, O. & VON DEIMLING, A. (1995) Shared allelic losses on chromosomes 1p and 19q suggest a common origin of oligodendroglioma and oligoastrocytoma. *J Neuropathol Exp Neurol,* 54**,** 91-5.

KUHLENBECK, H. (1947) Neuroplastic Transformation of the Subependymal Cell Plate in the Floor of the IV Ventricle (Subependymal-Spongioblastoma). *J. Neuropathol. Exptl. Neurol.***,** 139-151.

LANTOS, P. & COX, D. (1976) The origin of experimental brain tumours: a sequential study. *Experientia,* 32**,** 1467-8.

LAPIDOT, T., SIRARD, C., VORMOOR, J., MURDOCH, B., HOANG, T., CACERES-CORTES, J., MINDEN, M., PATERSON, B., CALIGIURI, M. & DICK, J. (1994) A cell initiating human acute myeloid leukaemia after transplantation into SCID mice. *Nature,* 367**,** 645-8.

LEE, J. & HERLYN, M. (2007) Old disease, new culprit: tumor stem cells in cancer. *J Cell Physiol,* 213**,** 603-9.

LENDAHL, U., ZIMMERMAN, L. & MCKAY, R. (1990) CNS stem cells express a new class of intermediate filament protein. *Cell,* 60**,** 585-95.

LEWIS, P. (1968) Mitotic activity in the primate subependymal layer and the genesis of gliomas. *Nature,* 217**,** 974-5.

LEWIS, P. & EMERMAN, M. (1994) Passage through mitosis is required for oncoretroviruses but not for the human immunodeficiency virus. *J Virol,* 68**,** 510-6.

LIE, D., COLAMARINO, S., SONG, H., DÉSIRÉ, L., MIRA, H., CONSIGLIO, A., LEIN, E., JESSBERGER, S., LANSFORD, H., DEARIE, A. & GAGE, F. (2005) Wnt signalling regulates adult hippocampal neurogenesis. *Nature,* 437**,** 1370-5.

LIE, D., SONG, H., COLAMARINO, S., MING, G. & GAGE, F. (2004) Neurogenesis in the adult brain: new strategies for central nervous system diseases. *Annu Rev Pharmacol Toxicol,* 44**,** 399-421.

LIGON, K., HUILLARD, E., MEHTA, S. (2007) Olig2-regulated lineage-restricted pathway controls replication competence in neural stem cells and malignant glioma. *Neuron*, 53, 503-517.

LIM, D. & ALVAREZ-BUYLLA, A. (1999) Interaction between astrocytes and adult subventricular zone precursors stimulates neurogenesis. *Proc Natl Acad Sci U S A,* 96**,** 7526-31.

MARSDEN, H., KUMAR, S., KAHN, J. & ANDERTON, B. (1983) A study of glial fibrillary acidic protein (GFAP) in childhood brain tumours. *Int J Cancer,* 31**,** 439-45.

MAURER, M. & KUSCHINSKY, W. (2006) Screening the brain: molecular fingerprints of neural stem cells. *Curr Stem Cell Res Ther,* 1**,** 65-77.

MELLINGHOFF, I., WANG, M., VIVANCO, I., HAAS-KOGAN, D., ZHU, S., DIA, E., LU, K., YOSHIMOTO, K., HUANG, J., CHUTE, D., RIGGS, B., HORVATH, S., LIAU, L., CAVENEE, W., RAO, P., BEROUKHIM, R., PECK, T., LEE, J., SELLERS, W., STOKOE, D., PRADOS, M., CLOUGHESY, T., SAWYERS, C. & MISCHEL, P. (2005) Molecular determinants of the response of glioblastomas to EGFR kinase inhibitors. *N Engl J Med,* 353**,** 2012-24.

MERKLE, F., MIRZADEH, Z. & ALVAREZ-BUYLLA, A. (2007) Mosaic organization of neural stem cells in the adult brain. *Science,* 317**,** 381-4.

MERKLE, F., TRAMONTIN, A., GARCÍA-VERDUGO, J. & ALVAREZ-BUYLLA, A. (2004) Radial glia give rise to adult neural stem cells in the subventricular zone. *Proc Natl Acad Sci U S A,* 101**,** 17528-32.

MILLER, M. & NOWAKOWSKI, R. (1988) Use of bromodeoxyuridine-immunohistochemistry to examine the proliferation, migration and time of origin of cells in the central nervous system. *Brain Res,* 457**,** 44-52.

MORSHEAD, C., REYNOLDS, B., CRAIG, C., MCBURNEY, M., STAINES, W., MORASSUTTI, D., WEISS, S. & VAN DER KOOY, D. (1994) Neural stem cells in the adult mammalian forebrain: a relatively quiescent subpopulation of subependymal cells. *Neuron,* 13**,** 1071-82.

MURASE, S. & HORWITZ, A. (2004) Directions in cell migration along the rostral migratory stream: the pathway for migration in the brain. *Curr Top Dev Biol,* 61**,** 135-52.

NEALE, F., CLUBB, J., HOTCHKIS, D. & POSEN, S. (1965) HEAT STABILITY OF HUMAN PLACENTAL ALKALINE PHOSPHATASE. *J Clin Pathol,* 18**,** 359-63.

NOTTEBOHM, F. (2004) The road we travelled: discovery, choreography, and significance of brain replaceable neurons. *Ann N Y Acad Sci,* 1016**,** 628-58.

PALMER, T., MARKAKIS, E., WILLHOITE, A., SAFAR, F. & GAGE, F. (1999) Fibroblast growth factor-2 activates a latent neurogenic program in neural stem cells from diverse regions of the adult CNS. *J Neurosci,* 19**,** 8487-97.

PALMER, T., WILLHOITE, A. & GAGE, F. (2000) Vascular niche for adult hippocampal neurogenesis. *J Comp Neurol,* 425**,** 479-94.

PATHAK, S. (1990) Cytogenetic abnormalities in cancer: with special emphasis on tumor heterogeneity. *Cancer Metastasis Rev,* 8**,** 299-318.

PEREIRA, D. (1998) Retroviral transduction of TLS-ERG initiates a leukemogenic program in normal human hematopoietic cells. *Proc. Natl. Acad. Sci*., 95, 8239-8244.

POSEN, S., CORNISH, C., HORNE, M. & SAINI, P. (1969) Placental alkaline phosphatase and pregnancy. *Ann N Y Acad Sci,* 166**,** 733-44.

PRICE, J., TURNER, D. & CEPKO, C. (1987) Lineage analysis in the vertebrate nervous system by retrovirus-mediated gene transfer. *Proc Natl Acad Sci U S A,* 84**,** 156-60.

PUROW, B., HAQUE, R., NOEL, M., SU, Q., BURDICK, M., LEE, J., SUNDARESAN, T., PASTORINO, S., PARK, J., MIKOLAENKO, I., MARIC, D., EBERHART, C. & FINE, H. (2005) Expression of Notch-1 and its ligands,

Delta-like-1 and Jagged-1, is critical for glioma cell survival and proliferation. *Cancer Res,* 65**,** 2353-63.

RAINETEAU, O., RIETSCHIN, L., GRADWOHL, G., GUILLEMOT, F. & GÄHWILER, B. (2004) Neurogenesis in hippocampal slice cultures. *Mol Cell Neurosci,* 26**,** 241-50.

RAMON Y CAJAL, S. (1913) Degeneration and Regeneration of the Nervous System. London, Oxford Univ. Press.

RASHEED, B., WILTSHIRE, R., BIGNER, S. & BIGNER, D. (1999) Molecular pathogenesis of malignant gliomas. *Curr Opin Oncol,* 11**,** 162-7.

RATHER, L. (1978) *The Genesis of Cancer: A Study in the History of Ideas,* Baltimore, Johns Hopkins University Press.

RAY, J., PETERSON, D., SCHINSTINE, M. & GAGE, F. (1993) Proliferation, differentiation, and long-term culture of primary hippocampal neurons. *Proc Natl Acad Sci U S A,* 90**,** 3602-6.

REYA, T. & CLEVERS, H. (2005) Wnt signalling in stem cells and cancer. *Nature,* 434**,** 843-50.

REYNOLDS, B. & WEISS, S. (1992) Generation of neurons and astrocytes from isolated cells of the adult mammalian central nervous system. *Science,* 255**,** 1707-10.

RIETZE, R., VALCANIS, H., BROOKER, G., THOMAS, T., VOSS, A. & BARTLETT, P. (2001) Purification of a pluripotent neural stem cell from the adult mouse brain. *Nature,* 412**,** 736-9.

ROTH, W., WILD-BODE, C., PLATTEN, M., GRIMMEL, C., MELKONYAN, H., DICHGANS, J. & WELLER, M. (2000) Secreted Frizzled-related proteins inhibit motility and promote growth of human malignant glioma cells. *Oncogene,* 19**,** 4210-20.

ROY, N., BENRAISS, A., WANG, S., FRASER, R., GOODMAN, R., COULDWELL, W., NEDERGAARD, M., KAWAGUCHI, A., OKANO, H. & GOLDMAN, S. (2000) Promoter-targeted selection and isolation of neural progenitor cells from the adult human ventricular zone. *J Neurosci Res,* 59**,** 321-31.

SANAI, N., TRAMONTIN, A., QUIÑONES-HINOJOSA, A., BARBARO, N., GUPTA, N., KUNWAR, S., LAWTON, M., MCDERMOTT, M., PARSA, A., MANUEL-GARCÍA VERDUGO, J., BERGER, M. & ALVAREZ-BUYLLA, A. (2004) Unique astrocyte ribbon in adult human brain contains neural stem cells but lacks chain migration. *Nature,* 427**,** 740-4.

SANES, J., RUBENSTEIN, J. & NICOLAS, J. (1986) Use of a recombinant retrovirus to study post-implantation cell lineage in mouse embryos. *EMBO J,* 5**,** 3133-42.

SCHERER, H. (1940) The forms of growth in gliomas and their practical significance. *Brain***,** 1-35.

SERI, B., GARCÍA-VERDUGO, J., MCEWEN, B. & ALVAREZ-BUYLLA, A. (2001) Astrocytes give rise to new neurons in the adult mammalian hippocampus. *J Neurosci,* 21**,** 7153-60.

SERI, B., HERRERA, D., GRITTI, A., FERRON, S., COLLADO, L., VESCOVI, A., GARCIA-VERDUGO, J. & ALVAREZ-BUYLLA, A. (2006) Composition and organization of the SCZ: a large germinal layer containing neural stem cells in the adult mammalian brain. *Cereb Cortex,* 16 Suppl 1**,** i103-11.

SHEN, Q., GODERIE, S., JIN, L., KARANTH, N., SUN, Y., ABRAMOVA, N., VINCENT, P., PUMIGLIA, K. & TEMPLE, S. (2004) Endothelial cells stimulate self-renewal and expand neurogenesis of neural stem cells. *Science,* 304**,** 1338-40.

SHERR, C. & WEBER, J. (2000) The ARF/p53 pathway. *Curr Opin Genet Dev,* 10**,** 94-9.

SHOSHAN, Y., NISHIYAMA, A., CHANG, A., MÖRK, S., BARNETT, G., COWELL, J., TRAPP, B. & STAUGAITIS, S. (1999) Expression of oligodendrocyte progenitor cell antigens by gliomas: implications for the histogenesis of brain tumors. *Proc Natl Acad Sci U S A,* 96**,** 10361-6.

SIDMAN, R., MIALE, I. & FEDER, N. (1959) Cell proliferation and migration in the primitive ependymal zone: an autoradiographic study of histogenesis in the nervous system. *Exp Neurol,* 1**,** 322-33.

SINGEC, I., KNOTH, R., MEYER, R., MACIACZYK, J., VOLK, B., NIKKHAH, G., FROTSCHER, M. & SNYDER, E. (2006) Defining the actual sensitivity and specificity of the neurosphere assay in stem cell biology. *Nat Methods,* 3**,** 801-6.

SINGH, S., CLARKE, I., TERASAKI, M., BONN, V., HAWKINS, C., SQUIRE, J. & DIRKS, P. (2003) Identification of a cancer stem cell in human brain tumors. *Cancer Res,* 63**,** 5821-8.

SINGH, S., HAWKINS, C., CLARKE, I., SQUIRE, J., BAYANI, J., HIDE, T., HENKELMAN, R., CUSIMANO, M. & DIRKS, P. (2004) Identification of human brain tumour initiating cells. *Nature,* 432**,** 396-401.

SMART, I. (1961) The subependymal layer of the mouse brain and its cell production as shown by autography after [H3]-thymidine injection. *J. Comp. Neurol.***,** 325–27.

SONG, H., STEVENS, C. & GAGE, F. (2002a) Astroglia induce neurogenesis from adult neural stem cells. *Nature,* 417**,** 39-44.

SONG, H., STEVENS, C. & GAGE, F. (2002b) Neural stem cells from adult hippocampus develop essential properties of functional CNS neurons. *Nat Neurosci,* 5**,** 438-45.

STANFIELD, B. & TRICE, J. (1988) Evidence that granule cells generated in the dentate gyrus of adult rats extend axonal projections. *Exp Brain Res,* 72**,** 399-406.

TAYLOR, M., POPPLETON, H., FULLER, C., SU, X., LIU, Y., JENSEN, P., MAGDALENO, S., DALTON, J., CALABRESE, C., BOARD, J., MACDONALD, T., RUTKA, J., GUHA, A., GAJJAR, A., CURRAN, T. & GILBERTSON, R. (2005) Radial glia cells are candidate stem cells of ependymoma. *Cancer Cell,* 8**,** 323-35.

TEMPLE, S. (2001) The development of neural stem cells. *Nature,* 414**,** 112-7.

TOHYAMA, T., LEE, V., RORKE, L., MARVIN, M., MCKAY, R. & TROJANOWSKI, J. (1992) Nestin expression in embryonic human neuroepithelium and in human neuroepithelial tumor cells. *Lab Invest,* 66**,** 303-13.

UCHIDA, N., BUCK, D., HE, D., REITSMA, M., MASEK, M., PHAN, T., TSUKAMOTO, A., GAGE, F. & WEISSMAN, I. (2000) Direct isolation of human central nervous system stem cells. *Proc Natl Acad Sci U S A,* 97**,** 14720-5.

UHRBOM, L., DAI, C., CELESTINO, J., ROSENBLUM, M., FULLER, G. & HOLLAND, E. (2002) Ink4a-Arf loss cooperates with KRas activation in astrocytes and neural progenitors to generate glioblastomas of various morphologies depending on activated Akt. *Cancer Res,* 62**,** 5551-8.

ULLIAN, E., CHRISTOPHERSON, K. & BARRES, B. (2004) Role for glia in synaptogenesis. *Glia,* 47**,** 209-16.

VALTZ, N., HAYES, T., NORREGAARD, T., LIU, S. & MCKAY, R. (1991) An embryonic origin for medulloblastoma. *New Biol,* 3**,** 364-71.

VAN PRAAG, H., SCHINDER, A., CHRISTIE, B., TONI, N., PALMER, T. & GAGE, F. (2002) Functional neurogenesis in the adult hippocampus. *Nature,* 415**,** 1030-4.

VESCOVI, A., GALLI, R. & REYNOLDS, B. (2006) Brain tumour stem cells. *Nat Rev Cancer,* 6**,** 425-36.

VESCOVI, A., REYNOLDS, B., FRASER, D. & WEISS, S. (1993) bFGF regulates the proliferative fate of unipotent (neuronal) and bipotent (neuronal/astroglial) EGF-generated CNS progenitor cells. *Neuron,* 11**,** 951-66.

VICK, N., LIN, M. & BIGNER, D. (1977) The role of the subependymal plate in glial tumorigenesis. *Acta Neuropathol (Berl),* 40**,** 63-71.

VOGELSTEIN, B., FEARON, E., HAMILTON, S., KERN, S., PREISINGER, A., LEPPERT, M., NAKAMURA, Y., WHITE, R., SMITS, A. & BOS, J. (1988) Genetic alterations during colorectal-tumor development. *N Engl J Med,* 319**,** 525-32.

WECHSLER-REYA, R. & SCOTT, M. (2001) The developmental biology of brain tumors. *Annu Rev Neurosci,* 24**,** 385-428.

WOLF, H., BUSLEI, R., SCHMIDT-KASTNER, R., SCHMIDT-KASTNER, P., PIETSCH, T., WIESTLER, O. & BLÜMCKE, I. (1996) NeuN: a useful neuronal marker for diagnostic histopathology. *J Histochem Cytochem,* 44**,** 1167-71.

ZHU, H. & DAHLSTRÖM, A. (2007) Glial fibrillary acidic protein-expressing cells in the neurogenic regions in normal and injured adult brains. *J Neurosci Res,* 85**,** 2783-92.